CONTRACT NO. A732-085
FINAL REPORT
AUGUST 1991

Emissions of Volatile and Potentially Toxic Organic Compounds from Wastewater Treatment Plants and Collection Systems (Phase II)

Volume 2:

Wastewater Collection System Study

State of California
AIR RESOURCES BOARD
Research Division

EMISSIONS OF VOLATILE AND POTENTIALLY TOXIC ORGANIC COMPOUNDS FROM WASTEWATER TREATMENT PLANTS AND COLLECTION SYSTEMS (PHASE II)

VOLUME 2 - WASTEWATER COLLECTION SYSTEM STUDY

Final Report
Contract No. A732-085

Prepared for:

Research Division
California Air Resources Board
1800 15th Street
Sacramento, CA 95814

Submitted by:

Department of Civil Engineering
University of California
Davis, CA 95616

Prepared by:

D.P.Y. Chang
Principal Investigator

August 1991

ABSTRACT

This report was completed to assess the potential for volatile organic compound (VOC) emissions from wastewater collection systems. The study focussed on two important phenomena: 1) partitioning of VOCs between sewer atmospheres and wastewater, and 2) convective transport of VOCs by gas exchange with the ambient atmosphere. Tracer studies were completed in operating sanitary sewers, resulting in data used to evaluate methods for predicting VOC partitioning. An oxygen transfer model was suggested with theoretically based adjustments for VOCs. Several mechanisms were studied as driving forces for ventilation of sewer atmospheres. Fluid mechanical analyses were applied to hypothetical flow circuits, and the importance of individual mechanisms were compared. It was concluded that no single mechanism dominates sewer ventilation under all situations, but environmental conditions, wastewater flow conditions, and physical characteristics of a collection system were identified under which some mechanisms become dominate. A set of one-dimensional, two-phase finite volume models were developed to predict dynamic mass transport of VOCs in collection systems. Over one thousand hypothetical scenarios were simulated to ascertain the importance of physical characteristics of sewers, flow characteristics, and physico-chemical properties of VOCs. Results provide guidance in identifying potential points of high emission, and the relative importance of collection systems compared to wastewater treatment systems.

DISCLAIMER

"THE STATEMENTS AND CONCLUSIONS IN THIS REPORT ARE THOSE OF THE CONTRACTOR AND NOT NECESSARILY THOSE OF THE CALIFORNIA AIR RESOURCES BOARD. THE MENTION OF COMMERCIAL PRODUCTS, THEIR SOURCE OR THEIR USE IN CONNECTION WITH MATERIAL REPORTED HEREIN IS NOT TO BE CONSTRUED AS EITHER AN ACTUAL OR IMPLIED ENDORSEMENT OF SUCH PRODUCTS."

ACKNOWLEDGEMENTS

Many individuals contributed to the completion of this effort, especially the field experiment phase. We wish to thank Mssrs. Allen Turner of the City of Davis, Jack Wong, Frank Bechtel and Ron Linden of the County of Sacramento. Several other individuals made valuable suggestions for the field and modeling experiments: Mssrs. Chip Hellier of the East Bay Municipal Utilities District; Ross Caballero and Jeff Weiss, County Sanitation Districts of Los Angeles County; John Vasconcelos of James M. Montgomery, Inc. Fellow students and staff at the University of California, Davis also took part in the actual preparation for and conduct of the experiments and subsequent chemical analyses: Phil Jones, Jim Meyerhofer, Steve Donovan, Chris Pierce, Steve Teague and Dale Uyeminami.

The California Air Resources Board and their staff have been supportive of our efforts over the past years. In particular, we will always remember the friendship and efforts of our former research project manager Mr. Joseph R. Pantalone. Mr. Ralph Propper has capably taken over that task and we are thankful for his assistance and patience in completing it. Our friends in the Test and Evaluation Branch were probably never more joyful about not having to sample a specific source type, and we wish to thank Mr. Bob Okamoto for his help in constructing some of the sampling equipment.

TABLE OF CONTENTS

	Page
Abstract	ii
Disclaimer	iii
Acknowledgements	iv
List of Tables	vi
List of Figures	viii
List of Acronyms	x
Nomenclature	xii
Introduction	1
Background	4
Theoretical Review - Mass transfer	15
Theoretical Development - Sewer Ventilation	47
Theoretical Development - Quantitative Solutions	71
Mass Transfer Field Experiments	86
Interpretive Modeling	134
Summary, Conclusions and Recommendations	172
References	180
Appendix A - Source Code for Models	189
Appendix B - Schematics of Sewer Appurtenances and Structures	226

LIST OF TABLES

		Page
2-1.	Uses of VOCs	7
2-2.	Sources of VOCs	7
2-3.	Percent Occurrence and Average Concentrations of VOCs in Sewers	8
2-4.	VOCs in Top 20 List of Hazardous Contaminants Discharged to Sewers in the United States	11
2-5.	Industries which Discharge VOCs in Excess of 100 Metric Tons per Year to Sewers	11
3-1.	Experimental Values of Ψ with Respect to Oxygen	22
3-2.	Coefficients for Nakasone's Equation of Oxygen Transfer Over Weirs	33
3-3.	Sludge Stream Partition Fractions	45
4-1.	Ventilation Rates Based on 85% Oxygen Levels in the Atmospheres of Operating Sewers	65
4-2.	Estimates of Gas Mean Velocities Caused by Individual Ventilation Mechanisms	68
6-1.	Physical Properties of Experimental Systems	89
6-2.	Summary of Tracer Experiments	89
6-3.	Wastewater Flow and Depth Conditions	97
6-4.	Wastewater Temperature and Henry's Law Constant for TCM-d	97
6-5.	Gas Flow Conditions	102
6-6.	Tracer Concentrations and Injection Rates	102
6-7.	Summary of TCM-d Standards for GC/MSD Analyses	110
6-8.	Regression Analysis of TCM-d Standards	110
6-9.	Comparison of Methods to Compute Liquid Concentration	116
6-10.	Summary of Steady-State Concentrations of TCM-d in Wastewater	117
6-11.	Mass Transfer Coefficients Based on Experimental Data	122
6-12.	Ratio of Experimental to Predicted Mass Transfer Coefficients	122
6-13.	Summary of Steady-State Concentrations of TCM-d in Sewer Gas	130
6-14.	Contributions to Uncertainties in Mass Transfer Coefficients	132

7-1. Standard Conditions used for Parameter Variations on a Uniform Reach 135

7-2. Parameter Variations for MATES Analysis of Uniform Reaches 136

7-3. Conditions for Example Discharge at Varying Flowrates 145

7-4. Conditions for variable slope analyses at constant flowrate 146

7-5. Standard Conditions for Parameter Analyses on Drops 150

7-6. Removal of PERC from Drops with Varying Wastewater Discharge 153

7-7. Model Conditions and Results for Small Interceptor Discharging to Wet Well 156

7-8. Model Conditions and Results for Large Interceptor Discharging to Wet Well 159

7-9. Model Conditions and Results for House Connection Discharging to Street Sewer 162

7-10. Model Conditions and Results for Drop Manhole Connecting Two Reaches 165

7-11. Concentrations at End of Segments of Sewer Model 169

LIST OF FIGURES

Page

4-1. Hypothetical Circuit for Analysis of Ventilation Flows Caused by Liquid Drag 52

4-2. Hypothetical Circuit A for Analysis of Ventilation Flows Caused by Eduction by Wind (circuit B identical to circuit used for liquid drag and shown in Figure 4-1) 55

4-3. Hypothetical Circuits for Analysis of Ventilation Flows Caused by Temperature Differences Between Sewer and Ambient Atmospheres 60

4-4. Hypothetical Circuits for Analysis of Ventilation Flows Caused by Barometric Pressure Gradients 63

5-1. Gas and Liquid Control Volumes with a Common Interface 72

5-2. Gas-Phase Control Volume for a Wet Well Atmosphere 85

6-1. Simplified Schematic of the Two-Phase Tracer Method 87

6-2. Simplified Illustration of the El Macero Interceptor (not to scale) 91

6-3. Simplified Illustration of the Central Interceptor (not to scale) 92

6-4. Simplified Illustrations of Field Experiments (not to scale) 95

6-5. Duct Arrangement for Ventilation during Field Experiments 99

6-6. Gas Sampling Train used in El Macero and Central Interceptor Experiments 105

6-7. Example Chromatogram of TCM-d Standard 109

6-8. Example Calibration Curve Based on TCM-d Standards 111

6-9. Measured Aqueous Concentrations of TCM-d during Field Experiments 113

6-10. Gaseous Sulfur Hexafluoride Concentrations Downstream of Release Point 120

6-11. Measured and Predicted Concentrations of TCM-d in Sewer Gas 124

6-12. Normalized Residuals Indicating the Difference Between Measured and Predicted ConcentrationsofTCM-d in Sewer Atmosphere 129

7-1. Variable Combinations Exceeding Specified Removal for MATES Analysis of Standard Reach 138

7.2. Mass emissions for hypothetical sewer reach subject to variations in the spatial distribution of ventilation. 141

7-3. Mass removal versus ventilation rate for hypothetical sewer reach and dimensionless Henry's law constants of 0.1 to 1.0. 143

7-4. Mass removal versus ventilation rate for hypothetical sewer reach and dimensionless Henry's law constants of 0.1 to 1.0. 143

7-5. VOC mass removal versus Henry's law constant for hypothetical sewer reach. 145

7-6. VOC mass removal versus Henry's law constant for a hypothetical sewer reach. Uniform ventilation at 1.0 volume turnovers per day. 147

7-7. VOC mass removal versus Henry's law constant for a hypothetical sewer reach. Uniform ventilation at 10.0 volume turnovers per day. 147

7-8. Schematic Diagram of Collection System Emission Scenario from Residence to Wastewater Treatment Plant 170

7-9. Sewer Model TCM Predicted Concentration by Sewer Segment 171

LIST OF ACRONYMS

AN	acetonitrile
BDCM	bromodichloromethane
BOD	biochemical oxygen demand
BZ	benzene
BP	boiling point
CARB	California Air Resources Board
CFSTR	continuous-flow stirred tank reactor
CI	Central Interceptor
ClBz	chlorobenzene
CORAL	Collection System Organic Release Algorithm
CT	tetrachloromethane (carbon tetrachloride)
DBCM	dibromochloromethane
DCA	1,2-dichloroethane
DCE	1,1-dichloroethene
DCM	dichloromethane (methylene chloride)
EMI	El Macero Interceptor
ETBZ	ethylbenzene
GC/MSD	gas chromatography/mass selective detector
i.d.	inside diameter
MATES	Multi-Parameter Assessment of Toxic Emissions from Sewers
MGD	million gallons per day
MSD	mass spectrometry detector (or mass selective detector)
mtpy	metric tons per year
NEWPCP	North East Water Pollution Control Plant (Philadelphia)
PDE	partial differential equation
PERC	tetrachloroethene (perchloroethylene)
POTWs	publicly owned treatment works
ppb	parts per billion
ppm	parts per million
QSAR	quantitative structure-activity relationship
RCRA	Resource Conservation and Recovery Act
Re	Reynolds number
ROG	reactive organic gas

Sc	Schmidt number
SCAQMD	South Coast Air Quality Management District
SF_6	sulfur hexafluoride
SRWWTP	Sacramento Regional Wastewater Treatment Plant
SUDS	Sewer Uniform Reach and Drop Solution
TCA	1,1,1-trichloroethane (methyl chloroform)
TCE	trichloroethene (trichloroethylene)
TCM	trichloromethane (chloroform)
TCM-d	deuterated trichloromethane (deuterated chloroform)
TDS	total dissolved solids
THM	trihalomethane
TOL	methylbenzene (toluene)
UCD	University of California, Davis
USEPA	United States Environmental Protection Agency
VC	chloroethene (vinyl chloride)
VOC	volatile organic compound
VP	vapor pressure
WCS	wastewater collection system

NOMENCLATURE

A_0	surface area of undisturbed gas-liquid interface [L^2]
A_g	cross-sectional area of gas flow [L^2]
A_l	cross-sectional area of liquid flow [L^2]
A_s	actual interfacial surface area [L^2]
A_{si}	gas-
A_{sl}	area of slime layer on wetted wall of cell i [L^2]
c_e	escape coefficient in Tsivoglou-Neal reaeration model [L^{-1}]
C_1	liquid-phase concentration upstream of a drop [$M\ L^{-3}$]
C_2	liquid-phase concentration downstream of a drop [$M\ L^{-3}$]
C_a	gas--phase ambient concentration [$M\ L^{-3}$]
C_b	liquid-phase concentration at the bottom of a drop [$M\ L^{-3}$]
C_A	area correction term = A_s/A_0 [-]
C_g	gas-phase concentration in cell i [$M\ L^{-3}$]
C_{qi}	gas-phase concentration in cell i [$M\ L^{-3}$]
C_{gi-1}	gas-phase concentration in cell (control volume) i-1 [$M\ L^{-3}$]
$C_{g\ in}$	gas-phase concentration entering a wet well [$M\ L^{-3}$]
C_l	liquid-phase concentration in cell i [$M\ L^{-3}$]
C_l'	liquid-phase concentration in thermodynamic equilibrium with gas-phase concentration [$M\ L^{-3}$]
$C_{l\ i-1}$	liquid-phase concentration in cell i-1 [$M\ L^{-3}$]
C_{l0}	liquid-phase concentration at x = 0 [$M\ L^{-3}$]
C_s	C_l' [$M\ L^{-3}$]
d	mean hydraulic depth of wastewater flow [L]
D_I	turbulent diffusivity [L^2T^{-1}]
D_l	liquid-phase diffusivity [L^2T^{-1}]
D_m	molecular diffusivity in liquid = D_l [L^2T^{-1}]
E	rate of loss of potential energy [L^2T^{-3}]
E_s	rate of energy expenditure to overcome molecular forces at a liquid surface [L^2T^{-3}]
F	Froude number [-]
Fr_j	jet Froude number [-]
Fr_s	supercritical Froude number [-]

g	gravitational acceleration [$L\ T^{-2}$]
G	factor in analytical solution of concentration depletion in sewers [-]
h	drop height of falling wastewater stream [L]
H_c	dimensionless Henry's law constant defined as the ratio of gas-to-liquid phase concentrations at thermodynamic equilibrium [-]
I	ionic strength [$mol\ L^{-3}$]
J	mass flux across a liquid-gas interface [$M\ L^{-2}T^{-1}$]
k_a	anaerobic decay constant [$L\ T^{-1}$]
k_b	first-order biological decay constant [T^{-1}]
k_g	gas-phase mass transfer coefficient [$L\ T^{-1}$]
k_l	liquid-phase mass transfer coefficient [$L\ T^{-1}$]
k_l'	liquid-phase mass transfer coefficient per unit depth, i.e. normalized by mean hydraulic depth [T^{-1}]
k_{li}	liquid-phase mass transfer coefficient for VOC i or cell (control volume) i [$L\ T^{-1}$]
k_{lj}	liquid-phase mass transfer coefficient for volatile species j [$L\ T^{-1}$]
k_m	wall transfer coefficient used to describe uptake of VOCs at unwetted walls of sewer pipe [$L\ T^{-1}$]
k_s	salting-out coefficient for nonelectrolytes [-]
K_{ow}	octanol-water partition coefficient [-]
K_T	overall mass transfer coefficient [$L\ T^{-1}$]
q	specific conductance [$\mu mhos\ cm^{-1}$]
q_j	wastewater discharge per unit width [$L^2\ T^{-1}$]
Q_{ex}	ventilation outflow [$L^3\ T^{-1}$]
Q_{in}	ventilation inflow [$L^3\ T^{-1}$]
Q_g	gas flow rate into a wet well [$L^3\ T^{-1}$]
$Q_{gi\ out}$	gas flow rate in cell i [$L^3\ T^{-1}$]
$Q_{gi-1\ out}$	gas flow rate in cell i [$L^3\ T^{-1}$]
Q_l	wastewater flow rate into a wet well [$L^3\ T^{-1}$]
$Q_{li\ out}$	wastewater flow rate in cell i [$L^3\ T^{-1}$]
$Q_{li-1\ out}$	wastewater flow rate in cell i-1 [$L^3\ T^{-1}$]
Q_{out}	ventilation outflow [$L^3\ T^{-1}$]
r_i	depletion ratio used to describe liquid-phase concentration changes (relative to saturation conditions) upstream and downstream of drops [-]
r_{O2}	r_i for oxygen [-]

R	hydraulic radius [L]
Re	Reynolds number [-]
s	average rate of surface renewal [T^{-1}]
S	channel slope or slope of energy line [$L\ L^{-1}$]
Sc	Schmidt number [-]
t	time [T]
t'	liquid parcel contact time at gas-liquid interface [T]
t_f	mean transport time between two locations in Tsivoglous-Neal reaeration model [T]
T	temperature [^oC or K]
u_g	gas mean velocity [$L\ T^{-1}$]
u_l	wastewater mean velocity [$L\ T^{-1}$]
U	wastewater mean velocity = u_l [$L\ T^{-1}$]
U*	friction velocity [$L\ T^{-1}$]
v_l	supercritical velocity [$L\ T^{-1}$]
V_g	gas volume [L^3]
V_l	liquid volume [L^3]
w	surface width [L]
x	directional component [L]
yl	supercritical depth of flow [L]
Y	tailwater depth of falling wastewater [L]
z_0	effective liquid film thickness [L]
α	ratio of wastewater to clean water mass transfer coefficients [-]
$\phi(t)$	surface age distribution in Danckwerts penetration theory [-]
Ψ_i	ratio of transfer coefficients for VOCi and oxygen [-]
Ψ_{ij}	ratio of transfer coefficients for two volatile species i and j [-][
γ	activity coefficient [-]
μ	absolute viscosity of liquid [$M\ L^{-1}\ T^{-1}$]; or ionic strength of solution
ν	kinematic viscosity [$L^2\ T^{-1}$]
ρ	liquid or gas density [$M\ L^3$]
σ	surface tension [$M\ T^{-2}$]

1. INTRODUCTION

1.1 PURPOSE

Studies completed between 1981 and 1985 suggested that publicly owned treatment works (POTWs) were significant sources of volatile organic compound (VOC) emissions to the ambient atmosphere (Lurker et al., 1982; Pellizzari, 1981; Petrasek, 1983; Silverman, 1985). These studies raised several concerns including; health impacts on POTW employees and downwind populations, release of reactive organic gases (ROGs) in ozone non-attainment air basins, and effects of potential VOC emission strategies on the operation of municipal wastewater collection and treatment systems.

In 1986 the Department of Civil Engineering at the University of California, Davis (UCD) contracted with the California Air Resources Board (CARB) to assess VOC emissions from POTWs in California. A major conclusion of that study was that insufficient knowledge existed regarding VOCs in wastewater collection systems (WCS) to quantify their potential source strength. This volume deals with the results of a study to ascertain potential VOC emissions from sanitary sewers in California.

1.2 OBJECTIVES

The intent of this work was to understand emissions from WCS. This objective was met by an analysis of gas-liquid mass transfer in flowing streams, sewer ventilation, and factors that influence those processes. In particular, an effort was made to interpret effects of physical parameters of collection reaches, wastewater discharge conditions, VOC discharge conditions, physico-chemical properties of VOCs, environmental factors, and ventilation rates and patterns on emissions rates.

Specific objectives included:

1. assessment of methods to estimate partitioning of VOCs from wastewater to overlying sewer gas,

2. investigation of factors that affect air exchange (ventilation) between WCS and ambient atmospheres,

3. quantitative assessment of important variables or combination of variables that can lead to emission "hot spots", and

4. assessment of relative removal rates of VOCs from "typical" WCS reaches.

1.3 SCOPE

The complex, non-linear interactions of factors affecting VOC emissions from sewers made it impossible to address the problem entirely from laboratory, pilot, or field experiments, or from a set of closed analytical solutions. Therefore, central to this study was development of computational models that allowed for sequential variation in single or multiple factors. Models were coded in FORTRAN 77 and executed on a DEC VAX 750.

There exists an infinite number of combinations of factors affecting VOC emissions from WCS. Given computational and time resources, it was only feasible to assess discrete values of individual factors over reasonable (or typical) ranges, and hypothetical collection reaches that represented small, medium, and large sewer lines.

Prediction of emissions from an entire WCS was beyond the scope of this study. Therefore, hypothetical discharge conditions were modeled to study practical effects of variations in discharges. An emphasis was placed on sanitary sewers, which are the most common type found in California, as opposed to combined sanitary/storm sewers, which still prevail in many older urban communities. However, basic principles described in this report should also apply to combined WCS.

Because of the importance of interphase partitioning on VOC emissions, a set of field experiments were completed in operating sanitary sewers to collect data to be used in comparisons of partitioning models. A volatile tracer (deuterated trichloromethane; TCM-d) was introduced to each of two collection reaches of significantly different dimension and flow conditions. Cost constraints, concerns regarding the discharge of foreign substances to a collection reach, and constraints on the availability of analytical equipment limited the number of experiments to six, and the number of liquid and gas samples per experiment to approximately 20.

1.4 ORGANIZATION

Chapter 2 of this volume provides background on the sources and properties of VOCs, as well as previous studies of VOC occurrence in WCS. Chapter 3 presents an analysis of interfacial mass transfer, and Chapter 4 describes gas flow in sewers. Analytical and computational models are described in Chapter 5. A description of experimental and analytical methods, data interpretation, results, and discussions of field experiments are provided in Chapter 6. Chapter 7 includes a discussion of interpretive modeling, and an analysis of parameter variations. An example calculation of loss of chloroform from a typical hypothetical sewer reach running from a residential area to a MWTP is discussed. Conclusions and recommendations for future studies are presented in Chapter 8.

2. BACKGROUND

This chapter summarizes past and present studies associated with the fate of VOCs in wastewater collection systems (WCS). Volatile organic compounds have high vapor pressures. However, a precise definition of what constitutes a VOC does not exist. Operational definitions of VOCs often depend on a particular measurement or analytical procedure, or can be based upon a legal definition, e.g. compounds having vapor pressures at 25 ^{o}C greater than 0.1 mm Hg. Relevant physico-chemical properties that affect volatility include pure compound vapor pressure, solubility, boiling point, and Henry's law constant. The latter parameter has been used to classify organic compound volatility with respect to mass transfer from water or wastewater to ambient air (Matter-Muller et al., 1981; Thomas, 1982; Petrasek, 1983).

Uses and Sources of VOCs

Volatile organic compounds are used in a wide variety of applications ranging from household cleaners to fuel additives, and solvents. Specific uses for several VOCs are summarized in Table 2-1. Sources that may serve as dischargers of VOCs to municipal wastewater collection systems are listed in Table 2-2.

2.1 STUDIES OF THE FATE OF VOCS IN WASTEWATER

To date, most of the studies associated with VOCs in wastewater have focused on treatment facilities (Lawson and Siegrist, 1981; Pellizzari, 1981; Bishop, 1982; Lurker et al., 1982; Kincannon et al., 1983; Petrasek et al., 1983; Roberts et al., 1984; Cox et al., 1984; Dixon and Bremen, 1984; Lurker et al., 1984; Blackburn et al., 1985; California Air Resources Board, 1985; Silverman, 1985; Allen et al., 1986; Hannah et al. 1986; USEPA, 1986a; USEPA, 1986b; Berglund and Whipple, 1987; Chang et al., 1987; Corsi et al., 1987; Namkung and Rittmann, 1987; Weber et al., 1987; Eklund et al., 1988; Corsi et al.,

1989a; Melcer et al., 1989). Studies of VOCS in collection systems are reviewed below.

Four City Study

Levins et al. (1979) studied occurrences and concentrations of 129 priority pollutants in the sewers of four major metropolitan areas (Cincinnati, St. Louis, Atlanta, and Hartford). Wastewater samples were collected for sewers classified as residential, commercial, or industrial. A total of 11 residential, 10 commercial, and five industrial sewers were monitored, in addition to tap water and treatment plant influent. The St. Louis collection system was the only completely sanitary system, i.e. not a combined sanitary/stormwater system. The range of 24-hour or 48-hour composite samples was 30-60 per city.

Only 56 of the 129 pollutants studied were observed in sewers, including 13 of the VOCs listed in Table 2-1. A summary of percent occurrence and average concentrations in various water and wastewater conveyance categories is provided in Table 2-3. Standard deviations are also provided for all but treatment plant influent and industrial sewer samples. Although specific values were not provided, standard deviations were noted to be very high in the latter categories as a result of significant variations in the types of industrial dischargers.

Chloroethene (VC) and propenenitrile (acrylonitrile) were not detected in any samples. Dichloromethane (DCM) was detected in relatively high concentrations in nearly all samples. It was excluded from analyses on the basis of being an ubiquitous contaminant. It is clear from Table 2-3 that relatively few VOCs were observed in tap water, with the exception of trihalomethanes (THMs) and tetrachloroethene (PERC). The occurrence and concentration of VOCs generally increased from residential, to commercial and industrial reach categories. Treatment plant influent represented a flow-averaged mixture of contributions

from each category (concentrations generally higher than residential but lower than industrial). One important observation is the reduction in both occurrence and concentration of THMs from tap water to residential wastewater, suggesting volatilization during residential activities, e.g. showers. Another observation is the occurrence of highly volatile CT in industrial sewers, and absence in treatment plant influent, suggesting significant volatile emissions from combined sewer systems.

USEPA - Study of VOC Desorption in Sewers

Kyosai et al. (1981) described a theoretical approach to estimate transfer coefficients for VOCs given that a transfer coefficient for oxygen is available. The theoretical approach was verified by conducting non steady-state oxygen absorption tests simultaneously with DCM desorption tests in a bench-scale stirred tank reactor.

An analytical model was developed to estimate losses of DCM from a collection reach. Simplifying assumptions included infinite dilution , i.e. no build-up of gases in a sewer atmosphere, clean water conditions, characterization of an entire collection reach as a single well-mixed reactor, liquid levels such that a collection reach is flowing half-full, and temperature invariant at 20 ^{o}C. The model was used to quantify losses from sewers with diameters of 0.25 to 2.3 m i.d. and mean liquid flow velocities of 0.6 to 12 $m \cdot s^{-1}$. Results suggested that desorption rate at a constant mean velocity decreases as diameter increases, and that desorption rate at a fixed diameter increases significantly as velocity increases.

Table 2-1. Uses of VOCs

Compound	Uses
BZ	fuel additive; solvent.
TCM	solvent; soil fumigant.
ETBZ	solvent; conversion to styrene monomer.
DCM	solvent; fire extinguishing; beer flavoring; caffeine extraction from coffee.
PERC	solvent.
TOL	solvent; fuel additive; production of benzene, dyes, and explosives.
TCA	metal/plastic mold cleaning; aerosol formulation.
TCE	solvent.
VC	refrigerant; production of polyvinyl chloride.

Reference: Chang et al. (1987)

Table 2-2. Sources of VOCs

Compound	Sources
BZ	metal finishing; organic chemicals, plastics, and synthetics industries (OCPS); pharmaceuticals; auto services; manufacture of dyes, linoleum, varnishes.
TCM	adhesives industry; aluminum forming; leather tanning and finishing; pulp, paper, and fiberboard manufacture; OCPS; pharmaceuticals; rubber industry; chlorinated drinking water.
ETBZ	adhesives industry; production of electrical products; OCPS; leather tanning and finishing; motor vehicle services; pharmaceuticals.
DCM	adhesives industry; metal industries; production of electrical products; leather industry; OCPS; pharmaceuticals; wood finishing; food processing; photographic chemicals.
PERC	copper forming; metal finishing; textile mills; non-OCPS; dry cleaners; wood finishing.
TOL	adhesives industry; OCPS; leather industries; metal finishing; pharmaceuticals; motor vehicle services; laundries; wood finishing.
TCA	production of electrical products; metal finishing; plastic forming; pharmaceuticals; motor vehicle services.
TCE	adhesives industry; aluminum forming; textile mills; motor vehicle services; dry cleaners.
VC	polyvinyl chloride manufacturers.

Reference: Chang et al. (1987)

Table 2-3. Percent Occurrence and Average Concentrations of VOCs in Sewers

Compound		Tap %	Tap C	Res %	Res C	Com %	Com C	Ind %	Ind C	Inf %	Inf C
BZ		0	0	22	0.2	50	2.7	76	1.2	67	2.7
	sd		0		0.4		2.1				
BDCM		100	8.8	4	0	50	1.0	57	1.6	11	0.2
	sd		6.9		0.1		1.2				
CT	0	0	0	0	5	0.1	33	28.4	0	0	
	sd		0		0		0.2				
MCB	0	0	7	0.1	5	0	14	0.9	6	0	
	sd		0		0.1		0.1				
TCM		100	27.1	91	3.0	100	6.7	100	12.0	100	4.9
	sd		8.6		0.9		2.0				
DBCM		58	5.9	4	0	43	0.7	57	1.2	22	0.2
	sd		7.1		0		0.9				
DCA	0	0	2	0.1	5	0.1	14	0.6	11	0.2	
	sd		0		0.1		0.2				
DCE	0	0	0	0	5	0.3	38	11.6	17	2.4	
	sd		0		0		0.5				
ETBZ	8	0.1	17	0.4	50	3.0	76	100.4	67	16.3	
	sd		0.1		0.5		3.1				
PERC	25	0.8	78	6.3	98	21.4	100	69.9	83	77.9	
	sd		0.9		7.6		13.3				
TOL	8	0.3	63	2.6	90	11.0	100	52.3	78	25.8	
	sd		0.5		2.7		6.8				
TCA	0	0	30	2.3	52	2.9	71	85.1	78	28.9	
	sd		0		2.8		1.8				
TCE	0	0	11	0.4	14	12.8	100	25.4	67	50.5	
	sd		0		0.5		25.6				

Tap = tap water; Res = residential; Com = commercial; Ind = industrial; Inf = plant influent; % = occurrence; C = aqueous concentration [mg L^{-1}]; sd = standard deviation [mg L^{-1}].
Reference: Levins et al. (1979).

South Coast Air Quality Management District Vent Sampling

The South Coast Air Quality Management District (SCAQMD) completed limited gas-phase sewer sampling in an industrialized area of Los Angeles (Porter, 1986). A single gas sample was drawn from a building vent used for gas relief of building plumbing connected to a public collection system. Concentrations of four VOCs (BZ, PERC, TCA and TOL) were observed to be 4.6, 4.3, 60, and 5.8 ppm, respectively.

Report to Congress on Domestic Sewage Exclusion

In 1984 section 3018a of the Resource Conservation and Recovery Act (RCRA) was amended to remove specific contaminants from RCRA hazardous waste classifications if they happened to be mixed with domestic wastewater. Concerns regarding the impact of such an amendment on discharges of hazardous waste to sewers motivated a study by the USEPA which was reported to Congress in 1986 (USEPA, 1986a).

Various data bases were utilized to study discharges of 165 hazardous constituents from 47 industrial/commercial categories and the residential sector. A total of 160,000 industrial and commercial dischargers of hazardous wastes to sewers were identified in the United States. An estimated 37,000 to 52,000 metric tons per year (mtpy) of priority organic constituents were discharged to sewers. Residential loadings were estimated to account for 7.5% of those discharges.

Discharges of several VOCs listed in Table 2-1 were high among total loadings of hazardous constituents nationwide. Those estimated to be within the top 20 highest loadings are listed in Table 2-4, along with their relative rankings and estimated annual loadings. Industrial categories with total VOC discharges in excess of 100 mtpy are listed in Table 2-5. Estimates of speciated discharges by the Equipment Manufacturing and Assembly

industry included TCA (3819 mtpy), TCE (1681 mtpy), PERC (1299 mtpy), DCM (535 mtpy), TOL (229 mtpy), and BZ (153 mtpy).

The USEPA attempted to address VOC emissions from sewers and concluded the following:

1. Little is known regarding the fate of VOCs in sewers. Previous studies focused on fate during wastewater treatment.

2. Lack of knowledge regarding VOCs in sewers can be attributed to the complicated nature of such systems. In particular, wastewater characteristics, variations in flow volume, velocity, and level, sewer construction materials, rainfall events, and dangers and difficulties associated with sampling in such systems have led to a paucity of data regarding the occurrence of VOCs in WCS.

3. Previous work completed by the USEPA using a shallow-stream desorption model suggests rapid desorption of VOCs in well-ventilated combined sewers. It was concluded that losses should be virtually non-existent in separate sanitary sewers with limited air exchange. Technical arguments for that conclusion were not provided.

Philadelphia Integrated Environmental Management Project

The USEPA (1986b) completed a study in Philadelphia to develop methodologies for implementing human exposure reductions to toxic contaminants in multimedia. Ambient air, source gas, water, and wastewater monitoring were coupled with atmospheric transport and risk models to identify control options associated with eight pollutants (BZ, DCA, DCP, DCM, PERC, CT, TCE, and TCM) and 17 pollutant sources. Included in the latter was the 8.2 m^3-s^{-1} Northeast Water Pollution Control Plant (NEWPCP) and associated sewers which served several major industrial dischargers.

Table 2-4. VOCs in Top 20 List of Hazardous Contaminants Discharged to Sewers in the United States

Compound	Ranking	Discharge [mtpy]
DCM	2	5480
TCA	3	3925
TOL	4	3618
ETBZ	5	2179
TCM	7	1900
BZ	8	1859
TCE	9	1725
PERC	11	1506

mtpy = metric tons per year (1 metric ton = 1000 kilograms).
Reference: USEPA (1986a)

Table 2-5. Industries which Discharge VOCs in Excess of 100 Metric Tons per Year to Sewers

Industry Category	VOC Discharge in US [mtpy]
Equipment Manufacture and Assembly	7715
Pharmaceutical Manufacture	6995
Organic Chemicals Manufacture	4227
Petroleum Refining	1218
Pesticides Manufacture	1083
Plastics, Resins, and Synthetic Fibers	728
Pulp and Paper Mills	577
Industrial and Commercial Laundries	381
Textile Mills	253

mtpy = metric tons per year (1 metric ton = 1000 kilograms).
Reference: USEPA (1986a).

An upper-bound estimate of aggregate (all eight compounds) excess cancer incidence for a population of 1.7 million was 2.8 cases per year. Over 80% of the total risk was attributed to drinking water, particularly resulting from the ingestion of TCM. Exposure to airborne pollutants accounted for only 0.4 excess cancer incidence per year. The largest contribution to airborne risks was the NEWPCP (0.09 cases per year or 3.2% of total upper-bound cancer estimates). Emissions from wastewater collection systems were estimated to cause 0.021 upper-bound excess cancer cases per year (0.7% of total upper-bound cancer estimates). However, computational modeling significantly underestimated measured ambient levels of TCM and CT, and it was suggested that the difference might be due to area sources, e.g. sewers. Volatilization from sewers was observed to be a major loss mechanism for DCP and DCA.

Multi-Instrument Analysis in Cincinnati

Barsky et al. (1986) measured organic compounds in sewer head spaces in the City of Cincinnati. Although instrument limitations did not allow detailed results for individual VOCs, results did allow insight on predominant chemical groups in the atmospheres of various sewers. Sampling locations included a wet well and bar screen area at a large wastewater treatment facility, in sewers near each of two chemical plants, two reaches referred to only as "general" sewers, and a house sewer.

For the sampling periods reported, most of the compounds in the atmospheres of the wet well and all reaches other than the house sewer were predominantly condensible saturated aliphatics, e.g. hexanes, with saturated halogenated aliphatics, e.g. TCM, predominating during several sampling periods. Aromatics and halogenated alkenes were generally minor components of sewer atmospheres. The highest concentrations of total organics (in benzene equivalents) observed at the wet well were on the order of 1000 parts per million (ppm) by volume. In general, total

organic concentrations were less than 100 ppm near the two chemical plants and in the general sewers. Total organic concentrations in the house sewer were notably high (approximately 500 ppm in benzene equivalents). Unlike other sewer locations the concentration was almost entirely attributed to permanent combustible gases, e.g. methane.

Environment Canada Fuel Spill Studies

Fingas et al. (1988) used a physical model of a sewer to study measures to reduce explosion hazards after fuel spills to sewers. A 104 meter long, 3.8 cm i.d. pipe with a slope of 0.0048 $m \cdot m^{-1}$ was constructed in a laboratory. Automobile gasoline and diesel fuels were discharged to the model sewer by spilling them first into a concrete box and sewer entry designed to resemble a street and drain. Various dispersants and foams were also added before, during, and after fuel spills to ascertain their effectiveness at reducing explosive gas build-up. One important conclusion was that dispersants and foams generally increase gaseous concentrations of volatile components, thus increasing explosion hazards.

An interesting result was that gasoline produced two vapor peaks with respect to time at each sampling port along the model sewer. The first peak was found to consist primarily of high boiling fraction compounds attributed to fuel evaporation during water transport. It was observed to move faster than a second peak consisting of volatiles desorbed near the point of fuel spillage into the model sewer, i.e. drain drop. A possible explanation for the differences in peak velocities might be that VOCs lost during system entry were distributed across the gas flow cross-section with an average gas velocity lower than directly above the water surface.

USEPA - Control of VOC Emissions from Industrial Wastewater

The USEPA (1988) completed a review of VOC emission mechanisms and control technologies for industrial wastewater. Treatment processes in four general industrial categories were reviewed; organic chemicals, plastics, and synthetic fibers, pesticides, and pharmaceuticals manufacturing, and pulp, paper, paperboard, builder's paper and board mill industry. Collection of liquid waste streams was described, with two processes applicable to municipal collection systems; emissions through manhole covers and from lift stations.

Gas transport through manhole covers was described in terms of diffusive (molecular) and convective mechanisms. Temperature gradients (buoyancy-driven flows) and pressure differences caused by wind blowing over manhole covers (venturi-like effect) were major ventilation factors. Additional factors were described as manhole diameter, length of manhole cover to sewer line, thickness of manhole cover, number and diameter of vent holes wastewater composition and temperature, and physical properties of pollutants.

For lift stations, convective mass transfer was described as the predominant ventilation mechanism. Lift station design characteristics which affect air emission rates were noted to be liquid surface area, turbulence in wastewater, and hydraulic retention time in lift station wells. Increases in each parameter leads to increased partitioning between wastewater and overlying gases. Effects of lift station operation were also described including the piston-effect associated with displaced gases as liquid levels rise and fall, and increased partitioning to the gas phase during influent "spilling" into lift station wet wells when liquid levels in the wet well are low. Wastewater and pollutant characteristics also affect interfacial partitioning as described above for manholes.

3. THEORETICAL REVIEW: MASS TRANSFER

The most widely studied transfer process in environmental engineering has been absorption of oxygen from the atmosphere to natural water bodies or treated wastewater. Only recently have drinking water standards and effluent discharge requirements motivated studies of VOC desorption as water and wastewater treatment methods, respectively (Ball et al., 1984; Leighton and Calo, 1981). In particular, detailed studies have not been completed to investigate transfer of VOCs between raw wastewater and overlying gases in sewers.

3.1 MASS TRANSFER RATE COEFFICIENT

Most theories of interfacial mass transfer are based on the assumption that resistance to transfer is confined largely to thin regions in either phase. Potential or "driving force" for mass transfer is usually taken to be the difference between species concentration in the aqueous phase and the aqueous phase concentration that would exist in equilibrium with the bulk overlying gas-phase concentration. Overall transfer resistance is thus defined as the ratio of the gradient of a potential and the mass flux across an interface. The inverse of overall mass transfer resistance is referred to as the mass transfer rate coefficient, or simply transfer coefficient, so that mass flux across an interface from liquid to gas is modeled as

$$J = K_T \, (C_l - C'_l). \qquad (3\text{-}1)$$

The term J [$g \cdot m^{-2} \cdot s^{-1}$] is mass flux across a unit area of interface, C_l and C'_l are actual and equilibrium aqueous-phase concentrations of a species of interest [$g \cdot m^{-3}$], respectively, and K_T is an overall transfer coefficient [$m \cdot s^{-1}$]. The transfer coefficient has been noted to be a function of physico-chemical properties of chemical compounds and turbulent mixing characteristics of a bulk fluid. Variability of K_T from one appli-

cation to another results from differences in the nature and relative contributions of those effects.

3.2 THEORIES OF INTERFACIAL MASS TRANSFER

Three of the most widely applied theories of interfacial mass transfer are two-film theory, penetration theory, and film-penetration theory. Each theory is described below.

Two-Film Theory

Lewis and Whitman (1924) extended classical stagnant-film theory, reviewed by Sherwood et al. (1975), by allowing for two films separated by an interface. The interface was assumed to separate thin films in the gas and liquid phases through which molecular diffusion controls the rate of mass transfer. Resistance to mass transfer was assumed to occur only in the films themselves and not at the interface. Resistances were described as the inverse of a transfer coefficient through each film. Application of a flux-matching boundary condition with no accumulation at the interface led to

$$1/K_T = 1/k_l + 1/(H_c k_g) \qquad (3\text{-}2)$$

where k_l and k_g [$m \cdot s^{-1}$] are transfer coefficients across the liquid and gas films, respectively. The term H_c is the dimensionless Henry's law constant, defined as the ratio of gas and liquid-phase concentrations at equilibrium. Because diffusivities of VOCs are much greater in gas than in liquid, k_g is typically much greater than k_l. It has been shown that the product of H_c and k_g is generally much greater than k_l for H_c greater than 0.1 (Smith et al., 1980). For such a condition, liquid-phase resistance to mass transfer is limiting, and the overall transfer coefficient is approximated by the transfer coefficient in liquid.

Lewis and Whitman (1924) assumed steady-state conditions with a linear concentration gradient across each film. This assumption coupled with the assumption that overall mass transfer is limited by diffusion across the liquid film led to

$$K_T \simeq k_l = D_l/z_o. \qquad (3\text{-}3)$$

where z_o represents an "effective" liquid film thickness [m].

The most common criticism of Lewis and Whitman's (1924) presentation of two-film theory stems from the assumption of steady-state conditions across each film, i.e. fully-developed, linear concentration gradients across each film. It has been postulated that in a turbulent liquid, "parcels" of bulk liquid are intermittently transported to the interface where they remain for a time period, t', that is too short to attain a steady-state condition. Mathematical arguments by Dobbins (1956) suggested that convergence to a steady-state concentration profile is relatively rapid, and that steady-state conditions can be met if the interfacial region is fairly quiescent due to relatively low mixing rates from bulk liquid to the interface. However, the same work indicated that for rapid mixing to and from a surface, classical two-film theory is invalid, i.e. for short t'.

Penetration Theory

Penetration theory is based on the assumption that a species diffuses only a small distance into a liquid parcel, relative to the thickness of the parcel, during exposure time t'. Thus, a steady-state concentration profile across the parcel is not approached.

Higbie (1935) developed the first penetration theory solution. He solved the one dimensional diffusion equation for the interfacial region subject to non-steady state boundary conditions and the assumption that t' is constant for all eddies.

The liquid phase was assumed to dominate overall resistance to mass transfer, leading to:

$$K_T \simeq k_l = 1.13\ (D_l\ s)^{1/2}, \qquad (3\text{-}4)$$

where s is the inverse of t' and is referred to as the average rate of surface renewal (replacement).

Danckwerts (1951) generalized Higbie's solution so that t' could assume a wide spectrum of values. A surface age distribution F(t) was assumed such that

$$F(t) = r\ e^{-st}, \qquad (3\text{-}5)$$

where Fdt represents the probability that a liquid parcel is exposed to an interface for a time between t and t + dt. With these assumptions the transfer coefficient was derived to be

$$K_T \simeq k_l = (D_l\ s)^{1/2}. \qquad (3\text{-}6)$$

Unlike the power relationship predicted by two-film theory, penetration theory predicts that k_l is proportional to the square root of diffusivity.

Film-Penetration Theory

Dependency of K_T on D_l can be expressed as

$$K_T \propto D_l^{n}, \qquad (3\text{-}7)$$

where n is 1.0 for two-film theory and 0.5 for penetration theory. Dobbins (1956 and 1964a) recognized that limited experimental evidence indicated that the value of "n" exists within an envelope of 0.5 to 1.0, and that values of the exponent vary depending upon mixing characteristics of the flow. Similar observations have since been made by several researchers (Matter-Muller et al., 1981; Roberts et al., 1984; Smith et al., 1980). To reconcile variability of the power coefficient, Dobbins (1956)

developed a mathematical model for liquid-phase dominated mass transfer that was based upon solution of the one-dimensional diffusion equation given Danckwerts' surface age distribution and modified boundary conditions. The resulting transfer coefficient equation was

$$K_T \simeq k_l = (D_l\ s)^{1/2}\ \coth\{(s\ z_o^2/D_l)^{1/2}\}. \qquad (3\text{-}8)$$

From the form of Equation 3-8 it is seen that if the rate of surface renewal, s, is small, n approaches 1.0 in accordance with two-film theory. If the rate of surface renewal is large, the hyperbolic cotangent term approaches unity and n converges to a value of 0.5 as predicted by penetration theory. Tracer experiments completed by Dobbins (1964a) indicated that n decreases as speed of mixing, and hence s, increases. Experimental values of n varied from 0.648 to 0.985.

Additional Theories

Dobbins (1964a) reported studies by Russian researchers that led to

$$k_l = 1.13\ \{(D_l + D_I)\ s\}^{1/2}, \qquad (3\text{-}9)$$

where D_I is turbulent diffusivity. For turbulent streams $D_I >> D_l$, and n approaches zero. This theory can not be justified by numerous observations that k_l varies for different chemical species in the same well-mixed liquid sample (Matter-Muller et al., 1981; Roberts et al., 1984; Smith et al., 1980; Tsivoglou and Neal, 1976).

3.3 RELATING TRANSFER COEFFICIENTS BETWEEN COMPOUNDS

Mass transfer rate coefficients for volatile compounds for which resistance to mass transfer is dominated by molecular diffusion in the liquid phase can be related to one another. Matter-Muller et al. (1981) suggested that extrapolation of

transfer coefficients from one compound to another is possible if each compound has a dimensionless Henry's law constant that is greater than 0.1. Differences between transfer coefficients are attributed solely to differences in liquid-phase diffusivities.

The ratio of transfer coefficients of volatile species i and j can be expressed by a dimensionless factor

$$\Psi_{ij} = k_{li}/k_{lj} \quad . \tag{3-10}$$

Thus, k_{li} can be estimated if Ψ_{ij} and k_{lj} have been measured or estimated. Analysis of theoretical dependencies of k_l on D_l indicates that

$$\Psi_{ij} = (D_{li}/D_{lj})^n, \tag{3-12}$$

where n approaches 0.5 at high surface renewal rates and 1.0 at low surface renewal rates.

If diffusion coefficients of two volatile compounds have been measured experimentally under the same set of conditions, the ratio of diffusivities can be obtained directly. If diffusion coefficients are unknown, they can be estimated given solvent viscosity and molecular weight, temperature, molal volume of the solute, and an "association" parameter for the solvent (Welty et al., 1976).

Most studies that have focussed on determination of Ψ_{ij} have used oxygen as species j. For that reason, Ψ_{ij} will hereafter be referred to as Ψ_i, where oxygen is implicitly assumed as volatile species "j". Use of oxygen is considered to be valid, even though most comparisons have been for oxygen absorption and VOC desorption. The characteristic factor that distinguishes rate of oxygen absorption from rate of VOC desorption is molecular diffusivity in the liquid. Transport of a volatile compound into or out of a liquid has been shown to be insensitive to direction of transport (Tsivoglou and Neal, 1976).

Smith et al. (1980) argued that effects of temperature and solvent viscosity cancel upon division of two diffusion coefficients. Therefore, the ratio of diffusivities should remain constant over a wide range of environmental conditions. Their argument was consistent with earlier experimental results which showed that Ψ_i for both krypton and radon varied insignificantly over a wide range of mixing conditions, and temperatures ranging from 10 to 32 ^{o}C (Tsivoglou et al., 1965). Similar results were obtained by Matter-Muller et al. (1981) for PERC in water.

Tsivoglou and Neal (1976) indicated that although k_l may vary significantly, Ψ_i does not vary appreciably over a wide range in temperature, degree of mixing, or presence of pollutants. Smith et al. (1980) observed that for BZ, Ψ_i was independent of temperature within a range of 4 to 50 ^{o}C. They also noted little change in Ψ_i in the presence of surface films, in a salt mixture that approximated sea water, and after addition of components of pond water to fresh water. Similar results were observed for PERC, ethylene, and propane in the presence of surface active agents such as alkylbenzenesulfonates, bactopeptides, and palmitic acid (Matter-Muller et al., 1981).

Roberts et al. (1984) tested several VOCs in both bubble and surface aeration systems. They noted small variations in Ψ_i with changes in temperature, no significant difference in Ψ_i for secondary effluent and tap water, no significant change in Ψ_i following addition of surfactants to clean water, and a 10% increase in Ψ_i after a large increase in degree of turbulent mixing. Batch reactor experiments using PERC indicated that Ψ_i is independent of the type of aeration system, e.g. bubble or surface aeration, and degree and nature of mixing (Matter-Muller et al., 1981). Similarly, Smith et al. (1980) observed that Ψ_i is independent of k_l in the k_l range of 0.05 to 15 hr^{-1}. A summary of measured values of Ψ_i for several VOCs is provided in Table 3-1. For surface aeration, Roberts et al. (1984) concluded that Ψ_i is equal to 0.60 ± 0.06 for many VOCs.

Table 3-1. Experimental Values of Ψ with Respect to Oxygen

Compound	Ψ [-]
BZ	0.53 - 0.56
CT	0.58 - 0.63
MCB	0.61
TCM	0.54 - 0.57
DCE	0.62
PERC	0.52 - 0.55
TCE	0.57 - 0.59
TOL	0.53

References: Smith et al. (1980), Matter-Muller et al. (1981); Roberts et al. (1984)

3.4 OXYGEN TRANSFER MODELS

Many oxygen absorption (reaeration) models have been described in the literature. Several models developed for oxygen transfer to flowing streams, drops, and hydraulic jumps are described below.

Flowing Streams

Most existing reaeration coefficient models are empirical, and based upon data collected for clean water in laboratory flumes or natural waterways. Most models were developed from correlations using mean velocity and mean hydraulic depth of streams (Bennett and Rathbun, 1971; Isaacs and Gaudy, 1968; Owens et al., 1964). Others have incorporated slope of the energy line or channel slope (Bennett and Rathbun, 1971; Churchill et al., 1962). Many existing models are not dimensionally consistent, and empirical coefficients assume awkward dimensions in order to yield transfer coefficients with correct units. Furthermore, the empirical nature of reaeration coefficient models can cause significant errors if conditions to which the models are applied are different than those from which they were derived. Extension of clean water reaeration models to wastewater has required introduction of an empirical factor, a, defined as the ratio of wastewater to tap water transfer coefficients. Errors associated with existing reaeration models have been summarized in the literature (Rathbun, 1977; Wilson and Macleod, 1974).

Five reaeration coefficient models are summarized below. Each model contains some degree of theoretical reasoning or dimensional analysis that distinguishes it from purely empirical models. Development of each model is applicable to all volatile compounds. The oxygen-specific nature of each model stems from incorporation of oxygen diffusivity or regression coefficients based on oxygen data.

One of the first conceptual models for reaeration was developed by O'Connor and Dobbins (1956). They derived a pair of equations based on Equation 3-8 and application of turbulence theory to quantify rate of surface renewal. For non-isotropic turbulence, rate of surface renewal was assumed to equal velocity gradient in a turbulent stream. Velocity profiles were obtained from Von Karman's universal logarithmic velocity law for pipes. The resulting equation was

$$k_l = (480\ D_l^{1/2}\ S^{1/4})/d^{1/4}, \qquad (3\text{-}12)$$

where D_l is liquid-phase diffusivity for oxygen [$ft^2 \cdot hr^{-1}$], S is channel slope [$ft \cdot (1000\ ft)^{-1}$], d is mean depth of flow [ft], and k_l is oxygen transfer coefficient [$ft \cdot day^{-1}$]. Slope appears as a result of its use to quantify shear stress in the logarithmic velocity profile. Equation 3-12 is applicable to shallow flows characterized by large values of bottom shear that give rise to marked velocity gradients. Isotropic turbulence was assumed for deeper channels without significant velocity gradients. Rate of surface renewal was assumed to equal the ratio of mean velocity and mean flow depth. The resulting equation was

$$k_l = ((D_l\ U)^{1/2}/(2.31\ d^{1/2}), \qquad (3\text{-}13)$$

where units of k_l, D_l, and d are identical to those in Equation 3-12, and U is mean velocity [$ft \cdot s^{-1}$]. Dobbins (1964b) noted that Equation 3-13 has been observed to be more reliable than Equation 3-12 for most practical applications.

Dobbins (1964b) developed a reaeration coefficient model based on Equation 3-10. He argued that the source of energy required for production of turbulent kinetic energy, and subsequent mixing, is equal to rate of loss of potential energy, and that the molecular forces which are responsible for surface tension act to oppose surface renewal. Dimensional considerations were used to define energy expenditure to overcome surface forces, and Kolmogoroff similarity theory was used to predict

effective film thickness z_o by assuming a proportionality to smallest eddy size. The following equations for z_o and s result

$$z_0 = c_3 \ (u^3/E_s)^{1/4}, \qquad (3\text{-}14)$$

and

$$s = (c_5/c_4{}^3) * (r \ u^{3/4} \ E^{3/4}/s), \qquad (3\text{-}15)$$

where c_3 and c_5 are dimensionless proportionality constants, c_4 is a dimensionless factor that depends on flow dynamics, u is kinematic viscosity of the fluid $[L^2 \cdot T^{-1}]$, E_s is rate of energy expenditure to overcome molecular forces at a liquid surface $[L^2 \cdot T^{-3}]$, r is liquid density $[M \cdot L^{-3}]$, E is rate of loss of potential energy $[L^2 \cdot T^{-3}]$, and s is surface tension $[M \cdot T^{-2}]$. Equations 3-14 and 3-15 were substituted into Equation 3-8 to yield

$$k_1 = \{(0.12 \ c_A \ A \ E^{3/8} \ \coth(B \ E^{1/8}/c_4{}^{1/2})\}/c_4{}^{3/2}, \qquad (3\text{-}16)$$

where,

$$c_A = 1.0 + F^2, \qquad (3\text{-}17)$$

$$c_4 = 0.9 + F, \qquad (3\text{-}18)$$

$$A = 9.68 + 0.054 \ (T - 20 \ ^oC), \qquad (3\text{-}19)$$

$$B = 0.976 + 0.0137 \ (30^oC - T)^{3/2}, \qquad (3\text{-}20)$$

$$E = 30.0 \ S \ U, \qquad (3\text{-}21)$$

$$F = U \ (g \ d)^{-1/2}, . \qquad (3\text{-}22)$$

and U is mean velocity $[ft \cdot s^{-1}]$, S is slope of the energy line $[ft \cdot (1000 \ ft)^{-1}]$, d is depth [ft], T is temperature $[^oC]$, g is gravitational acceleration $[ft \cdot s^{-2}]$, and B is a dimensional constant $[s^{3/8} \cdot ft^{-1/4}]$. The product of 0.12 and A $[L^{1/4} \cdot T^{1/8}]$ is corrected to yield k_1 in units of $[ft \cdot day^{-1}]$. The terms 0.12, A, and B account for molecular diffusivity of oxygen, proportionality constant c_5, density and kinematic viscosity of water, and surface tension. The term c_A is a factor that accounts for

increased interfacial area in the presence of surface disturbances such that

$$A_S = c_A A_0 \ , \qquad (3\text{-}23)$$

where A_S is actual surface area, and A_0 is interfacial area based upon an undisturbed surface.

Equation 3-18 was one of the first reaeration models to relate transfer coefficients to rate of dissipation of potential energy. That relationship served as the basis for several later models (Cadwallader and McDonnell, 1969; Tsivoglou and Neal, 1976; Tsivoglou and Wallace, 1972).

Lau (1972) proposed a transfer coefficient model based on consideration of a set of dimensionless groups. In addition to hydraulic characteristics such as mean flow velocity, liquid density, liquid viscosity, and hydraulic radius, he considered roughness and turbulence characteristics of channels. The latter were assumed to be accounted for in a friction (shear) velocity term. Transfer coefficient was analyzed using the Buckingham Pi theorem to yield

$$k'_1 \cdot R/U = f\{(U \cdot R \cdot r/m), (D_m \cdot r/m), (U_*/U), (w/R)\}, \qquad (3\text{-}24)$$

where r is liquid density $[M \cdot L^{-3}]$, m is absolute viscosity of a liquid $[M \cdot L^{-1} \cdot T^{-1}]$, U is mean flow velocity $[L \cdot T^{-1}]$, R is hydraulic radius [L], U_* is friction velocity $[L \cdot T^{-1}]$, D_m is molecular diffusivity in liquid $[L^2 \cdot T^{-1}]$, and w is surface width [L]. The author neglected gravitational acceleration based on reasoning that effects of wave action on reaeration are not appreciable for a stream. Nevertheless, Dobbins (1964b) included a Froude number based on his experiments. The term k'_1 was taken to be the transfer coefficient per unit depth (ratio of k_1 to hydraulic radius or mean hydraulic depth). The first term in parentheses is Reynolds number (Re) and the second term is the Schmidt number (Sc).

Lau (1972) used data which were available in the literature to investigate effects of each dimensionless group. He observed that variations in Re had no effect on transfer coefficients for Re greater than 2000. Variations in width-to-depth ratio had no appreciable effect on the transfer coefficient. Effect of Sc could not be ascertained because of its relatively small range of values. The only term which had a significant effect on transfer coefficient was the term including friction velocity. Furthermore, it was observed that substitution of hydraulic radius for mean hydraulic depth had no effect on the analysis. From these observations Lau proposed the model

$$k_l = 0.0126\ (U_*^3/U^2). \qquad (3\text{-}25)$$

Units used in Equation 3-25 must be consistent, and the transfer coefficient assumes the same units as mean velocity of the stream. Conditions for which Equation 3-25 was developed were a temperature of 20 ^{o}C, width-to-hydraulic depth ratio of 6 to 290, Re of 2000 to 2000000, and friction-to-mean velocity ratio of 0.06 to 0.25. Lau (1972) argued that these conditions are commonly met in all but small streams with depths of only two to three feet, mean flow velocities of less than 0.5 ft$\cdot$s^{-1}, and friction-to-mean velocity ratios of greater than 0.25.

Tsivoglou and Neal (1976) proposed a model of the form

$$(k_l/d) = k'_l = c_e\ (D_h/t_f), \qquad (3\text{-}26)$$

where k_l is the transfer coefficient [m$\cdot$s^{-1}], c_e is an empirical "escape" coefficient [m^{-1}], D_h [m] is the change in water surface elevation between two locations A and B in a flowing stream, and t_f [s] is mean transport time between A and B. For flow without pooling, falls, or non-uniformities in depth, the ratio of D_h to t_f is simply the product of mean flow velocity and channel slope (US).

To estimate an escape coefficient for oxygen, Tsivoglou and Neal (1976) analyzed results of over 500 field tracer measurements. Streams that were tested had flows that varied from 0.006 to 85 $m^3 \cdot s^{-1}$, temperatures that varied from 3 to 35 ^oC, and five day BODs ranging from 1 to 100 $mg \cdot L^{-1}$. It was observed that c_e was inversely proportional to flow rate. Low values of c_e were associated with streams that were characterized by large, deep, unobstructed, and straight channels (uniform in slope and cross-sectional geometry). A summary was provided for average values of c_e during high and low flow conditions. For flow rates greater than 0.7 $m^3 \cdot s^{-1}$, a value of 0.177 m^{-1} was suggested for c_e at a temperature of 20 ^oC. The range of c_e values was 0.036 to 0.387 m^{-1}, with 80% of the results lying between 0.1 and 0.26 m^{-1}. It was also suggested that c_e be adjusted to limiting values of 0.08 to 0.10 m^{-1} for flowrates above 8.5 $m^3 \cdot s^{-1}$, and for heavily polluted streams. For streams with flows less than 0.28 $m^3 \cdot s^{-1}$, c_e was observed to exceed 0.3 m^{-1}, adjusted downward to 0.2 m^{-1} for heavily polluted water. Variations in c_e led Tsivoglou and Neal (1976) to describe it as a mixing coefficient that relates mass transfer to surface renewal. It was noted that c_e is affected by hydraulic features that influence quality and intensity of mixing, e.g. changes of slope.

Only one model was found in the literature for the prediction of oxygen absorption in sewers. Parkhurst and Pomeroy (1972) developed a reaeration model based on tests in 12 operating sewers in Los Angeles County. To overcome complications added by biological activity, oxygen balances on wastewater were completed after "shock" treating sewers with caustic soda. A continuous dose of hypochlorite was added during tests. Dissolved oxygen content was monitored at upstream and downstream ends of selected sewer reaches. Wastewater flow rate, velocity, depth, and temperature were also measured, along with oxygen concentration in the gas phase above the wastewater. The resulting equation was

$$k_l = 0.96\ (1 + 0.17\ F^2)\ g\ (SU)^{3/8}, \qquad (3\text{-}27)$$

where k_l is the transfer coefficient for oxygen [$m \cdot hr^{-1}$], S is slope of the energy gradient [$m \cdot m^{-1}$], and U is average velocity of wastewater [$m \cdot s^{-1}$]. The term g is a temperature correction factor, and F is the Froude number as defined by Equation 3-24. The term $(1 + 0.17\ F^2)$ is a correction for increased interfacial area resulting from surface disturbances.

Free-Falling Water

Interfacial mass transfer can occur as a result of free-falling water. Examples in sewers include drop manholes, drops into pump station wet wells, and pressurized force mains discharging to gravity-flow sewers. Mass transfer can occur during the fall, as a result of splashing or agitation at the surface of a receiving pool, or by transport into or out of air bubbles which become entrained in a receiving pool. It has been observed that entrained air can account for greater than 95% of mass transfer for streams falling freely into receiving pools (Nakasone, 1986). An important variable is retention time of entrained air bubbles, which can be influenced by size and shape of a receiving pool, as well as characteristics of jet entry into a receiving pool Ψ e.g. discharge rate, fall height, downstream pool depth, shape of falling jet (Apted and Novak, 1973).

Factors which affect mass transfer include energy loss, discharge rate, receiving pool geometry, channel width, and jet shape. Energy loss of a falling stream is described by drop height. However, if either the depth of a receiving pool decreases or jet penetration increases, mechanisms for energy loss will vary, and drop height may not be a sufficient variable to correlate with turbulent mixing and mass transfer (Apted and Novak, 1973). Discharge rate is important as it affects depth to which a falling stream penetrates a receiving pool, a condition that affects retention time of entrained air bubbles. Similarly,

depth of a receiving pool limits the depth of bubble penetration and, hence, air contact time (Apted and Novak, 1973). Avery and Novak (1978) noted that mass transfer increases as pool depth increases until an "optimum" depth is reached which maximizes bubble contact time. Nakasone (1986) noted that channel width can affect mass transfer as a large fraction of entrained air bubbles originate at the outer edges of a stream impacting the surface of a receiving pool. Avery and Novak (1978) also suggested that jet shape affects the quantity of entrained air. However, no work has been completed to assess the significance of channel width or jet shape in terms of mass transfer.

Equations developed to predict mass transfer for falling streams have focused on oxygen transfer for clean water flowing over weirs. Existing equations are highly empirical, relying on regression analyses using laboratory or field data to correlate drop height, discharge, and/or pool depth to the dimensionless ratio

$$r_{O2} = \{(C_S - C_1)/(C_S - C_2)\}, \qquad (3\text{-}28)$$

where r_{O2} is referred to as the depletion ratio [-], and C_S, C_1, and C_2 are saturation, upstream, and downstream concentrations of oxygen, respectively [$mg \cdot L^{-1}$]. Using previous arguments to relate transfer coefficients for two volatile compounds it can be shown that

$$r_i = r_{O2}^{a\Psi}, \qquad (3\text{-}29)$$

for VOC "i", and "a" is the transfer coefficient ratio between wastewater and tap water, as defined previously. Methods to estimate r_{O2} are reviewed below. An important caveat is that all available transfer models were developed for solid (as opposed to disintegrated) jets impacting downstream surfaces.

Gameson (1957) and Gameson et al. (1958) conducted extensive field studies of oxygen transfer over river structures and proposed the equation

$$r_{O2} = 1 + 0.11\ a\ (1 + 0.046\ T)\ h, \qquad (3\text{-}30)$$

where "a" is a coefficient dependent upon the quality of water, T is liquid temperature in ^{o}C, and h is drop height in feet. Gameson (1957) suggested values of "a" ranging from 1.25 in slightly polluted water to 0.85 in treated wastewater effluent. However, later researchers observed that the effects of contaminants present in the liquid on mass transfer to entrained air bubbles in turbulent streams is insignificant, and may even increase mass transfer if pollutants limit bubble growth (Avery and Novak, 1977).

Avery and Novak (1977 and 1978) completed extensive experimental work to analyze oxygen transfer caused by flow over weirs. Their work led to the following two equations at 15 ^{o}C:

$$r_{O2} = p_3 \left(0.0110 \, Fr_j^{1.79} \, Re^{0.53} \right), \qquad (3\text{-}31)$$

and

$$r_{O2} = 1 + p_5 \, Fr_j^{1.78} \, Re^{0.53} , \qquad (3\text{-}32)$$

where the dimensionless coefficients p_3 and p_5 were observed to be 0.0057 and 0.0000627 in tap water. Reynolds number was evaluated as

$$Re = (q_j/\nu), \qquad (3\text{-}33)$$

where ν is kinematic viscosity of water $[m^2 \cdot s^{-1}]$, and q_j is equal to discharge per unit jet perimeter at impact $[m^2 \cdot s^{-1}]$. Discharge was calculated as

$$q_j = R \, (2 \, g \, h)^{1/2}, \qquad (3\text{-}34)$$

where R is the hydraulic radius of a jet at impact [m], and g is gravitational acceleration $[m \cdot s^{-2}]$. The jet Froude number at point of impact was given as

$$Fr_j = (g \, h^3/2 \, q_j^2)^{0.25}. \qquad (3\text{-}35)$$

Although Equations 3-31 and 3-32 have been successfully applied to a number of prototype structures, their use is valid only for pool depths (Y) such that

$$Y > 7.5\ (h^{0.58}/Fr_j^{0.53}), \qquad (3\text{-}36)$$

where Y has units of centimeters when h is expressed in meters.

While Gameson (1957 and 1958) accounted only for fall height, and Avery and Novak (1977 and 1978) accounted for fall height and discharge, Nakasone (1986) was the first to develop an equation incorporating receiving pool depth. It was based upon an analogy with bubble aerators, data from laboratory tests with horizontal pool bottoms, and field tests of weirs placed in rivers. The form of Nakasone's equation at 20 ^{o}C is

$$\ln (r_{O2}) = C_a\ h^n\ q^B\ Y^{0.31}, \qquad (3\text{-}37)$$

where the units of h and Y are [m], q is [$m^2 \cdot hr^{-1}$] (discharge per meter width of weir). Nakasone selected the values shown in Table 3-2 for the dimensionless coefficients. A caveat is that for Y > 2/3 h, Y should be set equal to 2/3 h in Equation 3-37, i.e. aeration efficiencies remain stable for tailwater depths greater than 2/3 h.

A correction for temperatures other than 20 ^{o}C was provided by Gameson et al. (1958):

$$\ln (r_T) = \ln (r_{20\ oC})\ \{1 + 0.0168\ (T - 20\ ^{o}C)\}. \qquad (3\text{-}38)$$

Equation 3-38 is empirical and based on experimental data that should have accounted for several factors affecting oxygen transfer, e.g. solubility and molecular diffusivity. Changes in

Table 3-2. Coefficients for Nakasone's Equation of Oxygen Transfer Over Weirs

Conditions				
h [m]	q [m^3 h^{-1} m^{-1}]	C_a	n	B
< 1.2	< 235	0.0785	1.31	0.428
> 1.2	< 235	0.0861	0.816	0.428
< 1.2	> 235	5.39	1.31	-0.363
> 1.2	> 235	5.92	0.816	-0.363

Reference: Nakasone (1986)

diffusivity should have similar effects on oxygen absorption and VOC desorption, i.e. increasing diffusivity increases both oxygen absorption and VOC desorption. However, an important caveat is that solubility changes should have opposite effects on oxygen absorption and VOC desorption. Therefore, use of Equation 3-38 to correct for the effects of temperature changes on VOC desorption is not recommended. No other temperature relationships for drops were found in the literature.

Pincince (1989) completed field studies of dissolved oxygen concentrations upstream and downstream of clarifier weirs. Multiple linear regression was used to determine best-fit coefficients for data, assuming a relationship similar in form to Equation 3-37. For primary clarifiers the values of C_a, n, and B, in Equation 3-37 were observed to be 0.042, 0.872, and 0.509, respectively. For secondary clarifiers the values were 0.077, 0.623, and 0.66, respectively. Unlike the Nakasone model, oxygen transfer was observed to be insensitive to pool depth. However, Pincince noted that for clarifier weirs wastewater usually trickles down the wall of the clarifier to the channel flow, unlike free-fall conditions described by Nakasone.

Hydraulic Jumps

Although sewers are designed to avoid rapid energy dissipation, hydraulic jumps can occur where channel slopes are suddenly decreased. Early equations for oxygen uptake at jumps were based on correlations using energy loss or changes in kinetic energy of a flowing stream (Apted and Novak, 1973; Holler, 1971). Avery and Novak (1977) later described the importance of entrained air bubbles and bubble contact time in terms of Reynolds number and supercritical Froude number. They provided the following equation, valid for discharges between 145 and 710 $cm^2\ s^{-1}$ and at a temperature of 15 ^oC:

$$r_{O2} = 1 + p\ Fr_s^{2.1}\ Re^{0.75}, \qquad (3\text{-}39)$$

where p is 1.0043×10^{-6} for tap water, Re is Reynolds number as described previously, and Fr_s is the supercritical Froude number

$$Fr_s = (v_1/(g\ y_1)^{1/2}), \qquad (3\text{-}40)$$

where v_1 and y_1 are supercritical velocity and depth, respectively.

Other Areas of Turbulence

Models have not been reported for mass transfer at pipe bends, confluence of two or more wastewater streams, or other areas associated with increased turbulent mixing or splashing of wastewater. As described for uniform reaches, drops, and jumps, such models might include correlation of parameters associated with energy loss, i.e. head loss, rate of energy dissipation, i.e. head loss per unit time, or bubble entrainment. Analogies could then be drawn with models presented in Section 3.4 to estimate effective reach lengths or drop heights for estimating volatilization losses.

3.5 FACTORS AFFECTING INTERFACIAL TRANSFER OF VOCs

Numerous factors can affect partitioning of VOCs. Mass transfer rate coefficients are dependent upon factors that affect rate of surface renewal or diffusivity of solutes. The transfer coefficient, as well as any factors that affect liquid and gas-phase concentrations of a species, and the interfacial area affect transfer rates.

Characteristics of solute

The physico-chemical properties of VOCs vary, thus they have different tendencies to volatilize under similar environmental conditions. A review of physico-chemical properties that affect volatilization in sewers was provided by Matthews (1975). Parameters include solubility, pure compound vapor pressure, diffusivity, and Henry's law constant of the contaminant.

Theories discussed earlier indicate that mass transfer rate constants are proportional to diffusivity raised to a power between 0.5 and 1.0.

As indicated by Equation 3-1, an increase in aqueous-phase concentration of a chemical increases mass transfer rate, all other factors being equal. Thus, for the same amount of mass discharged to a system, emissions will be higher during periods of low wastewater flow when dilution is not as significant as during periods of high flow.

Wastewater characteristics

Characteristics of wastewater that can affect interfacial mass transfer include water temperature and presence of surfactants and other impurities that act to enhance or retard transfer processes.

Tests completed in sewers of several cities in southern California indicated wastewater temperatures ranging from 20 to 28 ^{o}C, with an average of 24.5 ^{o}C (USEPA, 1974). Values of H_C and D_l vary with temperature, each increasing with an increase in temperature. Since k_l is proportional to D_l to a positive power, an increase in temperature also increases k_l. The effect of temperature on transfer coefficients was described by Daniil and Gulliver (1988). Gossett (1987) presented regression equations for the temperature dependence of Henry's law constant for 13 VOCs, and Nirmalakhandan and Speece (1988) used quantitative structure-activity relationship (QSAR) techniques to develop models which can be used to estimate Henry's law constants for a wide range of chemicals. A more complete description is contained in Appendix H of Volume IV.

Surface active agents, or surfactants, are compounds that when dissolved in a solvent, adsorb onto interfaces between liquid and a solid, liquid and liquid, or liquid and gas. Effects of surfactants at air-water interfaces have been

described in the literature (Backman et al., 1987; Hiemenz, 1977; Sherwood et al., 1975). It is generally agreed that surfactants, even in small amounts, reduce mass transfer by concentrating at a liquid phase boundary causing marked reductions in surface tension (Backman et al., 1987; Sherwood et al., 1975). Principal effects of surfactants on mass transfer processes have been described as; 1) formation of a more hydrodynamically stable interface with a reduction or elimination of fine-scale surface motion, and 2) introduction of an additional surface resistance to mass transfer (Sherwood et al., 1975).

Effects of surfactants on mass transfer of volatile compounds have been documented through laboratory and field experiments. Smith et al. (1980) observed that for several VOCs in clean water, k_l was reduced by as much as a factor of two in the presence of some surfactants. Frexes et al. (1984) summarized laboratory studies that showed substantial reductions in k_l in the presence of chemical or biological films at a water surface. Rathbun (1977) described reduction of K_T for oxygen in clean water in the presence of detergents. However, addition of nitriloacetic acid had no effect, and mineral oil actually increased reaeration rate during laboratory experiments. The same author noted higher reaeration rates in the Chattahoochee River on weekends, when discharges from municipal wastewater treatment plants were lower than on weekdays. Experiments by Roberts et al. (1984) indicated that transfer coefficients for several VOCs were 10 to 15% lower in filtered wastewater effluent than in clean water. Parkhurst and Pomeroy (1972) reviewed several studies regarding effects of impurities on reaeration of water. Addition of 25% sewage to tap water reduced reaeration rate by 66%. They described other studies showing little effect on K_T for oxygen in tap water after addition of thin oil films, a foam suppressor, and secondary effluent from a municipal wastewater treatment plant. They also reviewed a study which indicated that addition of synthetic anion surfactants (concentrations of 0.6 to 3.5 $mg \cdot L^{-1}$) to clean water had little

effect on high values of K_T for oxygen. However, surfactants reduced low values of K_T by as much as 40%. Results of the latter study were consistent with findings that suppression of transfer rates in the presence of surfactants may be negligible under conditions of high intensity mixing (Backman et al., 1987). For such conditions, short liquid contact times do not allow surfactant diffusion and formation of a surfactant layer at an interface (Sherwood et al., 1975).

For water with a high ion concentration, transfer of VOCs from liquid to gas may be enhanced by an increase in vapor pressure. The "salting-out" action can be expressed as an increase in apparent aqueous-phase concentration, or activity, with respect to actual concentration in solution. The ratio of apparent to actual concentrations is referred to as the activity coefficient γ, which can be related to ionic strength I of a solution by the empirical expression

$$\log(\gamma) = k_S I, \qquad (3\text{-}41)$$

where k_S is a salting-out coefficient for nonelectrolytes (Snoeyink and Jenkins, 1980). Snoeyink and Jenkins (1980) noted that k_S generally falls in the range of 0.01 to 0.15. Ionic strength, I [mol L^{-1}] can be estimated from total dissolved solids content (TDS) or specific conductance of the water by

$$I = 2.5 \times 10^{-5} \text{ TDS}, \qquad (3\text{-}42)$$

or

$$I = 1.6 \times 10^{-5} \text{ q}, \qquad (3\text{-}43)$$

where TDS has units of [$mg \cdot L^{-1}$], and q is specific conductance [$\mu mhos \cdot cm^{-1}$]. Using a high value of k_S equal to 0.15 and a typical TDS concentration of 500 $mg \cdot L^{-1}$ for domestic wastewater (Tchobanoglous and Schroeder, 1985), the value of γ predicted using Equations 3-44 and 3-45 is 1.004. Thus, enhancement of VOC emissions from ionic species in domestic wastewater is predicted to be less than 1% greater than from most tap waters. Enhance-

ment might be more significant for industrial wastewaters with higher ionic strengths. Little is known regarding the impact of dissolved non-ionic species on mass transfer, however it is likely that they also increase solution phase activity, but the effect is also probably small.

Flow Characteristics

Wastewater flow affects interfacial mass transfer through mixing characteristics, depth over which species must be mixed, and interfacial area available for the transfer process. Several authors have noted the importance of hydrodynamic mixing characteristics on mass transfer (Dobbins, 1964b; Krenkel and Orlob, 1962; Tsivoglou et al., 1965; Lau, 1972). Mixing is most often described in terms of rate of energy dissipation (Dobbins, 1964b; Tsivoglou and Neal, 1976). Dobbins (1964b) and Tsivoglou et al. (1976) described the dependence of liquid film thickness on degree of turbulent mixing. Lau (1972) noted that the rate of surface renewal is related to turbulent mixing characteristics near air-water interfaces. Krenkel and Orlob (1962) suggested that mass transfer does not depend solely on how much energy is imparted to an aqueous system, but also on how energy is distributed and ultimately dissipated. They argued that system geometry of must also be considered. Parkhurst and Pomeroy (1972) suggested that it is possible to have sheltered regions of flow away from a surface where a disproportionate amount of energy dissipation occurs. However, they argued that such effects are minimized for regular cross-sections such as sewer channels.

A summary of reaeration and energy dissipation in sewers has been presented (USEPA, 1974). It was noted that reaeration is reduced as wastewater is conveyed from small collecting sewers to larger lines, during which time channel slope typically decreases and depths of flow increase. It was argued that for high flows, at low slope and large depths, effects of junctions and other

points of significant turbulence are more important for reaeration than they are for normal flows. A positive correlation between energy dissipation and sulfide build-up in sewer gases was observed, especially near drops or falls and other locations of high turbulence which enhance interfacial partitioning. Increases in mixing may also occur at changes in channel slope leading to surface drawdown or a hydraulic jump. Depth changes occur at areas where pipe diameter is enlarged. However, most collection systems are designed to avoid rapid changes in surface elevation which can lead to release of corrosive gases. Other areas of increased turbulence or splashing include line connections (intersecting flows), curves or changes in direction of pipe flow, and drops encountered in drop manholes or wastewater entry into lift-station wet wells. A few examples of sewer structures are provided in the Appendix for those readers unfamiliar with their physical geometry.

A factor that further complicates estimation of mass transfer is the presence of erratic surface motions or ripples at an interface. Such motion can cause an increase in mass transfer rate by enhancing mixing, as well as increasing interfacial area. Interfacial turbulence can be caused by turbulence in bulk fluid and the action of turbulent eddies near a gas-liquid interface. Scriven and Pigford (1958) indicated that strong surface dilation and contraction at a fluid interface can substantially increase mass transfer. In sewers, surface ripples might be caused by turbulence generated at pipe walls in the region near a liquid surface. Increases in interfacial area were accounted for by introduction of an area correction factor in models proposed by Dobbins (1964b) and Parkhurst and Pomeroy (1972). Each correction factor was empirical, and proportional to the square of the Froude number.

The relationship between depth and interfacial area, and their combined effects on mass transfer across an interface, differ depending on whether relative depth is less or greater

than 0.5. As depth increases there is a tendency to reduce rate of mass transfer. For relative depths of less than 0.5, an increase in depth is associated with an increase in interfacial area over which mass transfer occurs. The opposite is true for relative depths greater than 0.5.

Transient Conditions of a Collection System

Several factors described above vary with location in a collection system as a result of changes in channel or discharge characteristics. In addition to spatial variations, all of the factors vary to some extent with time. Temporal variations, or transient conditions, can be classified as short term, diurnal, weekday-weekend, seasonal, and long term.

a) Short-term variations occur over periods of a few hours or less. An example is change in flow rate, which affects wastewater depth, interfacial area, energy dissipation, and time of transport in a collection system.

b) Diurnal variations occur over a twenty-four hour cycle. Examples include diurnal variations in flow rate, as well as reductions in ambient temperature at night. The latter enhances buoyancy-driven ventilation.

c) Some factors may change significantly from weekday to weekend. Flow rate patterns may be quite different, in accordance with differences in industrial or domestic activities.

d) Seasonal variations occur on the order of months. They generally result from changes in discharger activity or environmental conditions. Examples include changes in ambient temperature and wind speeds that affect ventilation, and discharge characteristics of contaminants as a result of seasonal industries.

e) Long-term variations occur on the order of years. Examples include changes in wastewater flow rate as population and industrial input changes, in make-up of industrial and commercial dischargers, and in the condition of a collection system, e.g. changes in roughness, slope, infiltration.

3.6 COMPETING REMOVAL MECHANISMS

Several mechanisms can influence VOC emissions from sewers by changing VOC concentration in the aqueous phase, or consuming VOCs in the gas phase. There is a complete lack of information regarding such mechanisms for VOCs in sewers. However, analogies with other systems lends insight to the potential importance of such mechanisms.

Chemical Reactions in Wastewater and Sewer Atmospheres

Most VOCs are not appreciably affected by photolysis or hydrolysis in aqueous systems. This is particularly true for photolysis in dark sewer environments. However, growing evidence of trihalomethane (THM) formation following chlorination of both raw and treated wastewater suggests the potential for such formation in sewers given the presence of available chlorine, e.g. from household bleach use. The presence of reduced inorganic species and ammonia may significantly inhibit THM formation as they out-compete THM precursors for free chlorine in the process of oxidation or forming chloramines.

Based on a lack of ultraviolet radiation in sewers and reported reaction rates for highly reactive VOCs such as TOL (Finlayson-Pitts and Pitts, 1986), time scales for chemical reactions in sewer atmospheres are expected to be too long for significant losses from that mechanism.

Adsorption in Wastewater

Matthews (1975) suggested that halogenated hydrocarbons can become trapped in sewer detritus which workers may disturb with their feet, thus releasing accumulated compounds. However, recent studies have indicated that most VOCs do not have a great affinity for adsorption to solid particles or biomass (Melcer et al., 1989; Petrasek et al., 1983; USEPA, 1986a).

One parameter used to assess a compound's relative affinity for sorbing to particles is the octanol/water partition coefficient (Table 2-2). Blackburn et al. (1985) developed a model for estimating equilibrium solute concentration after exposure of organic compounds to biomass. Petrasek et al. (1983) developed an empirical expression for first-order adsorption rate constants for VOCs exposed to biomass. However, both the Blackburn and Petrasek models were based on assumptions or experiments in which sorption was the sole removal mechanism. Furthermore, solids had different characteristics, e.g. smaller size and higher mass concentration than are expected in most sewers. A more appropriate analogy is sorption in primary sedimentation systems where non-viable particles dominate. Furthermore, hydraulic detention times in many sedimentation systems are on the order of hours, which is consistent with one to ten mile transport in a sewer with wastewater mean velocities of 0.5 to 1.0 $m \cdot s^{-1}$. Dobbs et al. (1989) completed experiments which indicated a rapid approach to sorption equilibrium (approximately one hour) for several organic compounds including DCM, MCB, CT, TCM, DCE, and PERC exposed to primary sludge, mixed-liquor solids, and digested sludge.

To study relative removal from sedimentation systems, VOCs were ranked in order of descending octanol/water partition coefficient (K_{OW}) and compared with estimated removal in sludge streams. Results are summarized in Table 3-3. The EPA partition fractions are suggested average values based on Henry's law constant and octanol/water partition coefficient. The values reported by Chang et. al (1987) were based on mass balances on data compiled in a USEPA data base (USEPA, 1982) for combined removal from primary and secondary sludge streams. The only clear trends are relatively high sorption fractions for ETBZ, MCB, and TOL, and low adsorption fractions for CT, DCE, PERC, and VC. High adsorption fractions compare positively with high octanol/water partition coefficients. However, sorption correlation with K_{OW} is not supported by PERC, CT, and DCM. With

the exception of ETBZ (fraction removal ranging from 0.04 to 0.33), most VOCs listed in Table 3-3 have maximum fractional adsorptions of 0.15, with some reported values considerably lower. Dobbs et al. (1989) developed partition coefficients for individual VOCs exposed to primary sludge, mixed-liquor solids, and digested sludge. Variations between coefficients were small after coefficients were normalized by percent of organic carbon content in solids. After accounting for organic carbon content, measured partition coefficients were observed to be highly correlated with K_{ow} (correlation coefficient of 0.99). Similar experimental results were reported for the less-volatile compounds lindane, diazinon, pentachlorophenol, and 2-chlorobiphenyl (Tsezos and Bell, 1989).

The degree of reversibility of sorption of VOCs has not been extensively reported in the literature. If VOC adsorption to particles in wastewater is reversible, it is conceivable that dynamic adsorption/desorption in sewers occurs as VOC concentrations in the wastewater change with time. Tsezos and Bell (1989) studied adsorption and desorption of lindane, diazinon, pentachlorophenol, and 2-chlorobiphenyl by living fungus cells (R. arrhizus) and activated sludge. Sorption reversibility varied by compound and type of solid. Sorption was observed to be completely reversible for lindane on fungus. However, sorption was only partially reversible for other compound-biomass combinations.

Biological Degradation in Wastewater and Sewer Atmospheres

Moisture that accumulates on sewer walls can serve as a medium for gas absorption. Aerobic bacterial degradation can subsequently occur. However, unless bacterial action is so rapid that the walls approximate a perfect sink, VOC mass accumulation in thin liquid films of low volume would lead to negligible mass removal.

Table 3-3. Sludge Stream Partition Fractions

Compound	Log_{10} (K_{ow})	EPA Partition Fraction[a]	Bishop Removal Factors (primary)[b]	UCD Combined Removal Factors[c]
ETBZ	3.15	0.15	0.33	0.04
PERC	2.88	0.04	nr	0.04
MCB	2.84	0.15	0.11	0.05
TOL	2.69	0.15	0.09	0.10
CT	2.64	0.04	< 0.01	0.04
TCE	2.29	0.04	0.18	0.04
TCA	2.17	0.15	nr	< 0.01
BZ	2.13	0.15	0.16	0.01
DBCM	2.09	0.08	nr	nr
TCM	1.97	0.14	< 0.01	< 0.01
BDCM	1.88	0.14	nr	< 0.01
DCE	1.48	< 0.01	nr	< 0.01
DCA	1.48	0.14	nr	0.01
DCM	1.25	0.14	0.03	0.08
VC	0.60	< 0.01	nr	0.01
AN	-0.14	0.10	nr	nr

a: USEPA (1986a)
b: Bishop (1982)
c: Chang et al. (1987)
nr: not reported

Generally, raw wastewater is aerobic only in small sewers (less than 0.5 m i.d.) with mean flow velocities greater than 0.6 $m \cdot s^{-1}$ (USEPA, 1974). For larger systems dissolved oxygen levels tend toward zero, and biological activity in bulk fluid and slime layers which occur along wetted walls is anoxic or anaerobic.

Although little is known regarding anaerobic degradation of VOCs, there is growing evidence to suggest breakdown of chlorinated compounds such as PERC to form less chlorinated compounds such as TCE, DCE, and VC (Bouwer and McCarty, 1983). While VC is infrequently detected in influent streams to wastewater treatment facilities, it has been observed at high concentrations in anaerobic digester gas (California Air Resources Board, 1985).

There is still much to learn regarding anaerobic breakdown of VOCs, and obvious differences between anaerobic digesters and sewers precludes a direct analogy between the two systems. Still, anaerobic degradation can not be ruled out as a potential VOC loss (or formation) mechanism in sewers, since anaerobic degradation rates under sewer conditions are not known. Important characteristics that should affect such losses or gains include presence, area, and microbial characteristics of a slime layer, characteristics of individual VOCs, and rate at which VOCs come in contact with a slime layer.

4. THEORETICAL DEVELOPMENT: SEWER VENTILATION

Studies of ventilation of collection systems have focused on control of pipe corrosion, release of odorous gases, accumulation of explosive gases, and maintenance of a safe environment for sewer workers. Natural ventilation received its greatest attention when modern collection systems were first developed. The primary concern at that time was the unknown health impacts of public exposure to "sewer gases" (Adams, 1880).

The diversity and physical complexity of wastewater collection systems have been major obstacles to successfully quantifying factors that affect their ventilation. Consideration of ventilation during design of collection systems has developed into something of an "art-within-engineering." This section is intended to summarize information regarding locations where gas exchange between ambient and sewer atmospheres can occur, and to provide a review of existing knowledge related to factors that affect sewer ventilation.

4.1 POINTS OF GAS EXCHANGE WITH THE AMBIENT ATMOSPHERE

Openings which allow for gas exchange between sewer and ambient atmospheres vary in number among collection systems, as well as among portions of the same system. A large number of openings can lead to high ventilation rates and well-distributed (spatially) ventilation. A paucity of openings may restrict ventilation and lead to gaseous emissions at relatively few, discrete locations. Locations of openings and their effects on ventilation can be important for deciding how to characterize an emission source for input to atmospheric dispersion models, for describing risks posed by the source, and for assessing potential control strategies. The most numerous locations for gas exchange in sanitary collection systems are manhole covers and vents associated with gas relief from building connections. Combined

sanitary/storm sewers also include large openings which serve as gutter drains.

Collection systems are typically designed to provide manholes at changes in pipe diameter, slope, or direction for sewer pipes with diameters less than 1.2 m (48 inches). The need to access and clean sewers necessitates a maximum manhole separation of less than approximately 150 m. For pipes with diameters greater than 1.2 m, easier access through the system allows for manhole spacings of up to 500 m, e.g. in large interceptors.

Manhole covers usually have a pick hole for removing the cover. The effective diameter of pick holes is up to 2.5 centimeters (one inch), and additional holes with diameters of approximately one inch are often found in manhole covers. These "finger holes" serve the purpose of providing ventilation to combat production and accumulation of hydrogen sulfide gas and subsequent odor and corrosion problems, to reduce concentrations of explosive and asphyxiating gases which can accumulate in sewer atmospheres, and for infiltration of storm water in combined sewers. Paradoxically, finger holes can serve as passageways for odorous and toxic gases to the ambient atmosphere, or inflow of unwanted storm water. For these reasons, the area available for gas exchange through manhole covers in sanitary sewers is often minimized, e.g. by plugging finger holes. For sanitary sewers it is common to observe between zero and four holes per cover.

Flow of gases upstream of an inverted siphon or wet well is often blocked from the downstream section. Inverted siphons and wet wells are sometimes equipped with a gas bridging pipe allowing for gas transport from the upstream to downstream section. However, most systems simply vent the gases. Perforated manhole covers or ventilation stacks are used for that purpose. In the case of wet wells, changes in wastewater depth due to intermittent pumping leads to gas displacement and an enhancement of ventilation. Blowers may also be used, typically on an intermittent basis, to assure worker safety in or near wet wells.

Building connections are used to convey waste from a building to collector pipe. Building connections usually consist of pipes with diameters of four to six inches. Gases within the sewer are capable of diffusing up building connections. In the event of leakage, this phenomenon can pose an explosion or health hazard to building occupants. Early observations of odorous gases emanating from household plumbing led to the practice of providing main traps on house sewers external to a building structure. However, pressure changes in collection systems, either above or below atmospheric, often broke main trap seals and sometimes broke seals of traps on fixtures within buildings (Babbitt and Baumann, 1958). Main traps were abandoned when it was realized that flow through building vents served as an important mechanism for sewer ventilation.

The number of vent stacks varies from building to building. For detached residential dwellings, a general rule of thumb is that the maximum number of stacks will correspond to the number of points of discharge to a sewer. However, the same vent stack may be used for adjacent fixtures. Pipes that are commonly used today as vent stacks have diameters ranging from 3.8 to 7.6 cm.

4.2 NATURAL VENTILATION MECHANISMS

Natural ventilation is the gas exchange between sewer and ambient atmospheres that is not the result of forcing air through the system with a mechanical device. Little work exists quantifying the importance of factors that affect natural ventilation in collection systems. Factors believed to most influence natural ventilation of sewers have been noted to be barometric pressure gradients, liquid drag, rise and fall of wastewater, eduction by wind (venturi effect), differences in temperature between sewer and ambient atmospheres (buoyancy effects), and changes in barometric pressure (barometric pumping).

Liquid drag

Wastewater flow has the effect of entraining overlying gas. Of all the factors that affect movement of sewer gases, liquid drag is the only one that acts continuously. Thus, without opposing factors, gas flow in sewers is generally in the same direction as wastewater flow (Thistlethwayte, 1972). Wastewater drag is responsible for some degree of ventilation, with actual magnitudes dependent in part on availability of openings to draw air in, and exhaust gases from, a collection system. Thistlethwayte (1972) estimated that a flow circuit characterized by air entry through vents and downstream transport of gas by liquid drag can induce maximum gas velocities of 0.3 to 0.5 $m \cdot s^{-1}$.

Pescod and Price (1981 and 1982) completed laboratory tests to study wastewater drag in a circular conduit. A 30 cm i.d. pipe with an adjustable slope was used. However, resistance to air flow into and out of the pipe was not considered. Nine tests were reported, with average water velocities varying from 0.2 to 0.8 $m \cdot s^{-1}$ and relative depths (normalized by pipe diameter) ranging from 0.25 to 0.75. Mean water surface velocity varied from 0.25 to 0.96 $m \cdot s^{-1}$. Mean air velocity varied from 0.07 to 0.21 $m \cdot s^{-1}$, and was observed to be highly correlated to the product of water surface velocity and a shape factor. The shape factor was defined as either surface width divided by unwetted perimeter, or surface width divided by hydraulic radius of the head space. Mean gas velocities converged to approximately 0.2 $m \cdot s^{-1}$ as the shape factor increased to greater than 0.6 based on unwetted perimeter, and 4.0 based on hydraulic radius. Except near walls, air velocity was observed to decrease exponentially above the water surface, with a velocity equal to underlying water velocity at the surface and zero velocity at pipe walls. The ratio of mean air velocity to mean water surface velocity was 0.29, with a standard deviation of 0.07. Wastewater movement had a greater effect on overlying gases at larger relative depths. All other factors being equal, average air velocity increased

with an increase in surface width and/or mean water surface velocity. Pescod and Price (1982) explained these results in terms of energy transfer to the air space occurring at the gas-liquid interface. All other factors being equal, average air velocity decreased with an increase in unwetted perimeter or "hydraulic" radius of the air space.

As part of this study, relationships reported by Pescod and Price (1982) were used to estimate air velocities in 0.25, 1.0, and 2.5 m i.d. sewers flowing with relative depth of 0.5 and wastewater surface velocity of 1.0 $m \cdot s^{-1}$ (calculations in Corsi, 1989d). Energy imparted to gas by flowing wastewater was assumed to be independent of inlet and outlet conditions, and an effective driving force was calculated based on head loss necessary to oppose gas acceleration per unit length of sewer pipe. Resulting pressure drops were 0.012, 0.0024, and 0.00072 $Pa \cdot m^{-1}$ for 0.25, 1.0, and 2.5 m i.d. pipes, respectively. Air entry to the sewer was assumed to occur at a specified number of vents "lumped" together at the extreme upstream boundary of each system (Figure 4-1). Exhaust was assumed to occur at the same number of vents located at the downstream boundary. These assumptions should underestimate gas flows since intermediate vents were neglected, thus increasing head loss by flow through the entire length of sewer pipe.

With only one inlet vent and one exhaust vent, mean gas velocity in a 200 m reach of 0.25 m i.d. sewer was 0.04 $m \cdot s^{-1}$, a factor of five lower than the 0.2 $m \cdot s^{-1}$ observed by Pescod and Price (1982) for open-ended systems. Increasing the number of vents to 10, 100, and 1000 led to gas mean velocities of 0.14, 0.19, and 0.20 $m \cdot s^{-1}$, respectively.

Total gas flow for 1000 vents was 0.0049 $m^3 \cdot s^{-1}$. Total volumetric turnovers per day (TPD - gas flow rate/total sewer volume) were estimated to be in the range of 8.6 to 43.2, depending on the number of vents. For one inlet and one exhaust vent, the greatest contribution to head loss was from vent risers

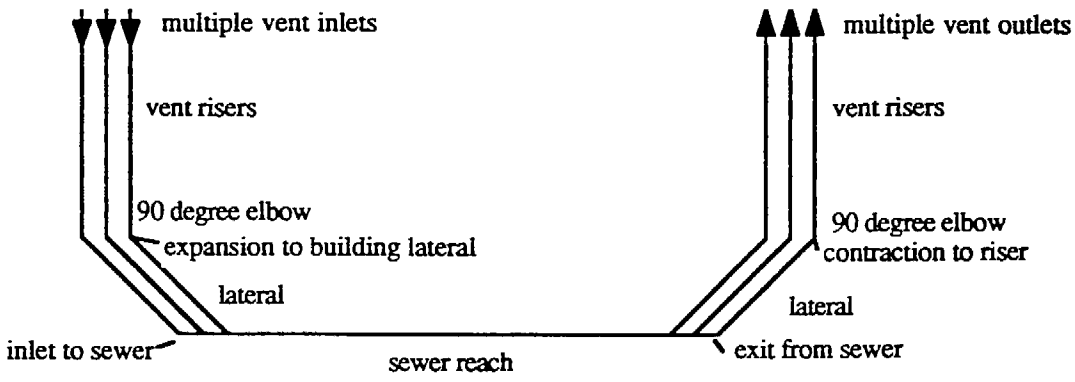

Figure 4-1. Hypothetical Circuit for Analysis of Ventilation Flows Caused by Liquid Drag

(72% of total losses). The 200 m reach of sewer pipe accounted for approximately 2% of total head loss. However, for 1000 inlet and exhaust vents, energy losses were dominated by the sewer reach (96% of total losses).

In a 1.0 m i.d. sewer with a reach length of 1000 m, one inlet vent and one exhaust vent led to a gas mean velocity of 0.003 $m \cdot s^{-1}$. Increasing the number of vents to 10, 100, and 1000 led to gas mean velocities of 0.023, 0.18, and 0.20 $m \cdot s^{-1}$, respectively. Total volumetric TPD ranged from 0.13 to 8.2, depending on the number of vents. The sewer reach contributed a greater fraction of total head loss as the number of vents increased, and approached an "open ended" system with as few as 100 inlet and exhaust vents.

Gas mean velocities in a 5000 m reach of 2.5 m i.d. sewer were estimated to be 0.005, 0.05, 0.16, and 0.18 $m \cdot s^{-1}$ for 10, 100, 1000, and 10000 inlet and exhaust vents, respectively. Total volumetric TPD ranged from only 0.04 to 1.6 for ten and ten thousand vents, respectively. Again, a greater fraction of the total head loss was contributed by the sewer reach as the number of vents increased.

Eduction by wind

Wind which blows across manhole covers or house vents can cause a small pressure difference between a sewer and the atmosphere immediately above a manhole or vent. This pressure difference can cause gases to be exhausted from and drawn into a collection system. In the case of building vents, increased wind speeds, as air is accelerated over a building, can increase pressure differential and hence ventilation rate. Some building vents are shielded from wind and may serve as inlets for air replacing gases which are exhausted from other building vents. Design of collection systems with alternating high and low vents to enhance natural ventilation has been used in some parts of the

world (Thistlethwayte, 1972; Pescod and Price, 1981). Although such practice is not common in the United States, Pomeroy (1945) stated that building vents and manhole covers provide a necessary circuit for sewer ventilation. He cautioned that reduction of manhole openings would reduce effectiveness of a flow circuit.

Pescod and Price (1981 and 1982) studied wind eduction by conducting field tests, experiments in a wind tunnel, and fluid mechanical calculations for a hypothetical sewer reach. Field and wind tunnel experiments led to the conclusion that wastewater drag should be subservient to wind eduction, particularly with a large air space above low-velocity wastewater. With wind effects and drag acting in the same direction, drag tended to increase air flows caused by wind by reducing overall head loss, but only marginally as losses along sewer pipe made up only a small fraction of total head loss. Analyses of a hypothetical sewer indicated that less than 0.3% of total loss occurred along a 150 m reach of 0.91 m i.d. sewer. Most losses were estimated to occur along vent riser pipes and bends in those pipes. Wind eduction proved to be an important mechanism for ventilating sewers.

As part of this study, energy analyses were completed using hypothetical sewer networks and assumed environmental conditions (calculations in Corsi, 1989d). Two flow circuits were studied along a 30 m reach of variable diameter sewer. Circuit A involved air entry through a manhole cover with a variable number of finger holes, and exhaust through a variable number of vents (1 - 100) associated with each manhole (Figure 4-2). Circuit B involved air entry through a variable number of vents (1 - 100), and exhaust through the same number of vents at the opposite end of a reach (Figure 4-1).

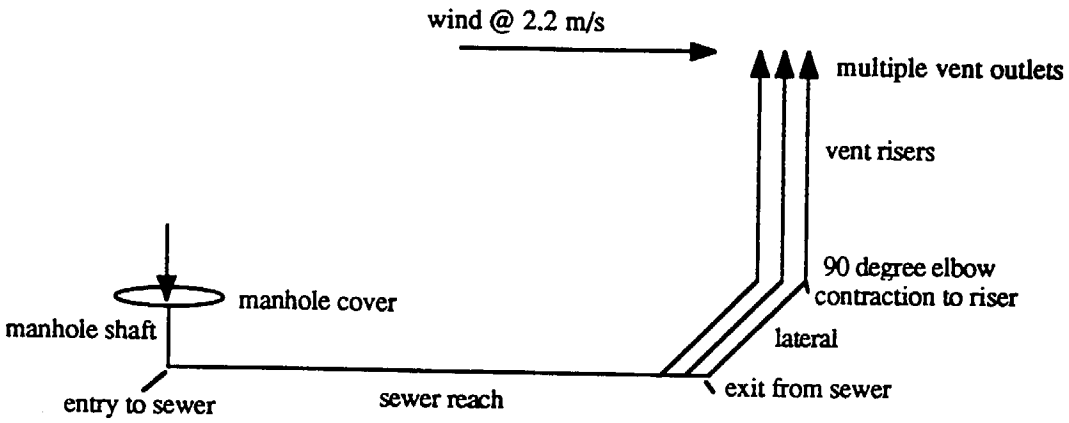

Figure 4-2. Hypothetical Circuit A for Analysis of Ventilation Flows Caused by Eduction by Wind (circuit B identical to circuit used for liquid drag and shown in Figure 4-1)

Wind speed across exhaust vents was assumed to be 2.2 $m \cdot s^{-1}$ (5 mph) with no flow across inlet manholes or vents, i.e. shielded inlets. Differences in kinetic energy of the flow were associated with a pressure differential of 2.9 Pascals.

For circuit A it was observed that head loss across manhole covers dominated overall flow resistance. For a collection reach flowing with relative depth of 0.5, gas mean velocities ranged from 0.029 to 0.10 $m \cdot s^{-1}$ (41 to 137 TPD) for a 0.25 m i.d. pipe, to 0.0018 to 0.0067 $m \cdot s^{-1}$ (2.5 to 9.3 TPD) for a 1.0 m i.d pipe. The upper-bound of each estimate was associated with three finger holes and 100 vents per manhole cover. Lower bounds were associated with only one finger hole and one exhaust vent.

For circuit B, gas mean velocities in 0.25 m i.d. and 1.0 m i.d. sewers were 0.041-1.2 $m \cdot s^{-1}$ and 0.0026-0.25 $m \cdot s^{-1}$ (58-1700 and 3.7-354 TPD), respectively. Lower bound estimates were for a flow circuit consisting of only one inlet and one exhaust vent. Upper-bound values were for 100 inlet and 100 exhaust vents.

Gas mean velocities induced by eduction by wind were generally greater than those caused by liquid drag for smaller diameter reaches, and approximately equal to those caused by liquid drag in larger diameter reaches. For smaller pipes with many openings to the ambient atmosphere, e.g. residential areas, it should be common to observe gas mean velocities of the same order or greater than wastewater mean velocities. In larger diameter sewers with many openings, e.g. combined sanitary/storm sewers, liquid drag and wind eduction may lead to gas mean velocities of greater than 0.1 times wastewater mean velocity. In larger diameter sewers with few openings, gas mean velocities are likely to be less than 0.01 times wastewater mean velocity, in the absence of ventilation mechanisms other than liquid drag or eduction by wind.

The analysis described above is not representative of the many scenarios that could be associated with wind eduction. Flow

circuits may act to counter one another, or counter effects associated with other ventilation mechanisms. In addition, wind speeds greater than 2.2 $m \cdot s^{-1}$ are common, and gas velocities in sewers should be roughly linearly proportional to ambient wind speeds (calculations in Corsi, 1989d). The possible configurations are innumerable and further detailed analysis does not appear to be practical.

Temperature Differences Between Sewer and Ambient Atmospheres

Ventilation resulting from differences between sewer and ambient atmospheres has been discussed only qualitatively in the literature. Adams (1880) was one of the first to note the effects of introduction of hot and cold liquids into a sewer, as well as heat generated by bacterial decomposition. It has been reasoned that warm sewer air should travel upstream, counter to wastewater flow, with colder air introduced at the lower end of a collection system (Metcalf and Eddy, 1928; Metcalf and Eddy,Inc., 1981). Manhole covers and building vents can serve as points of cold air entry or warm air exhaust. Thistlethwayte (1972) discussed seasonal variations of temperature differences between sewer and ambient atmospheres. He noted improved ventilation during winter months and cold summer nights as warm gases rise from sewers. He reported an Australian study during which high ventilation rates always occurred between the hours from about 9 or 10 p.m. to 6 or 7 a.m. in accordance with reduced atmospheric temperatures. Pescod and Price (1981) argued that temperature differences are probably not an important ventilation mechanism during summer months, and that in well-ventilated systems continual exchange of air between ambient and sewer atmospheres will tend to depress temperature differences.

Pescod and Price (1981) noted that a pressure equivalent of 0.057 Pa occurs per degree centigrade differential for every meter height of different air temperature. An approximate analysis assuming ideal gas conditions for a buoyant air parcel

(calculations in Corsi, 1989d) led to a pressure equivalent of 0.040 Pa for similar temperature conditions. It is likely that for many applications the column of air associated with differences in temperature between sewer and ambient atmospheres will be smaller than one meter, e.g. for relatively uniform sewer gas temperature, well-mixed below a manhole cover (height equal to thickness of cover). A one meter or greater height might occur for a sewer reach, at near ambient temperature, upstream of a hot industrial discharge stream. With an opening above or near the junction of hot discharge, a chimney-like effect might occur.

To be conservative, the Pescod and Price (1981) pressure equivalent was applied to a hypothetical sewer reach with a temperature differential of 20 ^{o}C over a one meter column of air (calculations in Corsi, 1989d). This led to an equivalent pressure driving force of 1.1 Pa. The hypothetical sewer reach was similar to that used for eduction by wind with the following exceptions:

A. Intake and exhaust both consisted of a single finger hole on each of two separated manhole covers.

B. Intake and exhaust both consisted of three finger holes on each of two separated manhole covers.

C. Intake and exhaust each consisted of a single low-elevation vent (0.05 m i.d.).

D. Intake and exhaust were each open-ended portions of pipe with relatively low resistance.

In each case, head loss was computed across intake and exhaust sites and along the hypothetical sewer reach (Figure 4-3).

Circuit A led to gas mean velocities of 0.012 $m \cdot s^{-1}$ and 0.00076 $m \cdot s^{-1}$ for 0.25 m i.d. and 1.0 m i.d. pipes, respectively. Circuit B led to gas mean velocities of 0.047 $m \cdot s^{-1}$ and 0.0030 $m \cdot s^{-1}$ for 0.25 and 1.0 m i.d. pipes, respectively. With two vents (circuit C), velocities increased to 0.052 $m \cdot s^{-1}$ and 0.0049 $m \cdot s^{-1}$ for 0.25 and 1.0 m i.d. pipes, respectively. For circuit D, gas mean velocities increased to 0.092 $m \cdot s^{-1}$ and 0.30 $m \cdot s^{-1}$

for 0.25 and 1.0 m i.d. pipes, respectively. For circuits A through C, gas flows were comparable to those associated with liquid drag and eduction by wind given restricted openings for gas exchange with the ambient atmosphere. However, results for circuit D suggest that for sewers with many openings, e.g. residential areas and combined sanitary/storm sewers, a 20 ^{o}C temperature difference between sewer and ambient atmospheres can lead to gas flows of the same order of magnitude as those caused by liquid drag and eduction by wind. It is conceivable that temperature gradients between sewer and ambient atmospheres can be much greater than 20 ^{o}C over a one meter column of air, and may be a dominant ventilation mechanism, e.g. during cold morning hours with hot domestic discharges to residential sewers or hot industrial discharges to combined sewers. However, such temperature differences will often be transient, or localized (spatially) with effects occurring over short segments of sewer, e.g. with hot discharge at one location.

Rise and Fall of Wastewater

Rise and fall of wastewater was recognized at an early date as a mechanism that causes sewer ventilation (Adams, 1880). It has since been discussed by several authors (Babbitt and Baumann; 1958; Pescod and Price, 1981; Pomeroy, 1945; Thistlethwayte, 1972). Only Pescod and Price (1981) attempted to quantify this factor in terms of ventilation. Known discharge variations with time were used as input to a wastewater flow model to obtain temporal wastewater depth changes at various stations in a collection system. Resulting turnover rates in 1000 m reaches of 1.5 and 0.45 m i.d. sewers were estimated to be 0.089 and 0.13 TPD, respectively. These translate to mean equivalent flow velocities of 0.002 $m \cdot s^{-1}$ and 0.003 $m \cdot s^{-1}$ for a relative depth of 0.5. The former is of the same order of magnitude as gas velocities caused by liquid drag, eduction by wind, and temperature differences in larger pipes, e.g. 1.0 m i.d. with a limited number of openings for gas exchange.

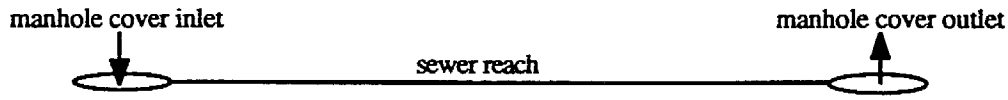

CIRCUITS A & B

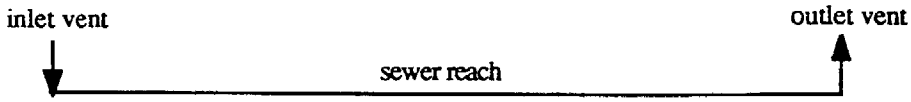

CIRCUIT C

CIRCUIT D

Figure 4-3. Hypothetical Circuits for Analysis of Ventilation Flows Caused by Temperature Differences Between Sewer and Ambient Atmospheres

Barometric Pumping

For ideal gases, changes in volume are inversely proportional to changes in pressure. Thus, all other factors being equal, a reduction in barometric pressure is associated with volume expansion. Estimates of sewer ventilation caused by barometric pumping have not been reported in the literature.

As part of this research the ideal gas law was used to estimate the relative significance of barometric pumping as a sewer ventilation mechanism (calculations in Corsi, 1989d). Simplifying assumptions of constant temperature and a 10 mb drop and rise over twenty-four hours were applied. Under such conditions barometric pumping was estimated to cause a one percent change in volume, or a ventilation rate of 0.01 day^{-1}. This translates to mean flow-through gas velocities of only 0.0002 $m \cdot s^{-1}$ and 0.0003 $m \cdot s^{-1}$ for the 1.5 m and 0.45 m i.d. systems considered for rise-and-fall of wastewater. Barometric pumping was thus concluded to be insignificant with respect to other ventilation mechanisms.

Barometric Pressure Gradients

Pescod and Price (1981) observed that barometric pressure gradients in England may be as high as 0.1 mb km^{-1} (0.01 $Pa \cdot m^{-1}$) under normal conditions. Values as high as 0.5 mb km^{-1} were reported during passage of severe depressions. However, Pescod and Price (1982) argued that there should not be frequent or prolonged occurrences of barometric pressure gradients during summer months. They also concluded that a pressure gradient of 0.1 $mb \cdot km^{-1}$ can give rise to ventilation rates greater than those induced by wind passing over extraction vents. However, they noted that significant barometric pressure gradients should coincide with unstable atmospheric conditions and high wind speeds. The resulting effect on sewer ventilation would depend on the magnitude and direction of flows induced by each mechanism. Thistlethwayte (1972) estimated that a change in

barometric pressure of one millibar (no distance provided) potentially equals 1.5 $m \cdot s^{-1}$ velocity, with the actual value being less due to frictional, entry, and exit losses in a collection system. No further work has been reported regarding effects of barometric pressure gradients on sewer ventilation.

As part of this study, a fluid/energy analysis was completed on hypothetical sewer reaches to assess ventilation by barometric pressure gradients (calculations in Corsi, 1989d). A 16 km (10 mile) reach of sewer flowing with relative depth of 0.5 was assumed, with a barometric pressure gradient of 0.1 $mb \cdot km^{-1}$ (0.01 $Pa \cdot m^{-1}$). This gradient is an extreme, leading to geostrophic winds on the order of 100 $m \cdot s^{-1}$. Two flow circuits were analyzed (Figure 4-4). Circuit A corresponded to minimal energy loss (resistance to ventilating flows) at the inlet andexit of the 16 km reach. The greatest energy losses occurred along walls of the sewer pipe (concrete pipe with 3 mm roughness elements assumed). Circuit B corresponded to a system of high resistance to air entry and exhaust, with a single manhole cover placed at each end of the reach. The number of finger holes (2.5 cm diameter) was varied from one to five on each manhole cover. There were no intermediate manholes. For circuit A, gas mean velocity increased from 0.16 $m \cdot s^{-1}$ to 0.81 $m \cdot s^{-1}$ for 0.25 and 2.5 m i.d. pipes, respectively. Gas mean velocity in a 1.0 m i.d. system was 0.43 $m \cdot s^{-1}$. These flows represent an upper-bound on flows caused by barometric pressure gradients, and should only occur in combined sewers. For such systems, gas flows induced by extreme barometric pressure gradients can rival those caused by liquid drag. Large pressure gradients would be associated with high wind speeds and result in wind eduction effects far exceeding those in hypothetical flow circuits described previously. Therefore, effects of barometric pressure gradients will be coupled with those of eduction by wind. For circuit B, velocities ranged from highs of 0.11-0.16 $m \cdot s^{-1}$ to lows of 0.0019-0.0094 $m \cdot s^{-1}$ for 0.25 and 2.5 m i.d. systems, respectively. Gas mean velocities were 0.012-0.058 $m \cdot s^{-1}$

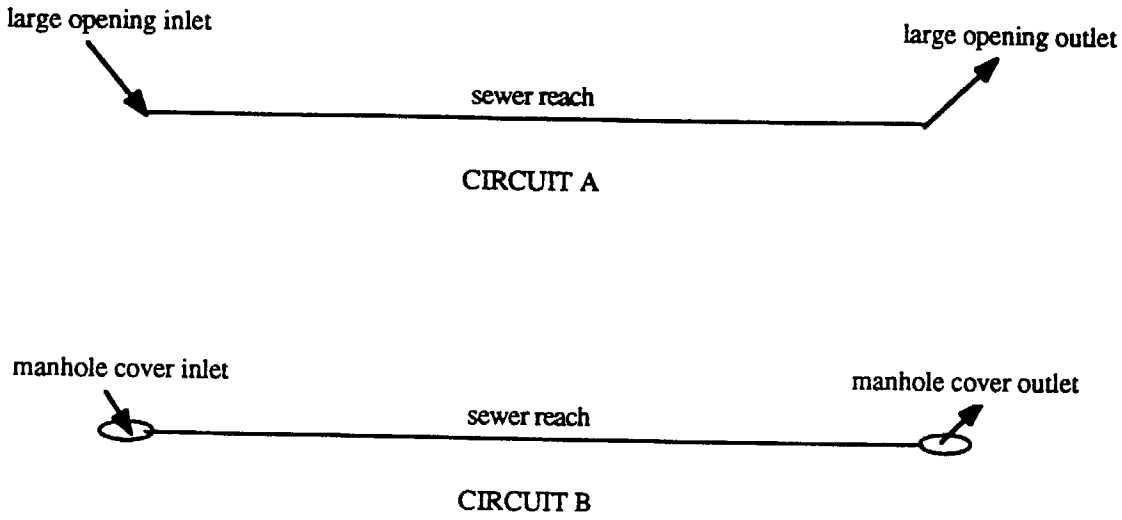

Figure 4-4. Hypothetical Circuits for Analysis of Ventilation Flows Caused by Barometric Pressure Gradients

for a 1.0 m i.d. pipe. Velocity ranges corresponded to one and five finger holes per manhole. Circuit B represented a condition of high resistance to air intake and exhaust. However, gas velocities in smaller diameter systems were still comparable to those induced by other ventilation mechanisms.

Combined Natural Ventilation Mechanisms

Because of the complexity of actual flow circuits, transient environmental conditions, and potential for opposing ventilation mechanisms, it is not possible to accurately estimate sewer gas flows from first principles. Pescod and Price (1982) suggested using carbon monoxide in individual sewer reaches to estimate gas flow rates. The use of sulfur hexafluoride, a non-toxic gas, is described in Chapter 6.

Given an accurate method to estimate gas-liquid partitioning, it should be possible to estimate ventilation flow rates based on gaseous oxygen measurements. Thistlethwayte (1972) argued that ventilation conditions necessary for satisfactory oxygen levels in sewers are volumetric turnover rates of 200 day^{-1} for 0.23 m i.d. pipes and smaller, and as low as 12 day^{-1} for larger pipes, e.g. approaching 3.7 m inside diameter. Pescod and Price (1981) applied a simple oxygen balance based on oxygen reaeration rates for standing water and bacterial respiration rates obtained for an actual sewer in Tyneside, England. They argued that oxygen levels of at least 85% of ambient are maintained in most sewer atmospheres, and used wastewater flow data from Tyneside to estimate ventilation requirements to maintain such an oxygen level. Results are listed in Table 4-1, and should serve as an approximate lower bound on ventilation flow rates for various pipe sizes. Estimated gas velocities at relative depth of 0.5 are not significantly different than values estimated previously for individual ventilation mechanisms. The concept of using routine gaseous oxygen measurements to estimate ventilation rate is

Table 4-1. Ventilation Rates Based on 85% Oxygen Levels in the Atmospheres of Operating Sewers

Diameter [m]	Length [m]	Gas Flow [m^3 day^{-1}]	Velocity[a] [m s^{-1}]	changes-day^{-1}
0.45	3000	955	0.05	2.34
1.05	3100	1189	0.03	0.52
1.50	1550	1195	0.02	0.51
2.0	870	1194	0.01	0.51
3.0	400	1204	0.004	0.50

a: Velocity based on relative depth of 0.5.
Reference: Pescod and Price (1981)

attractive in terms of simplicity. Gaseous oxygen measurements at upstream and downstream ends of isolated sewer reaches might be used in place of tracer releases to estimate sewer gas flows. This requires confidence in a model for interfacial mass transfer, which, as will be discussed in Chapter 6, appears to be resolved.

The simultaneous action of two or more ventilation mechanisms was considered previously for liquid drag and barometric pressure gradients. Pescod and Price (1982) considered combined effects of liquid drag and eduction by wind using a wind tunnel and experimental sewer system equipped with one flow extraction vent and one flow inlet vent. They observed that when eduction was greater than liquid drag, and in the same direction, effects were not additive. Instead, air flow was approximately the same as when wastewater was not flowing. Tracer experiments indicated a significant air flow counter to wastewater drag when eduction was greater than drag. It was reasoned that in the latter case air flow will be reduced to some extent in comparison to the case of no liquid flow. Thistlethwayte (1972) argued that opposing action of wind eduction and drag can lead to gas stagnation in a sewer.

4.3 FORCED VENTILATION

Forced (mechanical) ventilation is a procedure that has been applied to prevent corrosion of concrete sewer pipe, as well as for providing safe working environments for individuals who must enter collection systems. In order to prevent pipe corrosion by sulfuric acid, forced ventilation has been applied on a continuous basis. Intermittent forced ventilation for worker safety is common practice.

Forced ventilation along sewer reaches can be completed by either "pushing" air into one manhole and exhausting it at other locations in the system, or by drawing air out of a manhole and allowing for entry at other locations. The latter has been noted

as a preferred method, as polluted air release is fixed to a single location which can be controlled, dispersed to the atmosphere using an elevated stack, or located in an area where release will not present a public nuisance or health hazard (Pomeroy, 1945; Thistlethwayte, 1972).

Cost and practical design limitations of forced ventilation have been noted in the literature (Pomeroy, 1945; Thistlethwayte, 1972; USEPA, 1974). Because of such limitations, continuous forced ventilation is most often used only in large interceptors with relatively few openings to allow for natural ventilation to occur. It is common for an outfall interceptor to be mechanically ventilated using large exhaust fans at the headworks of a treatment plant.

Studley (1939) and Pomeroy (1945) were two of the first to describe results of an on-line ventilation system, with flows of 10 to 20 $m^3 \cdot s^{-1}$ (approximately 2 to 4 $m \cdot s^{-1}$) in large interceptors in Los Angeles. The City of Los Angeles faced odor problems at two inverted siphons upstream of the Hyperion Treatment Plant (USEPA, 1974). Gases upstream of each siphon were combined and drawn to the treatment plant using a large blower. The gases were then used as oxygen supply to activated sludge reactors. In a similar manner, the City of Palm Springs has drawn gas from their collection system and blown it through trickling filters, an odor control technique that has been used in several other cities (USEPA, 1974).

4.4 SUMMARY OF VENTILATION MECHANISMS

A summary of gas mean velocities caused by individual ventilation mechanisms is provided in Table 4-2. Velocities are only approximate, as they were based on a limited number of hypothetical flow circuits and values reported in the literature. It is clear that no mechanism always dominates. Relative importance of ventilation mechanisms is dependent on physical characteristics of a collection system, wastewater flow

Table 4-2. Estimates of Gas Mean Velocities Caused by Individual Ventilation Mechanisms

Liquid Drag	
0.25 m i.d.	0.04 - 0.20 m s^{-1}
1.0 m i.d.	0.003 - 0.20 m s^{-1}
2.5 m i.d.	0.005 - 0.18 m s^{-1}
Eduction by Wind: 2.2 m s^{-1} wind over vents	
0.25 m i.d.	0.029 - 1.2 m s^{-1}
1.0 m i.d.	0.0018 - 0.25 m s^{-1}
Temperature Differences: 20 ^{o}C m^{-1}	
0.25 m i.d. (restricted openings)	0.012 - 0.052 m s^{-1}
1.0 m i.d. (restricted openings)	0.00076 - 0.0049 m s^{-1}
0.25 m i.d. (open ended)	0.092 m s^{-1}
1.0 m i.d. (open ended)	0.30 m s^{-1}
Rise and Fall of Wastewater	
0.45 m i.d.	0.003 m s^{-1}
1.5 m i.d.	0.002 m s^{-1}
Barometric Pumping	
0.45 m i.d.	0.0003 m s^{-1}
1.5 m i.d.	0.0002 m s^{-1}
Barometric Pressure Gradients 0.1 mb km^{-1} (extreme)	
0.25 m i.d. (restricted openings)	0.11 - 0.16 m s^{-1}
1.0 m i.d. (restricted openings)	0.0012 - 0.058 m s^{-1}
2.5 m i.d. (restricted openings)	0.0019 - 0.0094 m s^{-1}
0.25 m i.d. (open ended)	0.16 m s^{-1}
1.0 m i.d. (open ended)	0.43 m s^{-1}
2.5 m i.d. (open ended)	0.81 m s^{-1}
Forced Ventilation up to 4 m s^{-1} has been reported in sanitary interceptors	

characteristics, and environmental conditions. Only barometric pumping can be neglected as a ventilation mechanism.

Based on calculations completed for this study, studies reported in the literature, and knowledge of collection system design, the following generalizations can be made regarding sewer ventilation:

1. For combined sanitary/storm sewers, gas flow rates are likely to be high, and a simplifying assumption of infinite dilution (zero VOC concentration above wastewater) is valid.

2. For small diameter systems with many vents, gas velocities should be relatively high. Examples include residential areas with many house vents. For such systems, infinite dilution can be reasonably assumed without a loss of significant accuracy in VOC emissions estimates.

3. For mid-to-large diameter sewers, particularly sanitary interceptors, gas velocity will be low relative to wastewater velocity. An assumption of infinite dilution is not valid, except where forced ventilation is practiced.

A summary of scenarios for which each ventilation mechanism might be important is described below.

Liquid drag: Particularly important for small diameter pipes in residential areas (many vent openings) when discharges are high and head space above wastewater is relatively small. Can also be important in combined sewers with large openings for air inflow and sewer gas exhaust.

Eduction by wind: Important in small diameter sewers with many vents, e.g. residential areas. May be dominant mechanism during unstable atmospheric conditions characterized by high wind speeds, e.g. during winter months. May be a localized mechanism affecting short regions or areas of a collection system.

Temperature differences: Important in residential sewers characterized by hot wastewater discharges during cold mornings and evenings. Can be important for combined sewer ventilation if hot discharges exist to maintain an elevated temperature in sewer atmospheres. Probably not a significant mechanism during summer months. May be a localized mechanism affecting short regions or areas of a collection system.

Rise and fall of wastewater: Can be a relatively important mechanism in larger diameter reaches, e.g. interceptors, with limited number of openings to the ambient atmosphere. Can also be significant during rapid discharges of storm water to combined sanitary/storm sewers.

Barometric pumping: Not an important ventilation mechanism.

Barometric pressure gradients: Can be significant in systems of any size, especially during unstable atmospheric conditions, and many openings for air exchange. Will always be coupled with effects of eduction by wind, and the two mechanisms may oppose one another. Should generally be insignificant during summer months.

Forced ventilation: Should dominate all other ventilation mechanisms if applied on a continuous basis. May be very significant in interceptors for several miles upstream of treatment plants, with subsequent point source emissions at the headworks of those plants.

5. THEORETICAL DEVELOPMENT: QUANTITATIVE SOLUTIONS

Analytical and computational solutions for VOC emissions from sewers are described in this chapter. Theoretical concepts developed in Chapter 3 are used to assess mass transport in uniform reaches and drops occurring at common sewer appurtenances. Section 5.1 involves VOC emissions from uniform reaches. Analytical and computational models are described, and two computer algorithms (CORAL and MATES) are summarized. Section 5.2 involves VOC emissions from drops existing at the downstream end of a uniform reach. A computational model is developed, and a computer algorithm (SUDS) is described.

5.1 GENERAL MASS BALANCE

Basic equations for mass transport in a collection reach can be derived from a consideration of gas and liquid control volumes sharing a common interface (Figure 5-1). Transfer of mass from one phase to another is taken into account by conserving species within control volumes in each phase such that

Accumulation = Input - Output + Generation - Destruction. (5-1)

Following Figure 5-1, mass is conveyed into each control volume by dispersion and mean convection across areas $A_{g,i-1/2}$ and $A_{l,i-1/2}$, respectively. Mass efflux is described by similar processes occurring across areas $A_{g,i+1/2}$ and $A_{l,i+1/2}$. Additional mass influx and efflux to/from gas cells can occur as a result of ventilation flows. The link between gas and liquid cells is provided by interfacial partitioning as described in Chapter 3.

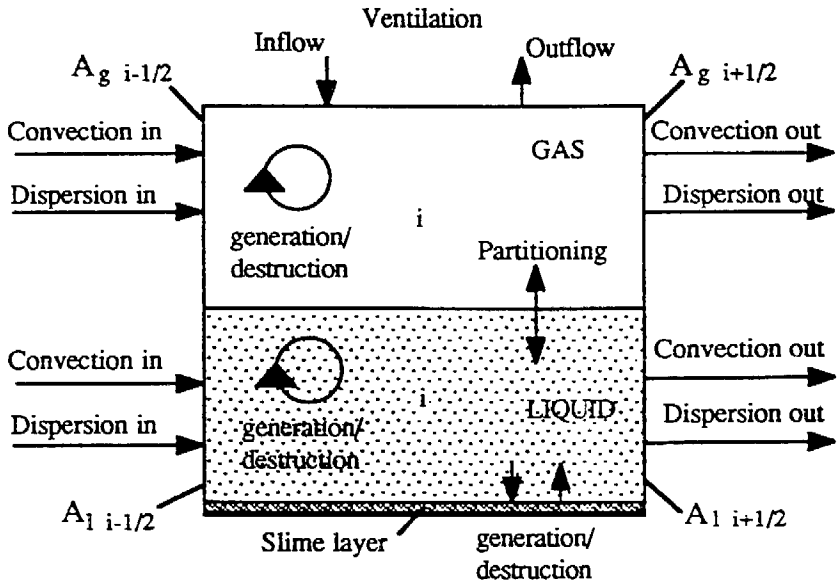

Figure 5-1. Gas and Liquid Control Volumes with a Common Interface

5.2 ANALYTICAL SOLUTIONS FOR UNIFORM REACHES

The following two partial differential equations (PDEs) result from a one-dimensional differential analysis of liquid and gas control volumes as Dx --> 0:

$$\partial C_g/\partial t = -u_g(\partial C_g/\partial x) + D_g(\partial^2 C_g/\partial x^2) + k_l(C_l - (C_g/H_c))(V_l/V_g) - (Q_{out}/V_g)\ C_g + (Q_{in}/V_g)\ C_a, \quad (5\text{-}2)$$

and

$$\partial C_l/\partial t = -u_l(\partial C_l/\partial x) + D_l(\partial^2 C_l/\partial x^2) - k_l(C_l - (C_g/H_c)), \quad (5\text{-}3)$$

where C_l, C_g, and C_a are liquid, gas, and ambient (gas) concentrations of a VOC, respectively [$mg \cdot m^{-3}$], t is time [s], u_g and u_l are mean velocities in gas and liquid phases, respectively [$m \cdot s^{-1}$], x is the spatial coordinate [m] in the direction of flow, D_g and D_l are gas and liquid-phase dispersion coefficients, respectively [$m^2 \cdot s^{-1}$], k_l is a liquid-phase mass transfer coefficient [$m \cdot s^{-1}$], Q_{in} and Q_{out} are ventilation flow rates into and out of a system [$m^3 \cdot s^{-1}$], V_g and V_l are gas and liquid volumes, respectively [m^3], and H_c is the dimensionless Henry's law constant [-].

An analytical solution of Equations 5-2 and 5-3 can be derived given the following assumptions:

1. uniform ventilation of the gas phase, i.e. equal quantities of ambient air inflow and sewer gas exhaust along an entire collection reach,
2. no net horizontal movement of gases,
3. $C_g >> C_a$,
4. convection >> dispersion in liquid, i.e. plug flow, $u_g(\partial C_g/\partial x) >> D_l(\partial^2 C_g/\partial x^2)$,
5. steady, continuous upstream discharge,
6. k_l, V_l, V_g, H_c, Q_{out} invariant with time, and
7. steady-state solution of concentrations (t --> ∞).

The two PDEs then reduce to an algebraic and an ordinary differential equation:

$$C_g = (k_l \cdot C_l)/\{(Q_{out}/V_l) + (k_l/H_c)\}, \qquad (5\text{-}4)$$

and

$$u_l(\partial C_l/\partial x) = -k_l\{C_l - (C_g/H_c)\}. \qquad (5\text{-}5)$$

Substitution of Equation 5-4 into Equation 5-5, and integration yields

$$ln_e(C_l/C_{l0}) = -(k_l/u_l)\ \{1 - 1/(G + 1)\}\ x, \qquad (5\text{-}6)$$

where C_{l0} represents liquid-phase concentration at $x = 0$, and

$$G = (Q_{out} \cdot H_c)/(V_l \cdot k_l)\ . \qquad (5\text{-}7)$$

Although Equation 5-6 is based on highly simplifying assumptions, it is of value for assessing the relative significance of individual variables, especially as they exist in term G, and for checking the accuracy of numerical solution algorithms.

Prediction of mass transfer from streams to open atmospheres is often completed by assuming infinite dilution (infinite ventilation) so that C_g always equals zero. Such an assumption is conservative from the point of atmospheric emissions, but very appealing for simplifying computational efforts if it can be justified. If $Q_{out} \dashrightarrow \infty$, Equation 5-6 reduces to the infinite ventilation solution

$$ln_e(C_l/C_{l0}) = -(k_l/u_l)\ x\ . \qquad (5\text{-}8)$$

Equations 5-6 and 5-8 can be used to assess variable combinations leading to minor deviations from infinite ventilation conditions.

5.3 COMPUTATIONAL SOLUTION FOR UNIFORM REACHES

A computational model was developed for conditions in which assumptions described in section 5.2 are not as restrictive. The model is based on a one-dimensional, finite-volume analysis of two-phase flow and interfacial mass transfer as illustrated in Figure 5-1. Important elements of the model are described below.

Hydraulic Characteristics

Flows are assumed to be uniform and are computed from Manning's equation. Required parameters include channel slope, roughness coefficient, depth of flow, and pipe diameter. In addition to wastewater flow, computations include cross-sectional area of the liquid stream, wetted perimeter, hydraulic depth and radius, surface width, and wastewater mean velocity.

Liquid Control Volumes

Flowing wastewater was treated as a series of continuous-flow stirred tank reactors (CFSTRs) with four important transport processes: mass inflow from cell (control volume) i-1 to cell i, mass outflow from cell i to cell i+1, interfacial transfer of mass to/from overlying gas cell i, and biodegradation losses.

Since each cell was treated as a CFSTR, the concentration transported across area $A_{l,i-1/2}$ into cell i was simply $C_{l,i-1}$ [$mg \cdot m^{-3}$]. The transport mechanism was wastewater flow $Q_{l,i-1}$ out (flow exiting cell i-1) [$m^3 \cdot s^{-1}$]. Mass inflow rate [$mg \cdot s^{-1}$] from cell i-1 to cell i was computed as

$$\text{Mass inflow} = Q_{l,i-1 \text{ out}} C_{l,i-1} \cdot \qquad (5\text{-}9)$$

Mass outflow [$mg \cdot s^{-1}$] is computed similar to mass inflow to yield

$$\text{Mass outflow} = Q_{l,i \text{ out}} C_{l,i} \cdot \qquad (5\text{-}10)$$

Dispersion of mass, i.e. by velocity gradients, turbulent mixing, and molecular diffusion, into and out of each cell was not explicitly included in the model. However, the use of a series of CFSTRs was assumed to yield a satisfactory simulation of the product of a dispersion coefficient and concentration gradient which would better describe actual dispersion phenomena.

Interfacial mass transfer [$mg \cdot s^{-1}$] was defined as negative from liquid cell i, and was modeled as a variation of Equation 3-1 such that

$$\text{mass transfer} = -(k_{l,i}/3600) \cdot \{C_{l,i} - (C_{g,i}/H_{c,i})\} A_{s,i}, \quad (5\text{-}11)$$

where $k_{l,i}$ is the mass transfer coefficient at cell i [$m \cdot hr^{-1}$], $C_{g,i}$ is gas-phase concentration of a VOC above liquid cell i, $H_{c,i}$ is the dimensionless Henry's law constant at cell i, and $A_{s,i}$ is total surface area defining a gas-liquid interface in cell i. Mass transfer is assumed to be liquid-phase dominated.

As discussed in Section 3.7, knowledge regarding anaerobic biodegradation of VOCs was lacking, and methods to quantify such a phenomenon are highly uncertain. However, for model utility and generality, and for determining model sensitivity, a first-order decay equation was used to describe anaerobic degradation losses [$mg \cdot s^{-1}$] such that

$$\text{Rate of anaerobic decay} = (-k_a \cdot C_{l,i} \cdot A_{s,l}/3600), \quad (5\text{-}12)$$

where $A_{s,l}$ is an effective slime layer area in cell i [m^2], and k_a is an anaerobic decay constant [$m \cdot hr^{-1}$]. Equation 5-12 does not account for VOC formation via degradation of other VOCs, e.g. chloroethene from dichloroethene, or for rate of VOC contact with a slime layer (assumed to be accounted for in k_a). Decay constants were not assumed or calculated within the model, and must be provided by the user. Slime layer area is calculated as the product of cell length and wetted wall perimeter.

Because of significant depletion of dissolved oxygen in wastewater, aerobic degradation of VOCs in sewers is expected to be low. Models to predict such losses include a great deal of uncertainty. For the reasons given above for anaerobic degradation, a first-order decay equation was again used to model either aerobic or anaerobic biodegradation losses [$mg \cdot s^{-1}$] in bulk liquid such that

$$\text{Rate of mass reduction} = -k_b(C_{l,i} \cdot V_{l,i}/3600), \qquad (5\text{-}13)$$

where k_b [hr^{-1}] is a first-order decay constant and $V_{l,i}$ is wastewater volume for cell i.

Sorption to solid particles and biomass were not considered and are not included in the model. However, the model can be modified to account for dynamic partitioning of VOCs between the solid and aqueous phases, if partition coefficients are known.

Gas Control Volumes

Mass transport in the gaseous phase was modeled using a series of n cells of equal length and identical "numbering" (i, i+1, etc.) as underlying liquid cells. Concentrations were assumed to be well-mixed (uniform) within each cell. Important transport processes are described below.

Similar to Equations 5-9 and 5-10 for liquid flow, convective processes were defined by

$$\text{Convection inflow} = Q_{g,i-1\ out} \cdot C_{g,i-1} \qquad (5\text{-}14)$$

and

$$\text{Convection outflow} = Q_{g,i\ out} \cdot C_{g,i} \qquad (5\text{-}15)$$

where $Q_{g,i-1\ out}$ and $Q_{g,i\ out}$ have units of $[m^3 \cdot s^{-1}]$ and $C_{g,i-1}$ and $C_{g,i}$ have units of $[mg \cdot m^{-3}]$.

Combined phenomena of turbulent and molecular diffusion, and non-uniformity in velocities across wastewater cross-sections, i.e. dispersion, can be simulated by choosing the number of CFSTRs used to model the system (as discussed for liquid cells). Instantaneous mixing throughout a sewer reach is simulated using one CFSTR, i.e. a slug of VOC entering the upstream boundary of a reach is instantaneously observed at the downstream boundary. A condition of plug-flow is simulated using an infinite number of CFSTRs. These extreme conditions can be used to approximately account for axial dispersion. Significance of the number of CFSTRs is described in Chapter 7.

Gas may be exhausted to or drawn from the ambient atmosphere to individual cells by one or more of a number of ventilation mechanisms (Chapter 4). For uniformly-mixed gas cells, each process (exhaust and intake) was assumed to affect gas concentrations throughout cell i. Exhaust and intake rates $[mg \cdot s^{-1}]$ were computed as

$$\text{Exhaust mass} = Q_{ex,i} \cdot C_{g,i}, \tag{5-16}$$

and

$$\text{Intake mass} = Q_{in,i} \cdot C_a, \tag{5-17}$$

where $Q_{ex,i}$ and $Q_{in,i}$ are exhaust and intake flow rates to cell i $[m^3 \cdot s^{-1}]$ and C_a is ambient concentration of a VOC $[mg \cdot m^{-3}]$. An additional equation was based on mass conservation of bulk gases (assuming incompressible conditions) so that

$$Q_{g,i\ out} = Q_{g,i-1\ out} + Q_{in,i} - Q_{ex,i}, \tag{5-18}$$

thereby allowing for spatial variations in bulk gas flow rates.

Mass transfer between phases [$mg \cdot s^{-1}$] was taken to be positive from liquid cell i to gas cell i, and was modeled as the negative of Equation 5-11 such that

$$\text{Mass transfer} = (k_{l,i}/3600) \cdot \{C_{l,i} - (C_{g,i}/H_{c,i})\} \cdot A_{s,i} \quad (5\text{-}19)$$

Biological activity is known to exist at moist walls of sewer atmospheres. However, data required to predict loss of chemical species to moist sewer walls did not exist. Removal by sorption from the gas phase is a function of aqueous concentration in the moisture layer, which in turn is a function of moisture volume film thickness and kinetics of biological degradation. A conservative assumption involves rapid depletion on the liquid side, so that sorption losses to walls [$mg \cdot s^{-1}$] were modeled as

$$\text{Gas phase removal to wall} = (-k_m/3600)\ C_{g,i} \cdot A_{m,i} \quad (5\text{-}20)$$

where $A_{m,i}$ is the area of moist wall in cell i [m^2]. The term k_m is a "wall transfer coefficient" defining transport to and uptake at walls. Equation 5-20 is believed to be very conservative, as bacterial action in the moisture layer should be far from instantaneous. Furthermore, total accumulation of VOC mass in the moisture layer should be small relative to VOC mass in the gas phase. Equation 5-20 was retained only for the purpose of model generality.

Upstream Boundary Conditions

Prescribed discharges to a collection reach set the upstream boundary conditions for gas and liquid. Upstream conditions can be specified at "apparent" cell i = 0. Gaseous concentrations are assumed to be constant at the upstream end of a collection reach. Liquid concentrations are user-prescribed as uniform "steps". Each uniform concentration step is associated with a discharge time that allows for continuous discharge (step time =

model simulation time), slug discharge (step time less than simulation time), or intermittent slug discharge (series of short discharges each followed by a period of zero discharge).

Solution Algorithm

Mass transport is solved explicitly with successive replacement (updating) of finite volume terms in time. A lagged interaction between phases is used in which mass transport is solved alternately between all liquid and all gas cells, with spatial "marching" in the liquid occurring first. By combining Equations 5-9 to 5-20, consistent with the application of Equation 5-1, using a finite difference approximation for accumulation, applying a successive replacement method where superscript n denotes a specific time step, grouping like terms and solving for C_{li} and C_{gi} leads to

$$C_{li} = \{Q_{l,i-1}^{(n+1)} \cdot C_{l,i-1}^{(n+1)} + k_l \cdot (C_{gi}^{(n)}/H_{ci}) \cdot A_{si}^{(n+1)} + (C_{li}^{(n)}/\Delta t) \cdot V_{li}^{(n+1)}\} / \{Q_{li}^{(n+1)} + k_l \cdot A_{si}^{(n+1)} + k_b \cdot V_{li}^{(n+1)} + k_a \cdot A_{si}^{(n+1)} + V_{li}^{(n+1)}/\Delta t\} \quad (5\text{-}21)$$

and

$$Z_1 = Q_{g,i-1}^{(n+1)} \cdot C_{g,i-1}^{(n+1)} \quad (5\text{-}22a)$$

$$Z_2 = [V_{gi}^{(n+1)}/\Delta t - (k_l/H_{ci}) \cdot A_{si}^{(n+1)}] \cdot C_{gi}^{(n)} + k_l \cdot C_{li}^{(n+1)} \cdot A_{si}^{(n+1)} + Q_{v,in,i}^{(n+1)} \cdot C_a^{(n+1)} \quad (5\text{-}22b)$$

$$Z_3 = V_{gi}^{(n+1)}/\Delta t + Q_{gi}^{(n+1)} + Q_{v,out,i}^{(n+1)} + k_m \cdot A_{mi}^{(n+1)} \quad (5\text{-}22c)$$

$$C_{gi}^{(n+1)} = (Z_1 + Z_2)/Z_3. \quad (5\text{-}22d)$$

To achieve conservation of mass, gas concentrations in the inter-phase transport term are assessed at time step n during both liquid and gas marching.

Equations 5-21 and 5-22 are solved by using user-prescribed initial conditions for both C_{li} and C_{gi} (usually set equal to zero), and upstream boundary conditions at cell i = 0.

Equations 5-21 and 5-22 form a basis for time-dependent solutions of mass transport in a confined sewer. Computational models to solve each equation were coded in FORTRAN 77. Model applications are discussed in Chapter 7. A brief summary of each model is provided below.

Collection System Organic Release Algorithm (CORAL)

The CORAL model is based on solution of Equations 5-21 and 5-22 given several supporting input, output, and computational routines. Major blocks of the algorithm include compound description, compound discharge specifications, wastewater hydraulics, options for mass transfer between phases, ventilation options, and discretization options.

Volatile compounds are selected interactively from a VOC "menu". Appropriate values of,i are assigned in accordance with Table 3-1. Values of $H_{c,i}$ are computed as functions of individual VOCs and temperature using expressions developed by Gossett (1987). Compound discharge conditions are specified as continuous, slug, or intermittent slug as described previously.

Wastewater hydraulic characteristics are computed using the solution to Manning's equation for circular conduits. Hydraulic computations are used to solve directly for wastewater flow rates, liquid and gas volumes, surface and cross-sectional areas, and indirectly for mass transfer coefficients. The latter are computed using Equations 3-13, 16, 25, 26 or 27. A user-specified option for computing mass transfer coefficients is also available.

Ventilation rates are prescribed on a turnover (total volume) per day basis. Uniform or cell-dependent spatial ventilation conditions can be chosen. The latter requires input of inflow and outflow cell locations. Total inflow is equally divided between inflow cells, and total outflow is equally divided between outflow cells.

Discretization options include a choice of Δx and Δt (cell size and time increment). Additional terms in Equations 5-21 and 5-22 are either user-specified or solved during execution.

Multi-Parameter Assessment of Toxic Emissions from Sewers (MATES)

The MATES model is based on an algorithm similar to CORAL, but is intended to assess effects of variations in specific variables. Those variables include pipe diameter, relative depth, Henry's law constant, channel slope, and ventilation rate. The basis for MATES is multiple model runs which summarize combinations of variables that exceed a specified VOC removal criteria (fractional mass emitted for a sewer of given length), given uniform ventilation conditions, continuous or slug discharge conditions, and transfer coefficients computed using Equations 3-13, 16, 25, 26 or 27.

Analytical and Computational Comparisons

Solutions obtained using Equation 5-6 and the CORAL model were compared for a wide range of system variables. A 2000 m reach was used, with spatial and temporal increments of 20 m and 10 s, respectively, for computational modeling. A continuous discharge of VOC was assumed, with steady-state conditions used for comparison. Uniform ventilation was assumed. However, ventilation rate, Henry's law constant, depth of flow, channel slope, and pipe diameter were varied over a wide range of values. The dimensionless parameter G (Equation 5-7) ranged from a low of 1.5 to 445 (closely approximating infinite dilution). Mass

transfer coefficients (normalized by mean hydraulic depth) computed using Equation 3-29 ranged from 0.06 hr^{-1} to 5.18 hr^{-1}. Estimated mass removals ranged from a low of 4% for G = 1.52 and k_l = 0.11 hr^{-1}, to a high of 81% for G = 445 and k_l = 3.29 hr^{-1}. For each of 16 analyses, the maximum absolute difference between analytical and computational solutions of mass removal was 0.1%, indicative of negligible computational errors There was no trend for model predictions to be higher or lower than analytical solutions.

5.4 COMPUTATIONAL SOLUTION FOR DROPS

Solution for mass transport from "drops" (elevation changes) in a confined atmosphere must consider mass balances in liquid and gas phases. Wastewater jetting from a sewer reach into a pump station wet well can be used as a reference case (Figure 5-2), and extended to drop-manholes, building connections, and other drops in sewers. Figure 5-2 illustrates mass input to a confined well-atmosphere by gas flow along an influent sewer pipe, mass outflow by ventilation to the ambient atmosphere, and mass loss or input caused by transfer to the falling wastewater stream. Mass transfer between liquid and gas can be estimated using Equations 3-28 and 29, and Equations 3-31, 32, or 37.

Computational Solution

Utilizing the mass balance concept of Equation 5-1, and an assumption of well-mixed conditions in the sewer atmosphere, a finite difference solution for gas concentration using Figure 5-2 as a simplified model yields

$$C_g^{(n+1)} = \{Q_l^{(n+1)} \cdot (C_l^{(n+1)} - C_b^{(n+1)}) + (C_{g,in}^{(n+1)} \cdot Q_g^{(n+1)} + (C_g^{(n)} \cdot V_g^{(n+1)}/\Delta t\} / \{V_g^{(n+1)}/\Delta t + Q_g^{(n+1)}\} \quad (5\text{-}23)$$

where superscripts denote time steps, Δt is a time step increment [s], C_g is gas concentration in the confined gas volume [$mg \cdot m^{-3}$],

Q_l and Q_g are liquid and gas flow rates into the wet well [m^3], C_l is liquid concentration at the top of the drop [$mg \cdot m^{-3}$], C_b is concentration in wastewater following the drop [$mg \cdot m^{-3}$], and $C_{g,in}$ is concentration in the gas flow entering the wet well [$mg \cdot m^{-3}$]. The variable C_b is found by rearranging Equation 3-28 to yield

$$C_b^{(n+1)} = [C_l^{(n+1)}/r_i] - [C_g^{(n+1)}/H_{c,i}] \cdot [(1/r_i) - 1], \quad (5\text{-}24)$$

where $H_{c,i}$ is the dimensionless Henry's law constant for species i, and r_i is solved given Equation 3-31 coupled with Equation 3-31, 32, or 37.

Emissions of VOCs from a confined chamber can be computed as

$$E = C_g \cdot Q_g \ , \quad (5\text{-}25)$$

where E is emission rate [$mg \cdot s^{-1}$].

Steady-state conditions were not assumed in deriving Equations 5-23 and 5-24. Thus, dynamic simulation of gas concentrations and emissions from a drop can be completed given a temporal history of input variables.

Sewer Uniform Reach with Drop Solution (SUDS)

The SUDS model draws on an algorithm similar to CORAL to provide necessary temporal input to a drop located at the end of a uniform reach. Slug or continuous discharges are prescribed at the upstream end of a reach. Computational solutions based on Equations 5-21 and 5-22 provide values of C_l and $C_{g,in}$ as input to Equations 5-23 and 5-24. The user prescribes a gas volume, tailwater depth, and drop height. Gas flow is computed based on reach cross-sectional area and a gas velocity equal to a prescribed fraction of wastewater mean velocity. The depletion ratio r_i in Equation 5-24 is computed based on Nakasone's model (Equation 3-37).

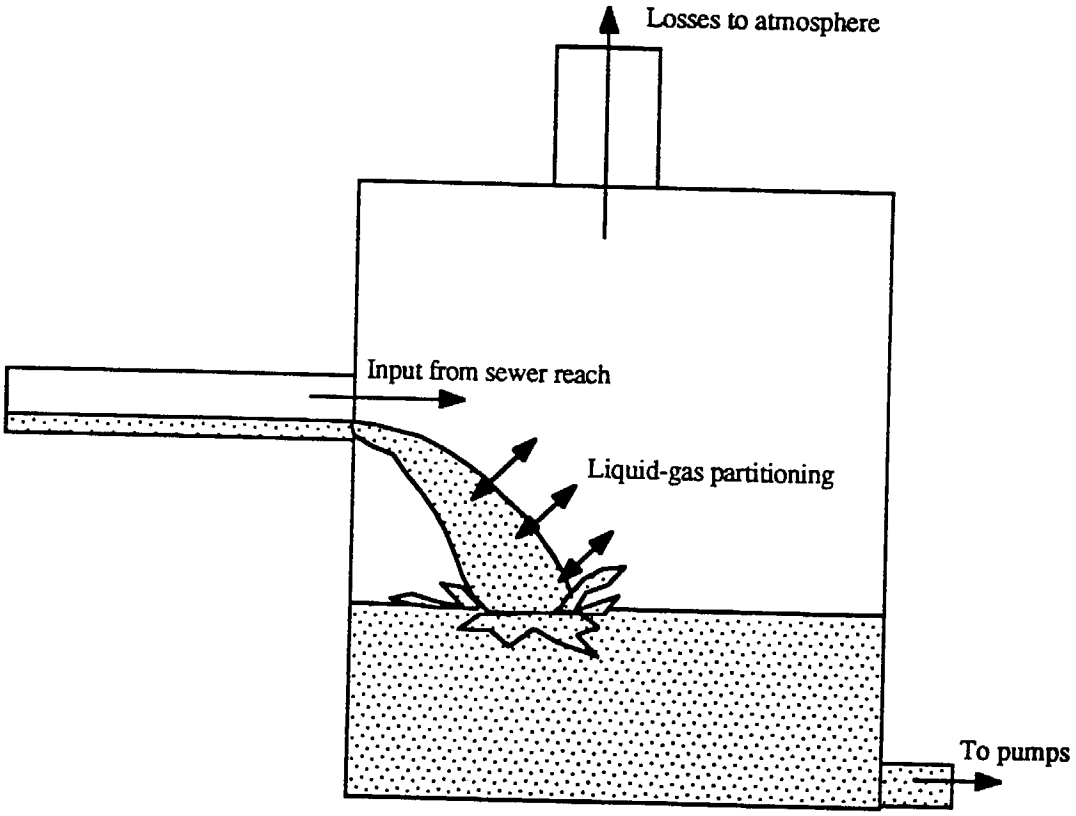

Figure 5-2. Gas-Phase Control Volume for a Wet Well Atmosphere

6. MASS TRANSFER FIELD EXPERIMENTS

Partitioning of a volatile tracer was studied in a series of six field experiments in operating sewers. Major objectives of the experiments were to obtain a data base for evaluation of the CORAL model, for use in back-calculating mass transfer coefficients, and for comparison with existing transfer coefficient models. The decision to conduct field studies, as opposed to laboratory or pilot, was motivated by concerns regarding 1) scaling from laboratory or pilot to actual sewer systems, 2) the importance of flow (mixing) conditions on interfacial mass transfer, 3) availability of operating sewers and cooperative municipalities, and 4) potential differences between raw wastewater and clean water. As described below, field experiments were completed on two operating interceptors with distinctly different physical characteristics.

6.1 GENERAL APPROACH: TWO-PHASE TRACER METHOD

A tracer method based on simultaneous monitoring in both gas and liquid phases was developed as illustrated in Figure 6-1. An essential element of each experiment was the ability to control gas flows by blowing ambient air into an otherwise sealed sewer, and venting sewer gases at an open downstream manhole. Therefore, constant and known ventilation rates were obtained. A volatile tracer was injected in the aqueous phase at the same manhole at which ambient air was forced into the sewer. Injection occurred at a known rate, and the tracer compound was transported downstream in both the wastewater and sewer gas. Downstream gas and liquid samples were collected while continuously injecting tracer. Thus, time profiles of tracer concentrations in both gas and liquid phases were compared with those predicted using CORAL, and steady-state concentrations were used to iteratively back-calculate transfer coefficients.

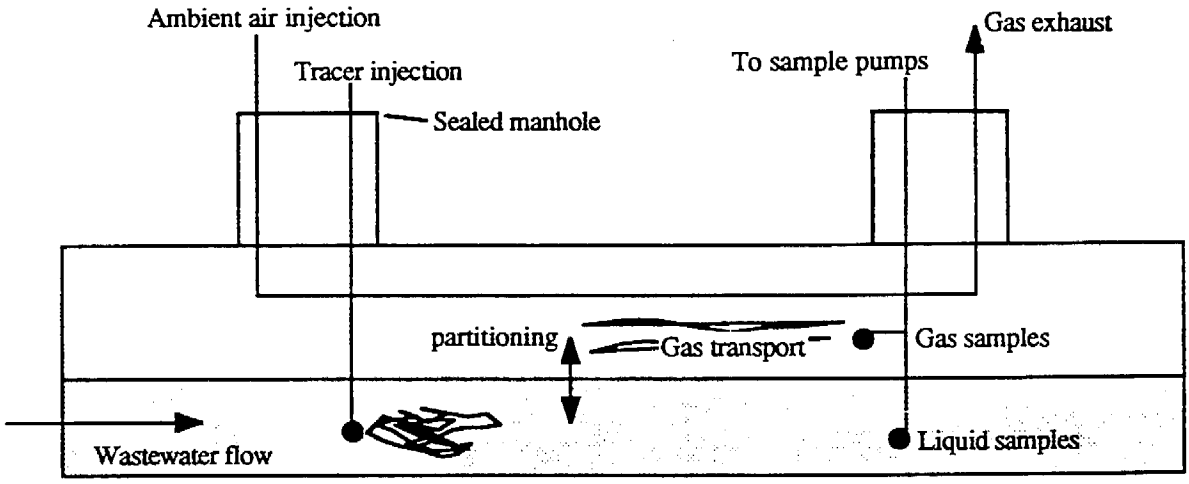

Figure 6-1. Simplified Schematic of the Two-Phase Tracer Method

Two operating sewers were selected for field experiments. Experiments (Tests) 1 through 4 were completed in the El Macero Interceptor, of the City of Davis. Tests 5 and 6 were completed in the Central Interceptor, of the County of Sacramento. The two systems were selected for a number of reasons including:

1. relative isolation from connecting sewer lines,
2. locations out of the flow of motor vehicle traffic,
3. controllable or measurable wastewater flow rates,
4. proximity to the University of California, Davis, and
5. significantly different physical conditions between the two systems, thus yielding a potentially wide range of mass transfer coefficients.

The physical properties of each experimental reach are listed in Table 6-1. Reach length corresponds to the distance between the manholes where experiments were conducted. A summary of locations, dates, times, and environmental conditions for each test is provided in Table 6-2. Additional characteristics of each system are described below.

City of Davis - El Macero Interceptor

The El Macero Interceptor (EMI) served primarily residential sources, with small contributions from commercial dischargers (grocery store, fast-food restaurants, gasoline stations, and several automobile sales and service companies). The EMI was located approximately five miles east of central Davis, and two miles northeast of South Davis and El Macero Estates.

As illustrated in Figure 6-2, wastewater was collected at a pump-station wet well in El Macero Estates. A combination of three variable-speed pumps was used to force wastewater through a 2.9 kilometer (km) pressurized main which discharged to a 0.53 m i.d. gravity-flow sewer. The latter was used to convey wastewater 2.0 km, parallel to County Road 105, to a 1.2 m i.d. main interceptor which led to the Davis Wastewater Treatment

Table 6-1. Physical Properties of Experimental Systems

	Davis	Sacramento
Reach Length [m]	131	291
Pipe Diameter [m]	0.533	2.59
Channel Slope [%]	0.24	0.063

Table 6-2. Summary of Tracer Experiments

Test	Location	Date	Time[a]	Comments
1	Davis	3-8-89	12:06-13:04	Significant precipitation
2	Davis	3-22-89	11:34-12:21	Sunny, slight breeze
3	Davis	4-13-89	11:39-12:39	Sunny, slight breeze
4	Davis	5-4-89	10:43-11:45	Sunny, windy
5	Sacramento	5-31-89	13:33-15:22	Sunny, hot
6	Sacramento	6-15-89	9:56-11:44	Sunny, slight breeze

a: Time during which tracer injected.

Plant. The only wastewater contribution to the 0.53 m i.d. gravity-flow reach was the pressurized main. There were also no points of air entry or exhaust between the wet well in El Macero Estates, and influent to the gravity-flow sewer, i.e. upstream of manhole 14.

Experiments were completed between manholes 13 and 11, with tracer injection and ventilation at manhole 13, gas and liquid sampling at manhole 12, and ventilation outflow at manhole 11. Channel slope between manholes 13 and 12 was 0.24% based upon a surveying effort completed prior to Test 1. The EMI was designed for a channel slope of 0.2% between manholes 14 and 1, and from 0.3% to 0.9% slightly upstream of manhole 14. Manhole depths (measured from outer lip to pipe invert) varied from 2.7 to 3.1 m for manholes 13 and 12, respectively.

County of Sacramento - Central Interceptor

The Central Interceptor (CI) served a mix of residential, commercial, and industrial dischargers. Except for a limited number of small lateral interceptors, its major purpose was to convey wastewater as a regional interceptor to the Sacramento Regional Wastewater Treatment Plant (SRWTP).

The CI consisted of about 16 km of gravity sewer pipe ranging in size from 2.1 m to 2.7 m i.d.. As illustrated in Figure 6-3, the CI began as a 2.6 m i.d. pipeline south of State Route 50 at the intersection of Fruitridge and Elk Grove-Florin Roads, where flows from the Arden and Northeast Interceptors were picked up. The CI continued south along Elk Grove-Florin Road for approximately six kilometers before turning west to the SRWTP.

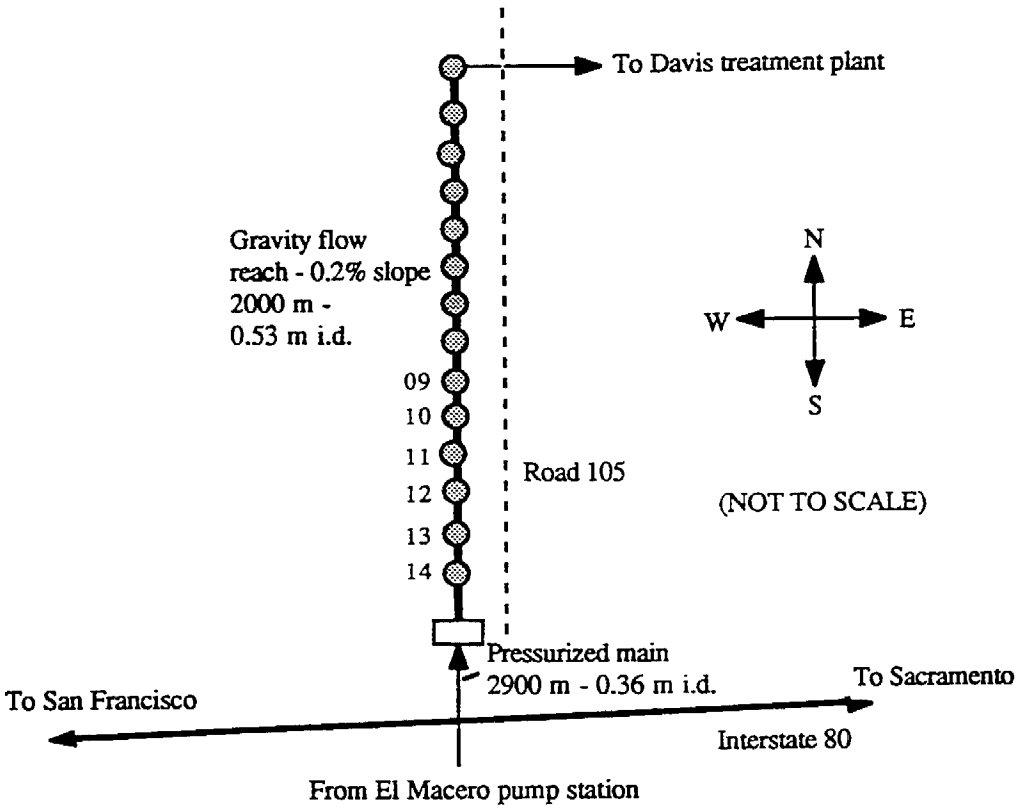

Figure 6-2. Simplified Illustration of the El Macero Interceptor (not to scale)

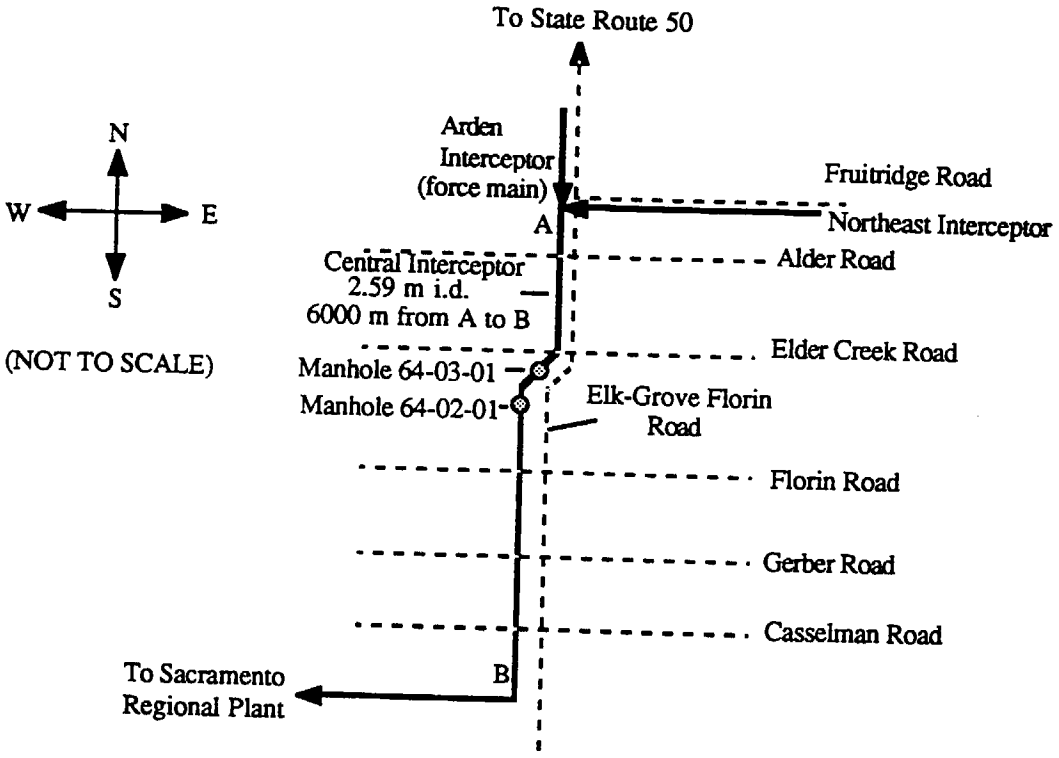

Figure 6-3. Simplified Illustration of the Central Interceptor (not to scale)

Experiments were completed in a 291 m section of 2.59 m i.d. pipe located south of Elder Creek Road, and north of Florin Road (manholes 64-03-1 to 64-02-1). Existing flowmeters (depth recorders) were located at Alder Road and Gerber Road, approximately 1.5 km upstream and 3.0 km downstream of manhole 64-03-1 (injection manhole), respectively. Manhole depths (outer cover lip to pipe invert) were approximately 10 m.

Volatile Tracer

The deuterated solvent TCM-d (MSD isotopes no. MD-591) was chosen as the tracer compound. Several properties of TCM are listed in Table 2-2. Trichloromethane-d had the following advantages for use as a field tracer:

1. properties nearly identical to TCM, a VOC frequently observed in raw wastewater,
2. distinguishable from TCM using gas chromatography / mass selective integration,
3. low affinity for adsorbing to solid particles and biomass, and not significantly affected by such processes along relatively short sewer reaches, and
4. low biodegradability and chemical reactivity, with low potential for degradation in samples during storage.

Tracer solutions were prepared within 24 to 48 hours of scheduled field experiments. A two-step dilution process was used to obtain concentrations of TCM-d below its solubility in water. The first step involved dissolution of 99.8% purity TCM-d in pure methanol to form a working stock solution. The second step involved dissolving the stock solution in water. A volume of 1980 ml of tap water was added to each of several 2.00 liter Florence flasks. Twenty milliliters of stock solution were added to each flask during the stirring period. Flasks were capped with ground glass stoppers immediately after stock addition. Stirring was continued, using magnetic stirrers and Teflon® stirring bars, until all of the TCM-d was dissolved. Dissolution

times varied from nearly instantaneous to approximately two hours, depending on the concentration of stock solution.

After complete dissolution, the contents of each flask were transferred by peristaltic pump, using a minimal amount of non-inert tubing, to an empty Tedlar® bag, where the tracer solution was stored until the beginning of the experiment. Minimal exposure of the tracer to the gas phase occurred. A flexible Tedlar® bag was used to prevent formation of a head space and possible loss of tracer from the solution phase. Total volume of tracer used varied with each experiment.

6.2 EXPERIMENTAL METHODOLOGY

Illustrations of experimental arrangements are shown in Figure 6-4. One difference between Davis and Sacramento experiments was the location of open manholes. In Davis, sampling was completed at a sealed manhole to avoid worker exposure to relatively high concentrations of TCM-d. In Sacramento, concentrations were relatively low, and sampling was completed at an open manhole. Smoke tests later confirmed significant gas exhaust at the open manhole in Davis, but similar experiments indicated continuous horizontal motion of gases along the sewer axis in Sacramento. It was subsequently ascertained that a ventilation fan was operating at the headworks of the plant, drawing air downstream along the sewer. Ventilation, injection, and sampling methods are described below.

Wastewater Flow Rates

Measurements of wastewater flow rate during each experiment were based on depth measurements and application of Manning's equation for circular conduits. In Davis, a plumb-bob assembly was used during experiments to measure distances from manhole lip to the wastewater surface, and depth was obtained by subtracting those measurements from previously surveyed invert-to-manhole lip

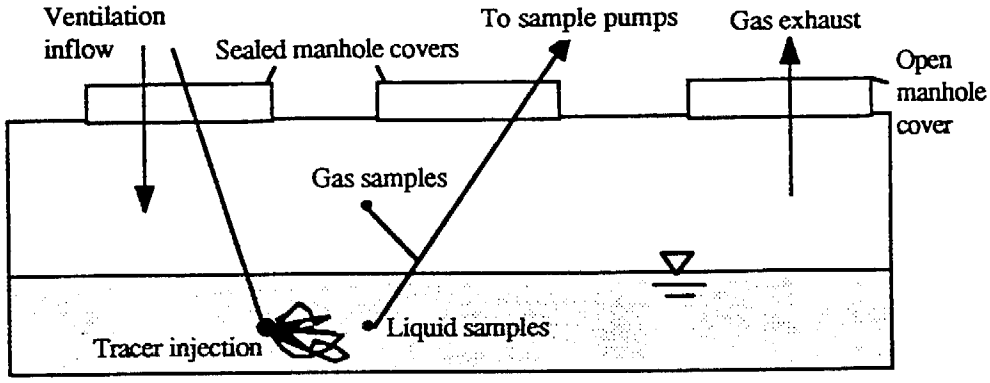

6-4a. El Macero Interceptor (City of Davis)

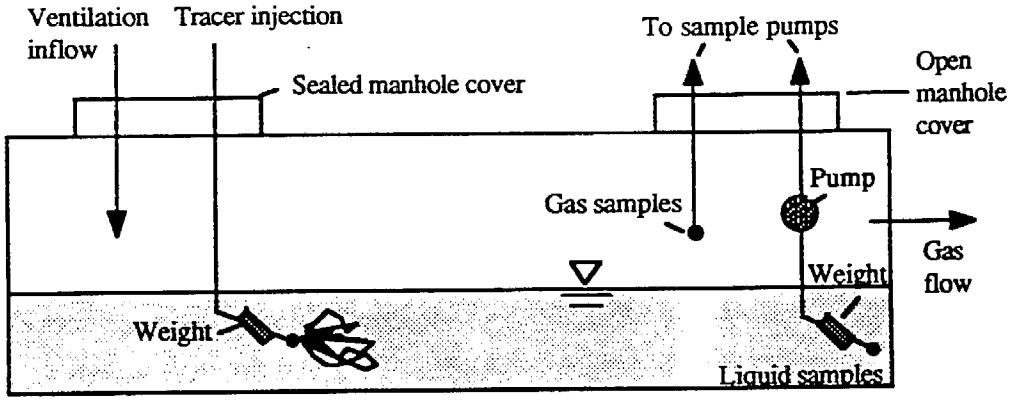

6-4b. Central Interceptor (County of Sacramento)

Figure 6-4. Simplified Illustrations of Field Experiments (not to scale)

distances. In Sacramento the measurement was facilitated by depth meters upstream and downstream of the experimental reach. Flows measured by the two meters separately were consistent when hydraulic lag time between meters was taken into account.

Wastewater flow, velocity, and depth conditions for each experiment are summarized in Table 6-3. In Davis, wastewater flows were controlled by appropriate pump settings at the El Macero pump station. Controlled flow conditions were not attainable in the Central Interceptor of Sacramento. Thus, experiments were completed during periods of relatively low flow variation. Flow rates differed by nearly two orders of magnitude between the two systems. Mean flow velocity varied between 0.67 $m \cdot s^{-1}$ and 1.31 $m \cdot s^{-1}$, encompassing a range commonly observed in sanitary sewers.

Wastewater Temperature

Because volatility of a compound varies with temperature, wastewater temperatures were measured at the beginning and end of each experiment. Wastewater was pumped through Teflon® tubing to a plastic jar containing a thermocouple probe. Maximum pumping speed was used to assure rapid liquid delivery with minimal heat transfer (preliminary testing indicated that temperatures of sewer gases were not significantly different from the underlying wastewater). Temperature readings equilibrated in less than one minute and remained stable as long as new wastewater was allowed to flow over the temperature probe. Wastewater temperature was constant during the course of an experiment.

Table 6-3. Wastewater Flow and Depth Conditions

Test	Flow [$m^3 s^{-1}$]	Mean Velocity [$m s^{-1}$]	Depth [m]	Relative Depth [-]
1	0.058	0.79	0.19	0.36
2	0.056	0.78	0.19	0.36
3	0.039	0.70	0.16	0.29
4	0.033	0.67	0.15	0.27
5	2.40 - 2.58	1.28 - 1.31	1.00 - 1.04	0.39 - 0.40
6	2.07 - 2.58	1.23 - 1.31	0.92 - 1.04	0.36 - 0.40

Table 6-4. Wastewater Temperature and Henry's Law Constant for TCM-d

Test	Wastewater Temperature [°C]	Henry's Law Constant [-][a]
1	20.8[b]	0.120
2	20.8	0.120
3	21.8	0.126
4	22.2	0.128
5	26.0	0.155
6	24.4	0.143

a: Based upon Gossett (1987).
b: Not recorded. Value assumed based upon Test 2 and other sampling during period.

Wastewater temperatures during each experiment, and associated Henry's law constants for TCM are listed in Table 6-4. Temperatures varied from approximately 21 ^{o}C to 26 ^{o}C. As noted in Chapter 3, this range is consistent with temperatures observed in other cities in California. Henry's law constants varied from 0.12 to 0.16.

Wastewater temperature was not measured during Test 1. A value of 20.8 ^{o}C was assumed based on Test 2 conditions, and values observed during preliminary testing just a few days prior to the experiment. Even though Test 1 was completed under relatively cool ambient conditions, the effects of small temperature changes in the sewer on the Henry's law constant would have been small as illustrated in Table 6-4.

Ventilation

Ambient air was introduced to injection manholes using a duct arrangement as shown in Figure 6-5. Portable blowers were used to force ambient air through a length of flexible duct connected to the inlet end of a one meter length of pipe. A small hole drilled at mid-length of the connecting pipe allowed measurement of air velocity, and hence air flow rate, using a hot-wire anemometer (Sierra Instruments, model 441). Air exited the connecting pipe through a second portion of flexible duct connected to a flanged circular jack mounted atop manhole covers constructed for field experiments. Smoke tests were completed to assure that ventilation manholes were well sealed.

Smoke tests were conducted after Test 6 indicated greater gas velocities in the sewer than could be accounted for by the volume of ambient air blown into the system. A separate experiment was completed to ascertain the nature of flows in the Sacramento CI. An amount of pure gaseous sulfur hexafluoride (SF_6) was bled into the connecting pipe used to monitor air velocity (Figure 6-5). Gas samples were drawn at the downstream

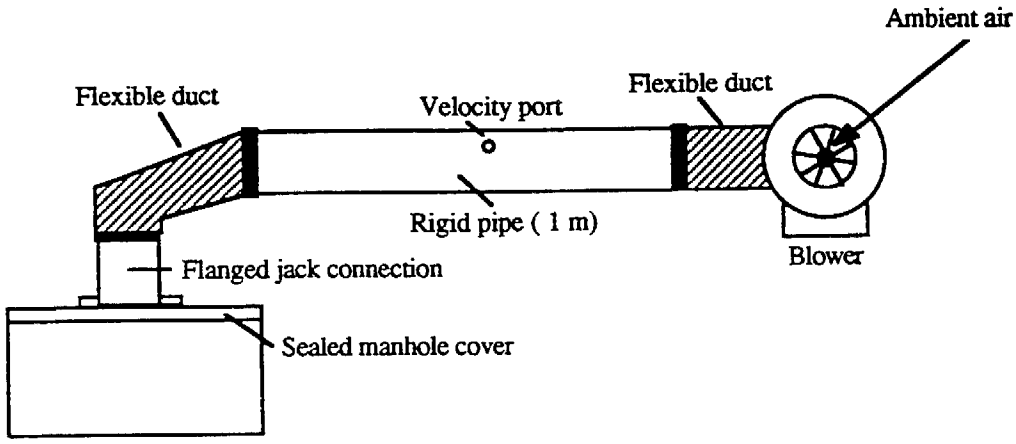

Figure 6-5. Duct Arrangement for Ventilation during Field Experiments

manhole using syringes attached to the exhaust side of gas sample pumps. Pumps were used to draw sewer gas through Teflon® tubing extended into the sewer head space. Samples were collected every five to ten minutes following injection, and analyzed on a gas chromatograph with an electron capture detector (Perkin-Elmer, model Sigma 3-B). Results of the tracer analysis indicated the following:

1. Sulfur hexafluoride concentrations were five times lower and arrived five times faster downstream than expected from forced ventilation rates.

2. Conditions were well-mixed in the gas phase.

The first result indicated the existence of gas flows unaccounted for by injection blowers used during experiments. It was later discovered that blowers used to draw air through the Sacramento CI system were continuously operating at the SRWTP. Based on the confined nature of the CI from the location of experiments to the SRWTP, it was concluded that unusually high gas flows were caused by forced ventilation at the plant.

Although SF_6 experiments were carried out on a different day than Tests 5 and 6, forced ventilation at the SRWTP was essentially the same each day. Therefore, flow rates observed during SF_6 experiments were applied to Tests 5 and 6. Additional discussion of SF_6 experiments is provided in Section 6-4. Gas flow conditions are summarized in Table 6-5. Ventilation rates in turnovers per day were based on total system volume extending between injection and gas exhaust manholes (manholes 13 and 11) in Davis, and injection and sampling manholes in Sacramento.

Tracer Injection

During each test a Tedlar® bag filled with TCM-d was brought to the field and used as a reservoir from which tracer was pumped. A variable speed peristaltic pump (Masterflex, 6-600 rpm) and speed controller (Masterflex), powered using a portable generator, were used for pumping tracer solution. As the volume

of tracer solution in the Tedlar® bag decreased, a head space was not formed as the bag continuously collapsed over the remaining solution.

Teflon® tubing (6 mm id) was used in each test to transport tracer solution to its point of discharge. For Tests 1 through 4, tubing was attached to a pole wedged into the effluent side of sewer pipe passing through the injection manhole. The total length of Teflon® tubing was approximately four meters, with minor variation between experiments. Deep manholes and high flows associated with Tests 5 and 6 did not allow injection similar to Tests 1 through 4. Instead, a large weight was attached near the discharge side of a 12 m length of Teflon® tubing. Tubing was submerged in the wastewater, with the force of wastewater flow conveying the weight and tubing approximately 5 meters downstream of the manhole. A summary of tracer concentrations, injection rates, and initial TCM-d concentrations in wastewater is given in Table 6-6.

Liquid Sampling

Liquid samples were drawn through 6 mm i.d. Teflon® tubing using a peristaltic pump (Masterflex, 6-600 rpm) and speed controller (Masterflex). Submergence of sample tubing was similar to injection tubing for both experimental systems. In Davis, tubing attached to a pole wedged into the influent pipe of the sampling manhole (Figure 6-4a). In Sacramento, weighted tubing extended approximately two meters downstream of the sampling manhole.

Table 6-5. Gas Flow Conditions

Test	Ventilation Rate [TPD]	Gas Flow rate [m^3 s^{-1}]	Gas Mean Velocity [m s^{-1}]	Re[b] (gas)
1	31.2	0.021	0.14	2700
2	37.1	0.026	0.17	3400
3	37.1	0.026	0.15	3500
4	35.4	0.024	0.14	3400
5[c]	100	1.8	0.51 - 0.56[a]	45500 - 48000
6[c]	100	1.8	0.51 - 0.56[a]	48000 - 49000

TPD: Total volume turnovers per day based upon experimental reach.
a: Gas mean velocity range based upon starting and ending cross-sectional areas.
b: Reynolds number defined with gas "hydraulic" depth as characteristic length.
c: Based in part on sulfur hexafluoride experiments of 7-20-1989.

Table 6-6. Tracer Concentrations and Injection Rates

Test	Tracer Concentration [mg l^{-1}][a]	Injection Rate [ml min^{-1}][b]	Instantaneous Concentration [mg m^{-3}][c]
1	658	210	40
2	500	320	48
3	469	264	53
4	412	277	57
5	1125	335	2.4 - 2.6[d]
6	1974	291	3.7 - 4.7[d]

a: Based on mass balance during preparation.
b: Based on change in bag volume over injection time.
c: Assuming instantaneous mixing upon injection to wastewater.
d: Based on wastewater flow rates at beginning and ending of experiments.

To avoid plugging of sample tubing, the point of wastewater intake was securely enclosed in a fine wire mesh. In addition, to avoid contributions from previous liquid samples, tubing was flushed for one to two minutes by pumping wastewater before a sample was collected. At maximum pump speed (used to draw most liquid samples), residence times in the sample tubing were about 20 s during Tests 1-4 and 60 s during Tests 5 and 6.

Liquid samples were collected in 40 ml glass sample vials and filled to capacity to minimize sample head space. Screw caps with Teflon®-faced silicone septa were used to immediately seal sample vials. In the field, samples were stored in a closed cooler filled with ice. Samples were refrigerated immediately following field experiments.

Gas Sampling

Gas samples were drawn through 6 mm i.d. Teflon® tubing by universal flow pumps (SKC, model 224-PCXR7). For Tests 1 through 4, sample tubing was attached to the same pole used to collect liquid samples. A rod affixed at a right angle to the pole was used to extend gas tubing into the sewer head space. For Tests 5 and 6, weighted Teflon® tubing was simply lowered to a point between the top of the sewer pipe and wastewater surface. For Tests 1 through 4, it was difficult to record the exact location of gas sample intake. Based on geometry of the sewer pipe and sample support pole, it was estimated that gas samples originated between 25 to 50 cm above the wastewater surface, with some variation between experiments. Total length of gas sample tubing was approximately four meters. During Tests 5 and 6, samples were drawn from approximately 80 and 10 cm above the wastewater surface, respectively. Total length of gas sample tubing was nine to ten meters.

The gas sampling train used for each experiment is illustrated in Figure 6-6. Sewer gases were drawn through multi-sorbent glass cartridges (4 mm i.d. packed with Tenax-TA® and

Ambersorb XE-340® resins). Twenty-four hours prior to sampling, each sorbent tube was conditioned by ramped heating to 300 °C using a thermal desorption system (Envirochem, model 785). Following exhaust from the sample pump, gases were passed through a bubble meter. At least three flow rates were measured for each sample. Flow measurements for each sample were found to be necessary, as differences in resin packing, the major resistance to gas flow, caused up to a factor of three difference in flow rates between tubes.

Before each sample was collected, sample tubing was flushed by drawing sewer gas for two or more minutes through the gas sample train (without sorbent tube). Gas residual remained in the tubing from the flushing period. Thus, gas samples represented a fraction of gas from each flushing period, as well as that drawn during the sampling period. Contributions from the flushing period were reduced for longer sampling periods, and should not have been significant when steady-state concentrations had already been attained. Sample times during Tests 1 through 4 varied from three to seven minutes, with an average sample volume of 453 ml. Sample times during Test 5 ranged from five to seven minutes, with an average sample volume of 714 ml. Test 6 consisted only of 15 minute samples, with an average sample volume of 1.7 liters.

Following each sample, sorbent tubes were placed in sealed glass tube holders. Tubes and holders were stored in a sealed glass Mason jar containing activated charcoal to scavenge VOCs present in the cannister head space. The cannister was refrigerated upon returning to the lab.

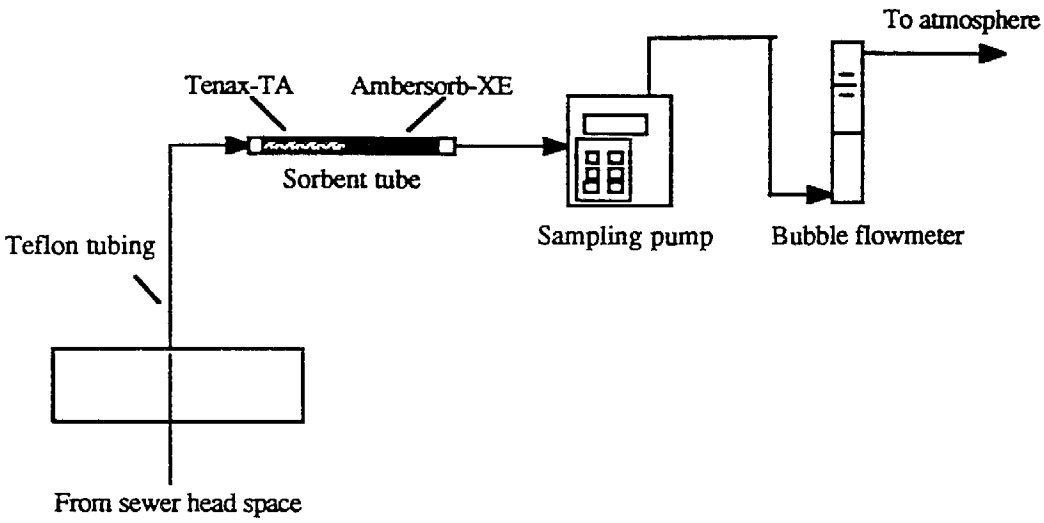

Figure 6-6. Gas Sampling Train used in El Macero and Central Interceptor Experiments

6.3 ANALYSIS METHODOLOGY

Sample analysis consisted of sample preparation, analytical detection, and quantitative assessment. Preparation included transfer of volatile species in liquid samples to multi-sorbent tubes, and mixing of TCM-d standards. Analytical detection was completed using gas chromatography/mass spectrometry (GC/MSD) with mass selective integration.

Liquid Sample Preparation

To avoid contamination of the GC/MSD system by high molecular weight compounds present in raw wastewater, liquid samples were first purged onto multi-sorbent tubes similar to those described in Section 6.2. Samples and conditioned sorbent tubes were first removed from refrigerated storage and allowed to warm to room temperature. Either 5 to 10 mL of sample was injected into a glass purging vessel (Supelco, model 2-2424) using a 5 mL glass syringe. Sorbent tubes were mounted on the only opening for gas passage so that all the purge gas passed through the tubes. Nitrogen gas was bubbled through a porous glass diffuser at the bottom of the purging vessel at flow rates varying from 50 to 65 $mL \cdot min^{-1}$ for 15 to 20 min (greater times and flows associated with greater liquid sample volumes). Lab tests conducted prior to field experiments indicated that an N_2 flow of 50 $mL^{®}min^{-1}$ for 10 min was sufficient to strip the TCM.

Liquid samples drawn from the Tedlar® bag before injection in sewers were also transferred to sorbent tubes by purging. This required a 1:10,000 dilution in distilled deionized water. The contents of 5 mL of diluted solution were purged onto a sorbent tube in a manner similar to field samples.

GC/MSD

Samples were analyzed with a gas chromatograph (Hewlett Packard, model 5890A) utilizing a glass capillary column (J & W Scientific, model DB-624). A mass selective detector (Hewlett Packard, model 5990) was used to identify and quantify compounds eluting from the GC and data were analyzed using a Hewlett Packard model 59970 Chem Station. A concentrating/capillary inletting system (Envirochem, model 810A) was used for sample desorption, pre-concentration (dual trap), and delivery to the GC column. The GC/MSD had an auto-tuning feature which was used at the beginning of each set of samples.

Desorption of sample tubes and two internal concentrating traps was completed by ballistic heating from 40 to 250 ^{o}C for each. The GC temperature program consisted of a three minute solvent delay, isothermal heating at 40 ^{o}C for four minutes, followed by a 10 ^{o}C per minute ramp to 200 ^{o}C, and cycle completion at 200 ^{o}C for six minutes. All gas transfer lines were maintained at a minimum of 150 ^{o}C throughout sample analyses. Helium served as the carrier gas.

A data acquisition system (Hewlett Packard, model 5890) and auxiliary tape were used to store data for future analyses. Hewlett Packard software was used for specification of ion abundance within a restricted atomic mass unit (amu) range of 85.5 to 86.5, with a TCM-d "fragment" (parent TCM-d with loss of one chlorine atom) noted at 85.8 amu (mass selective integration).

Analyses were always completed in the order of gas samples, standards, purged liquid samples, and bag samples. Within each of the four categories, samples were analyzed in order of estimated ascending concentration. Clean blank samples were also analyzed at the beginning of each set of analyses, after gas samples but before standards, after standards but before liquid samples, and after liquid but before bag samples. Contamination

was generally not found to be significant, and small amounts of residual TCM-d in the analytical system were observed to be removed by one blank run.

Deuterated Trichloromethane Standards

Standards were prepared from a stock solution of pure TCM-d dissolved in pure methanol and stored in a glass vial. Individual standards, were prepared by spiking successively larger quantities of stock solution onto the glass frit in the sorbent tubes and followed by N_2 purge at a rate of 50-60 $mL \cdot min^{-1}$ for 15 minutes. Standards were handled and stored in the same manner as described previously for liquid samples.

Three or more standards were prepared for each experiment, and analyzed on the GC/MSD in order of increasing TCM-d mass. An example chromatogram for a TCM-d standard is shown in Figure 6-7. Chromatograms all corresponded to mass selective integration between 85.5 and 86.5 amu. A summary of TCM-d standards for each experiment is provided in Table 6-7.

An example calibration curve is shown in Figure 6-8. A tabular summary of least-square fit, linear regression equations for all calibration curves is provided in Table 6-8. The form of regression equations is indicated at the bottom of Table 6-8, with ion abundance divided by 10^7. Squares of correlation coefficients were greater than 0.999 for three of the six sets of standards.

Sample abundances were compared with standard abundance ranges (Table 6-7) to assess deviations from low and high standards. Standards and samples were compared based on ion abundance at 85.8 amu. Only for liquid samples collected during Tests 3 and 4 did all sample abundances lie within the standard abundance range. However, most liquid samples for Test 6, and gas samples for Tests 1, 3, and 6 were near either the low or high bounds of the standard abundance range.

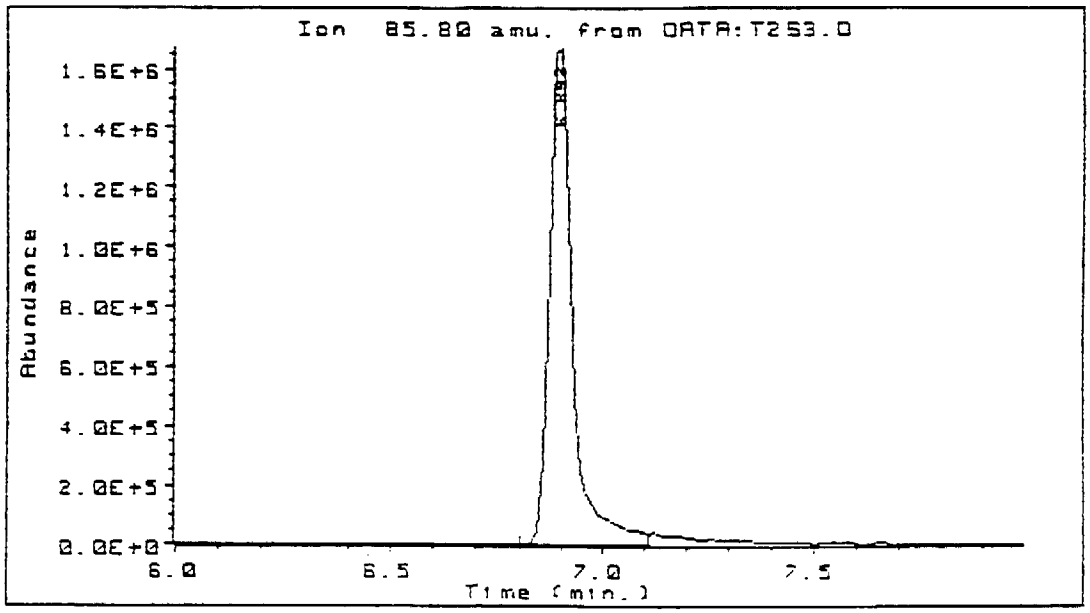


```
                                        T: --------------
                                        Z: Ion  85.80 amu. from DATA:
Redraw complete ...                     Y: Scan 7.147 min. of DATA:T2
[CHRO]                                  X: Scan 14.191 min. of DATA:T
```

Ion 85.80 amu. from DATA:T2S3.D 1 integration peaks found.

Peak#	Ret Time	Type	Width	Area	Start Time
1	6.892	PH	0.059	65523259	6.801

Figure 6-7. Example Chromatogram of TCM-d Standard

Table 6-7. Summary of TCM-d Standards for GC/MSD Analyses

Test	# standards	Abundance ($\times 10^7$)	Mass/Abundance (μg/A) x 10^{-9} Range	Average	Low/High
1	3	11.4 - 46.9	3.8 - 4.6	4.23	0.82
2	3	3.7 - 18.4	5.1 - 5.8	5.55	0.88
3	4	8.4 - 25.9	2.7 - 3.3	3.01	0.81
4	3	3.8 - 7.8	5.7 - 6.7	6.36	0.85
5	4	1.3 - 4.7	4.6 - 6.5	5.48	0.70
6	3	1.6 - 7.7	2.6 - 3.2	2.87	0.81

Table 6-8. Regression Analysis of TCM-d Standards

Test	Regression Terms m	b	r^2	Standard Errors Y	X
1	0.04827	-0.1261	0.9999	0.01299	0.00052
2	0.05711	-0.0211	0.9850	0.07409	0.00705
3	0.03040	0.0003	0.9768	0.04216	0.0033
4	0.07705	-0.0758	0.9990	0.00738	0.00244
5	0.07102	-0.0318	0.9946	0.01036	0.00370
6	0.03369	-0.0140	0.9999	0.00185	0.00041

Regression equation of form: $Y = mX + b$

Y = mass (μg)

X = ion abundance x 10^{-7}

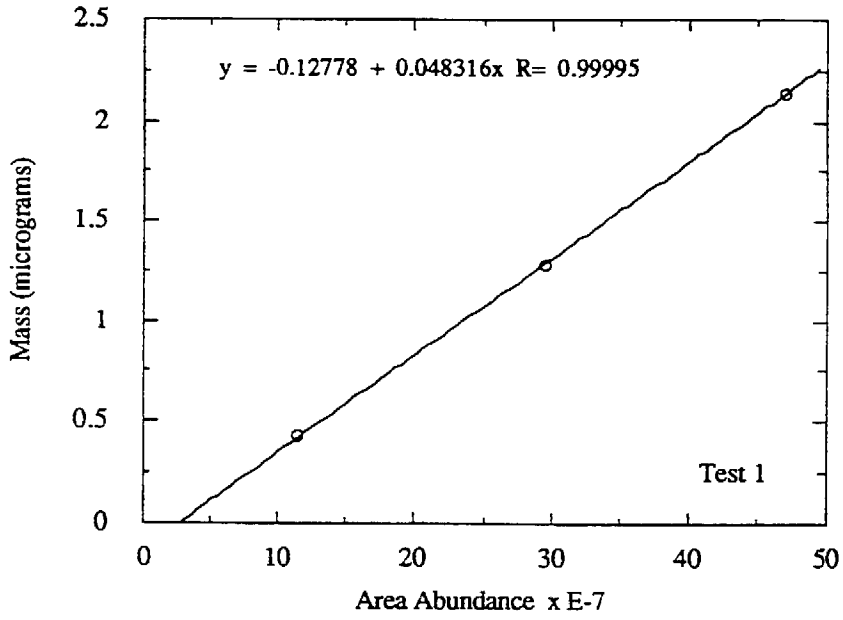

Figure 6-8. Example Calibration Curve Based on TCM-d Standards

It is common to quantify samples below the lowest standard using single-point calibration, i.e. using a calibration equation developed from the lowest standard and an assumed slope leading to a zero intercept. However, for this study it was observed that samples with abundance of greater than 0.3 of the lowest standard gave results consistent with theory when equations summarized in Table 6-8 were used. Thus, single-point calibration was only applied to samples with an ion abundance of less than 0.3 of the lowest standard abundance (11% of all samples; 3% of liquid and 18% of gas samples). Equations in Table 6-8 were used to quantify those samples with ion abundances greater than 0.3 of the lowest standard abundance, including those samples with an abundance greater than the highest standard abundance (12% of all samples; 0% of liquid and 23% of gas samples).

6.4 RESULTS

Results of field experiments completed in both the EMI and CI are presented below. Concentrations of TCM-d in wastewater are presented first, followed by concentrations in sewer gas. The latter includes an assessment of mass transfer coefficient models.

TCM-d in Wastewater

Scatter diagrams of liquid concentration versus time for all experiments are shown in Figure 6-9. Samples collected prior to or shortly after tracer injection had consistently low (near or at zero) TCM-d concentrations. Few samples were collected before steady-state conditions were reached. However, samples collected after termination of tracer injection exhibited an expected drop in concentration with time (Tests 2, 3, and 6).

Liquid concentrations were unexpectedly high for Test 2. It was later determined that the pump, and short length of tubing in the pump head, used to inject concentrated tracer solution during

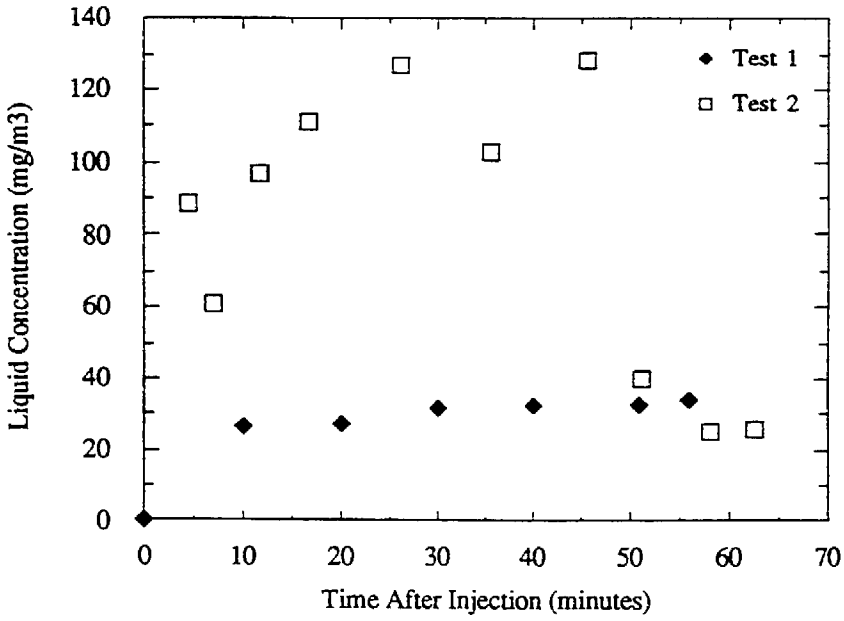

(a)

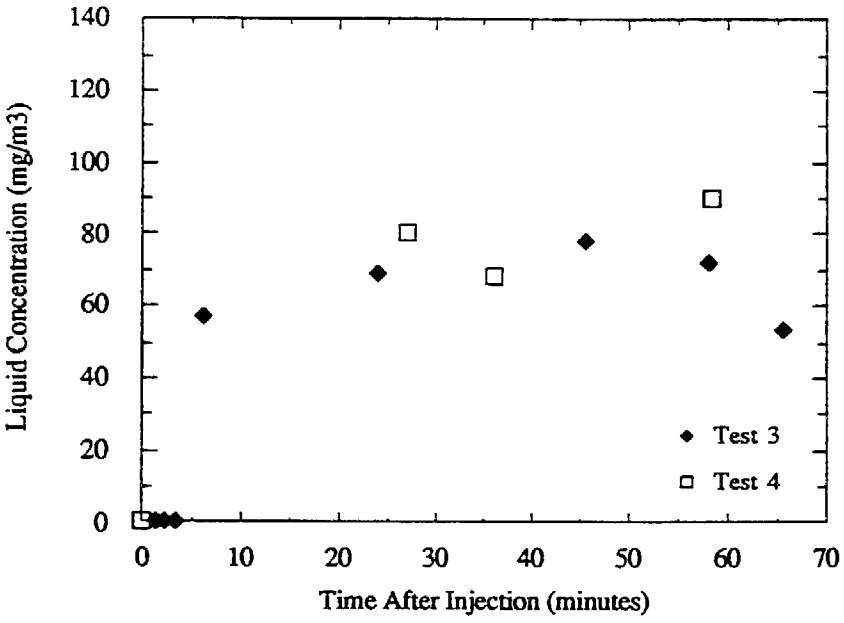

(b)

Figure 6-9. Measured Aqueous Concentrations of TCM-d during Field Experiments

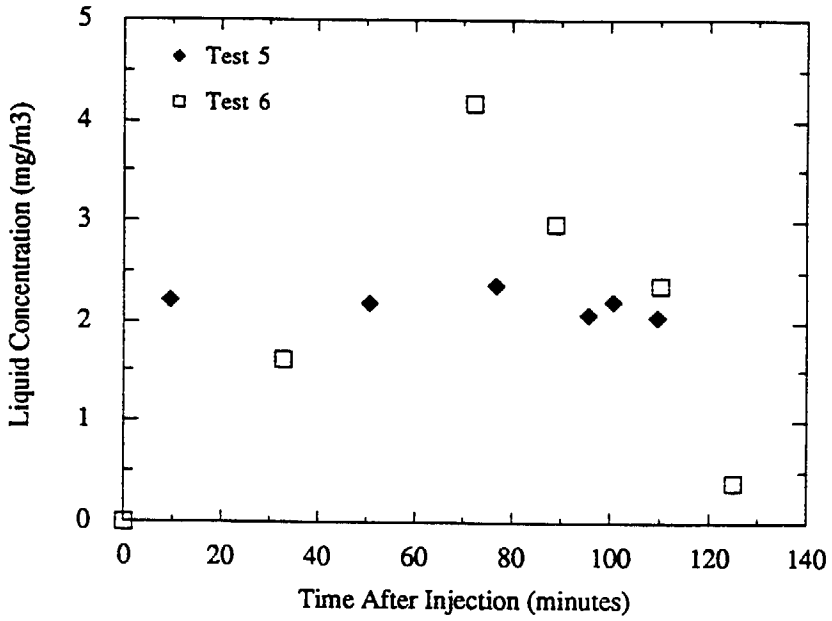

(c)

Figure 6-9. (cont.) Measured Aqueous Concentrations of TCM-d during Field Experiments

Test 1 were inadvertently used for sampling during Test 2. This is thought to have contaminated Test 2 samples. To avoid similar problems of contamination, new tubing was used in pump heads during each subsequent experiment.

Estimation of aqueous-phase concentrations, immediately after tracer injection, required knowledge of wastewater flow rate, and tracer concentration prior to injection. It was assumed that instantaneous mixing occurred during injection of tracer to wastewater. For all but Test 5, there was a significant difference between measured concentrations, i.e. from sampling contents of the Tedlar® bag prior to injection, and mass balanced concentrations, i.e. based on amount mixed in laboratory. Each was used to estimate TCM-d concentrations assuming instantaneous mixing with wastewater. Results are summarized in Table 6-9, and compared with the range of measured steady-state concentrations. It was assumed, and verified through modeling efforts, that only a small fraction (< 5%) of TCM-d was lost between the points of injection and sampling.

Because of contamination problems, the ratio of measured to "balanced" and measured to bag concentrations were both high for Test 2. For all but Test 3, the ratio of measured to balanced concentrations was closer to unity than was the ratio of measured to bag concentrations. After removing Test 2, and averaging the results of 5a and 5b, and 6a and 6b, average low and high bounds were computed for each comparative ratio. The average low-high range for measured/balanced concentrations was 0.87-1.18, thus encompassing unity. For measured/bag concentrations the range was 1.36-1.77. Initial liquid concentrations were based on mass balanced tracer solutions for all subsequent analyses.

A summary of steady-state TCM-d concentrations in wastewater is provided in Table 6-10. Coefficients of variation were less than 0.15 for all but Test 6. Modeled concentrations differed

Table 6-9. Comparison of Methods to Compute Liquid Concentration

Test	Liquid Concentration [mg m^{-3}] Mass Balance[c]	Bag[d]	Measured[e]	Meas/Balance	Meas/Bag
1	40	9.6	26 - 34	0.65 - 0.85	2.71 - 3.54
2	48	20	97 - 128	2.02 - 2.67	4.85 - 6.40
3	53	67	69 - 78	1.30 - 1.47	1.03 - 1.16
4	57	34	68 - 90	1.19 - 1.58	2.00 -2.65
5[a]	2.4	2.5	2.1 - 2.4	0.88 - 1.00	0.84 - 0.96
5[b]	2.6	2.8	2.1 - 2.4	0.81 - 0.92	0.75 - 0.86
6[a]	4.7	7.8	1.6 - 4.2	0.34 - 0.89	0.21 - 0.54
6[b]	3.7	6.1	1.6 - 4.2	0.43 - 1.14	0.26 - 0.69
average low-high range excluding Test 2:				0.87 - 1.18	1.36 - 1.77

a and b: Based on initial and final wastewater flow rates, respectively, for Tests 5 and 6.
c: Based on prepared concentration in bag and instantaneous mixing.
d: Based on measured concentration in bag and instantaneous mixing.
e: Steady-state concentration measured at downstream manhole.

Table 6-10. Summary of Steady-State Concentrations of TCM-d in Wastewater

Test	Average Concentration [mg m^{-3}]	Standard Deviation [mg m^{-3}]	cv	model / average 1 31
30.10	1.27			
2	113	14	0.12	0.42
3	73	5	0.06	0.71
4	79	11	0.14	0.70
5	2.2	0.1	0.05	1.14[a]
6	2.8	1.1	0.39	1.50[a]

cv:Coefficient of variation (standard deviation/average)
model: Based on mixed (mass balance) initial concentration.
a: Based on averaging model results for starting and ending flows during Tests 5 and 6.

from measured concentrations by less than 30% for all but Tests 2 and 6.

Instantaneous lateral mixing was assumed upon tracer injection to wastewater. Although lateral mixing was not studied experimentally, it occurred rapidly based on visual observation of highly turbulent streams during experiments. Reynolds numbers for wastewater streams varied from 7×10^4 (Test 4) to 1×10^6 (Test 6).

Axial dispersion was assessed by observing non-steady state concentrations of TCM-d in wastewater. For instance, during Test 3 the mean hydraulic transport time between injection and sampling manholes was 3.1 minutes and TCM-d was not detected in a liquid sample collected at three minutes after the beginning of injection. TCM-d concentration increased to within 78% of steady-state by 5.9 minutes after tracer injection. This was best modeled as a series of four CFSTRs (using CORAL), thus corresponding somewhere between a completely mixed reach (1 CFSTR) and a plug-flow system. The only other liquid-phase data which could be used to assess lateral mixing were those corresponding to concentration reductions after termination of tracer injection. Such data were available for Tests 2, 3, and 6. For all relevant data, the number of CFSTRs required to match relative reductions from steady-state (at specific times after tracer termination) was less than or equal to three. However, an important caveat is that after the intended completion of tracer injection, injection tubing contained some TCM-d which was slowly discharged to the wastewater stream. This effect could not be accounted for by the CORAL model, thus leading to somewhat lower predicted concentrations. Higher measured concentrations reduce the number of CFSTRs needed to match experimental conditions. Furthermore, under conditions of the six experiments, a small change in concentration, e.g., 10%, could lead to a substantial increase in the number of appropriate CFSTRs (by a factor of two or more).

TCM-d in Sewer Gas

During all experiments, gas samples were drawn over three to fifteen minute sampling periods, making it impossible to apply discrete comparisons with predicted concentrations during pre-steady state conditions. Furthermore, because of TCM-d introduction following the termination of tracer injection, post-steady state measured concentrations were consistently higher than predicted and could not be used to assess axial dispersion. Limited data were available from a sulfur hexafluoride experiment completed in the CI after the TCM-d research effort had ended.

Sulfur hexafluoride concentrations observed in the CI are plotted versus time after initial injection in Figure 6-10. Black diamonds correspond to samples collected approximately 10 to 15 centimeters above the wastewater surface (low influent). Open squares correspond to a sampling point approximately one meter above the surface (high influent). Both sampling points were located at the inlet (influent) side of sewer pipe flowing through the manhole used for sampling. There was a relatively small concentration difference between the two sampling locations, indicating well-mixed (lateral) conditions during experiments. Well-mixed conditions above wastewater were previously reported for the El Macero Interceptor based on oxygen concentration profiles (Corsi, et al. 1989b). Degree of axial mixing was analyzed by comparing pre-steady state measured SF_6 concentrations with predicted concentrations based on CORAL under variable CFSTR conditions. Concentration at 5 and 11 minutes after injection were best modeled by a series of 25 to 50 CFSTRs, suggesting near plug-flow conditions. Mass transfer coefficients were back-calculated using each measured gas-phase TCM-d concentration and mass balanced liquid concentrations at steady-state conditions. Steady state conditions were defined by the time required for predicted concentrations to reach 95% of the predicted steady state solution.

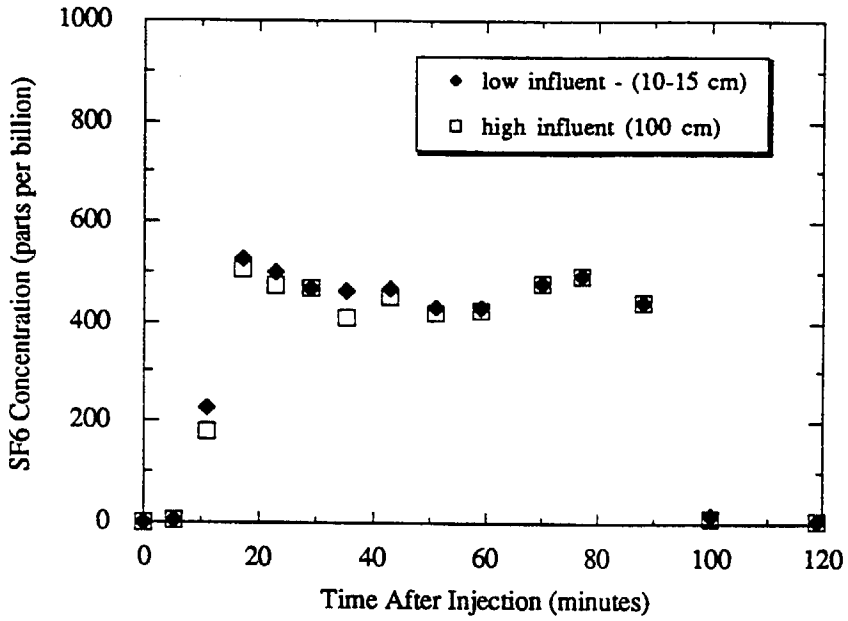

Figure 6-10. Gaseous Sulfur Hexafluoride Concentrations Downstream of Release Point (Central Interceptor)

The CORAL model was used with iterative selection of transfer coefficients to yield predicted gas concentrations equal to each measured concentration. Twenty-five liquid and gas cells were used to model each experiment, with numerical time increments of 30 seconds. Reductions in time increments and refinements to the one-dimensional grid did not significantly change computed transfer coefficients. The only free parameter used to adjust predicted concentrations to more closely represent experimental concentrations was the interfacial mass transfer coefficient. Results are summarized in Table 6-11. The third column corresponds to an average transfer coefficient (normalized by mean hydraulic depth) based on the number of steady-state data points listed in the second column. Coefficients of variation were less than or equal to 0.35 for all but Test 5, with low deviations from the mean for Tests 2 and 4. For Tests 5 and 6, transfer coefficients and gas concentrations were nearly linearly related. Back-calculated transfer coefficients were slightly more sensitive to concentration variations for Tests 1 through 4.

Mass transfer coefficients were predicted for each set of experimental conditions and each of the reaeration coefficient models described in Chapter 3. A TCM-to-oxygen transfer coefficient ratio of 0.57 was applied. The ratio of predicted to average experimental transfer coefficients was computed for each experiment, and averaged over all six experiments. Results are summarized in Table 6-12. The O'Connor-Dobbins, Dobbins, and Tsivoglou-Neal models, all developed for clean water, overestimated mass transfer coefficients. This was expected, and the ratio of experimental-to-predicted transfer coefficients served as an effective a value, as described in Chapter 3. Based on a values of 0.3 to 0.4 for oxygen transfer to treated wastewater (USEPA, 1972), "a" of 0.19 and 0.24 seems reasonable for raw wastewater. A ratio of 0.57 for the Tsivoglou-Neal model was higher than expected. The model attributed to Lau, also a clean

Table 6-11. Mass Transfer Coefficients Based on Experimental Data

Test	# points	k [hr^{-1}]	s [hr^{-1}]	cv
1	3	0.28	0.094	0.34
2	2	0.51	0.028	0.06
3	4	0.48	0.17	0.35
4	4	0.76	0.058	0.08
5[a]	5	0.032	0.029	0.92
6[a]	5	0.056	0.017	0.30

points: Number of steady-state data values used in analysis.
s: Standard deviation
cv: Coefficient of variation (standard deviation / average)
a: Average of values based on starting and ending wastewater flows.

Table 6-12. Ratio of Experimental to Predicted Mass Transfer Coefficients

	k_{expt} / k_{pred}		
Model	Average	sd	cv
Parkhurst-Pomeroy	0.98	0.34	0.34
O'Connor-Dobbins	0.24	0.06	0.26
Dobbins	0.19	0.06	0.34
Tsivoglou-Neal	0.57	0.43	0.75
Lau	4.96	1.60	0.32

Average of six tests.
sd: Standard deviation of transfer coefficient ratio.
cv: coefficient of variation of transfer coefficient ratio.

water model, significantly underestimated transfer coefficients by as much as a factor of five. The most appropriate clean water model, based on realistic "a" and lowest coefficient of variation, was the O'Connor-Dobbins model. The ratio of average-to-predicted transfer coefficient for the Parkhurst-Pomeroy model was 0.98, with a coefficient of variation of 0.34. Variations in experimental results easily encompassed unity. Because it was developed for raw wastewater, the Parkhurst-Pomeroy model is attractive for predicting VOC transfer coefficients in sewers, and was adopted for use in this study.

Measured and predicted gas concentrations are plotted versus time after initial tracer injection in Figure 6-11. Predicted concentrations were based on application of CORAL using the Parkhurst-Pomeroy transfer coefficient model. Predicted concentrations are plotted as a continuous solid line. For Tests 5 and 6, the two lines correspond to predicted conditions based on wastewater flow observed at the beginning and end of each test. Measured concentrations are volume-average values plotted at the midpoint of the sampling period. Twenty-five CFSTRs were used for each model simulation, i.e. no adjustments to calibrate to measured data.

The following observations were made regarding temporal variations in gas concentrations:

1. Test 1 was the only experiment during which gas sample tubing was not flushed (purged) prior to each sample. That could have accounted for the lower than predicted first measured value. However, it could not account for the large difference between the predicted and the second measured concentration. Cool, stormy conditions during Test 1 led to some condensation in sample tubes, which may have interfered with sample analyses.

2. The best fit between experimental and predicted gas concentrations occurred for Test 2. As illustrated in Figure 6-11b, measured gas concentrations exhibited a drop after termination of tracer injection. However, measured concentrations were typically greater than predicted due to continuous, unintentional TCM-d introduction as described previously.

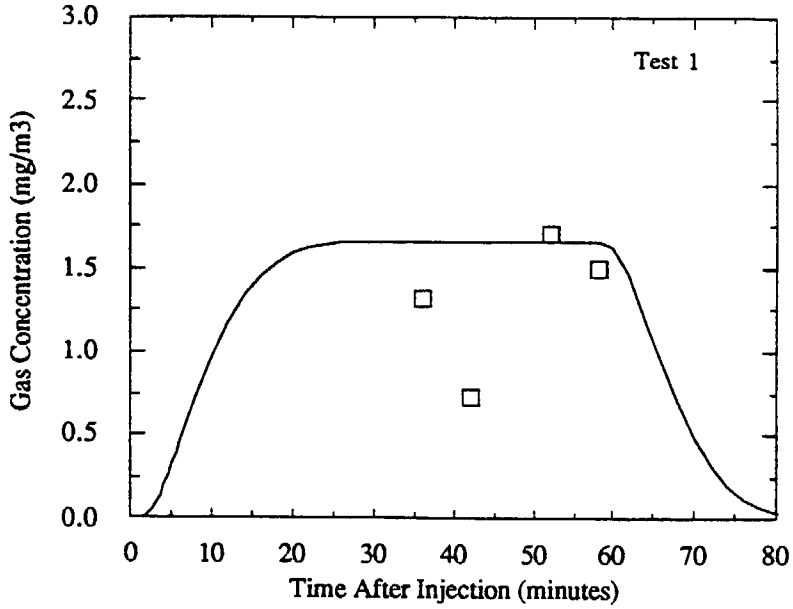

(a)

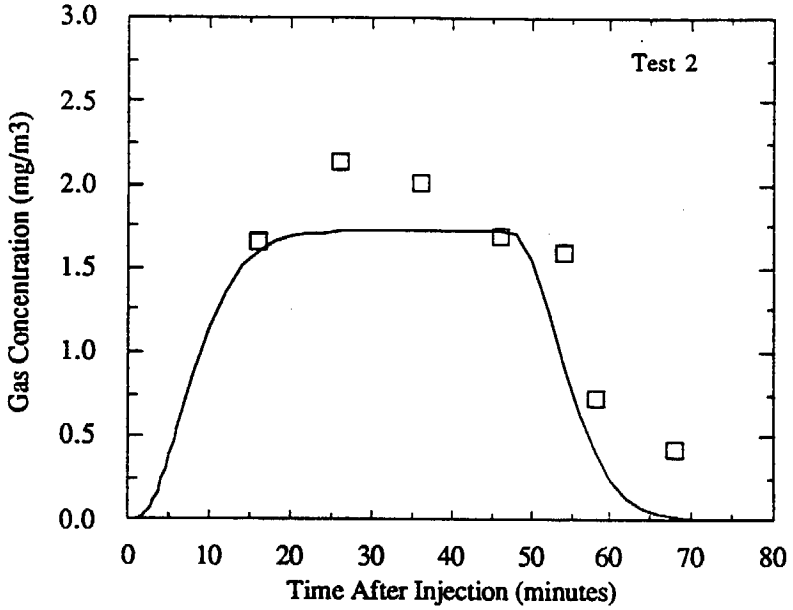

(b)

Figure 6-11. Measured and Predicted Concentrations of TCM-d in Sewer Gas (model results indicated by solid line, measured results by squares)

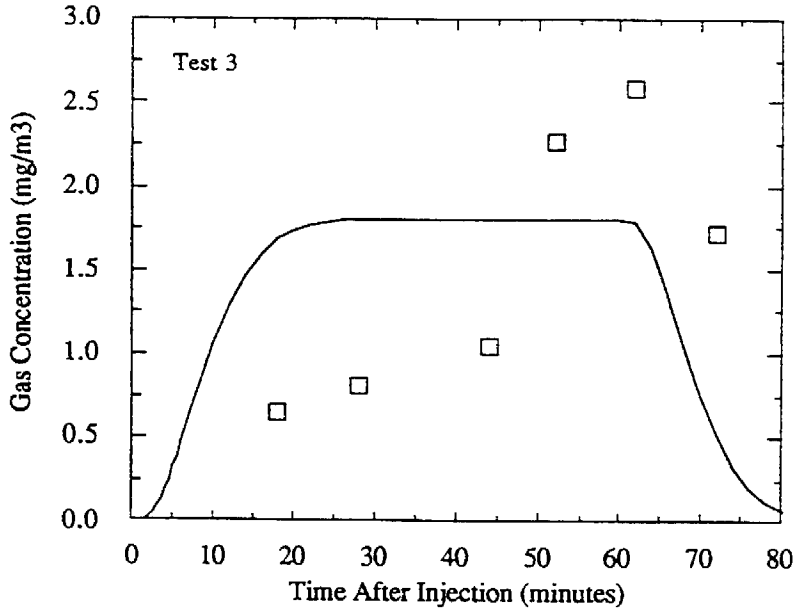

(c)

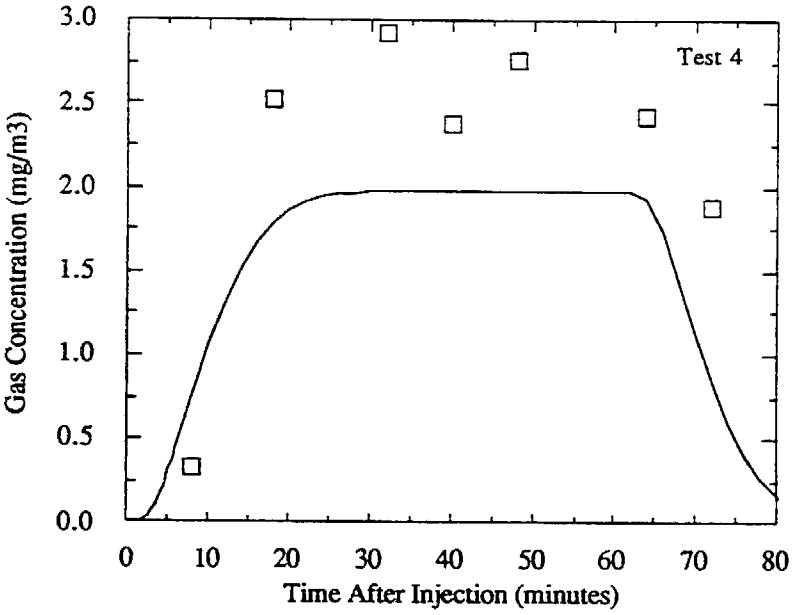

(d)

Figure 6-11. (cont.) Measured and Predicted Concentrations of TCM-d in Sewer Gas (model results indicated by solid line, measured results by squares)

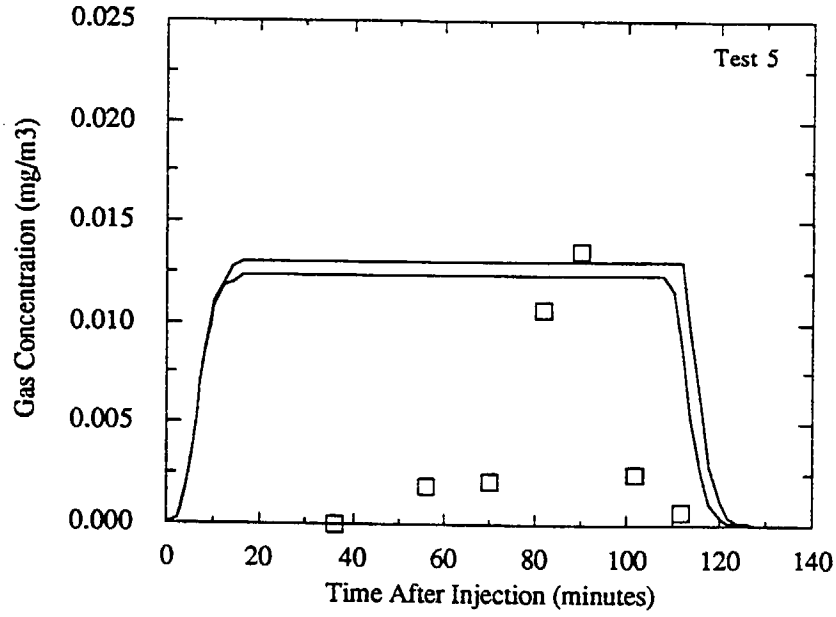

(e)

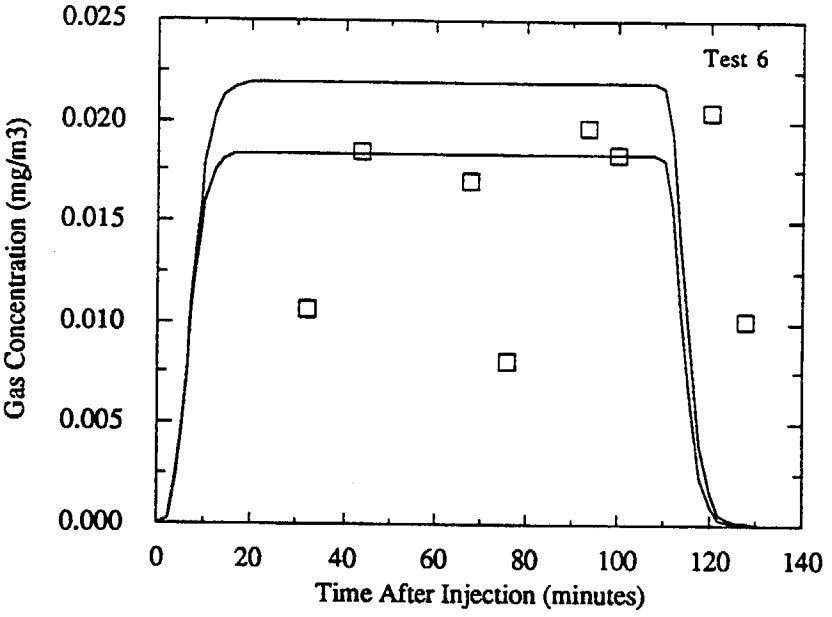

(f)

Figure 6-11. (cont.) Measured and Predicted Concentrations of TCM-d in Sewer Gas (model results indicated by solid line, measured results by squares) (model results based on both initial and final flow rates)

3. Following Test 3, it was discovered that Tygon' tubing used in the injection peristaltic pump head had crimped, leading to non-uniform volumetric flow rates. It is believed that such conditions occurred during Test 3 so that the predicted concentration profile was generated for liquid boundary conditions which did not correspond to experimental conditions. In subsequent experiments the Tygon' tubing was replaced with more flexible silicone tubing.

4. Measured concentrations for Test 4 were generally 30% greater than predicted concentrations. However, experimental and predicted time profiles were consistent in shape.

5. Except for two values, measured concentrations were significantly lower (by approximately a factor of five) than predicted concentrations for Test 5. It is possible that the ambient ventilation air introduced into the cooler sewer resulted in stratified flow near the crown of the sewer pipe. However, this is not known with certainty because a gas tracer release was not performed during Test 5.

6. For Test 6, three of eight samples fell within the predicted profiles generated using initial and final wastewater flow rates. Three measured values fell within approximately a factor of two (low) of predicted values. Two post-injection measurements were greater than predicted (see item 2 above).

To assess trends in the comparison of experimental and predicted gas concentrations, a normalized residual was defined as

$$(C_e - C_p)/C_p$$

where C_e and C_p were experimental and predicted gas concentrations, respectively. Results are plotted in Figure 6-12. Figure 6-12a includes residuals plotted versus sample number, with divisions indicating individual experiments. There was no apparent trend in residuals for the overall experimental program. With the exception of six residual values, all positive and at low C_p, residuals were bound between -1 and +1. Seventeen residuals were negative, and 22 were positive. Excluding the six outlying values, 17 residuals were negative, and 16 were positive. For four of the six tests, samples toward the end of

experiments led to high positive residuals. This was caused by low values of post-injection C_p, and C_e greater than C_p due to unintentional tracer introduction as described previously.

Figure 6-12b is a plot of residual versus time after tracer injection for lumped experimental data (independent of experiment). There was no trend in residuals as a function of time during experiments.

A summary of steady-state concentrations of TCM-d in sewer gas is provided in Table 6-13. Average concentrations during field experiments varied from 0.007 to 2.6 mg m^{-3}. Coefficients of variation ranged from a low of 0.04 (Test 2) to a high of 0.91 (Test 5). Predicted (using CORAL and the Parkhurst-Pomeroy model) concentrations differed from average experimental concentrations at steady-state by less than 30% for all but Test 5.

6.5 UNCERTAINTIES

Uncertainties were categorized as experimental, sample analysis, and computational. An emphasis was placed on uncertainties in measurements, techniques, and assumptions that could lead to differences in experimental and predicted mass transfer coefficients. Estimates were based on known or assumed accuracy of instruments, experience through repetition with laboratory methods, numerical experiments with the CORAL model, reported literature values, and engineering judgement. Upper-bound (conservative) uncertainties were assumed, and overall uncertainty was taken to be greater than largest individual uncertainty. Results are listed in Table 6-14 and discussed below.

Uncertainties in Field Experiments

Uncertainties in experimental measurements that could lead to greatest potential error in estimated transfer coefficients were those stemming from ventilation rates (Tests 5 and 6 only)

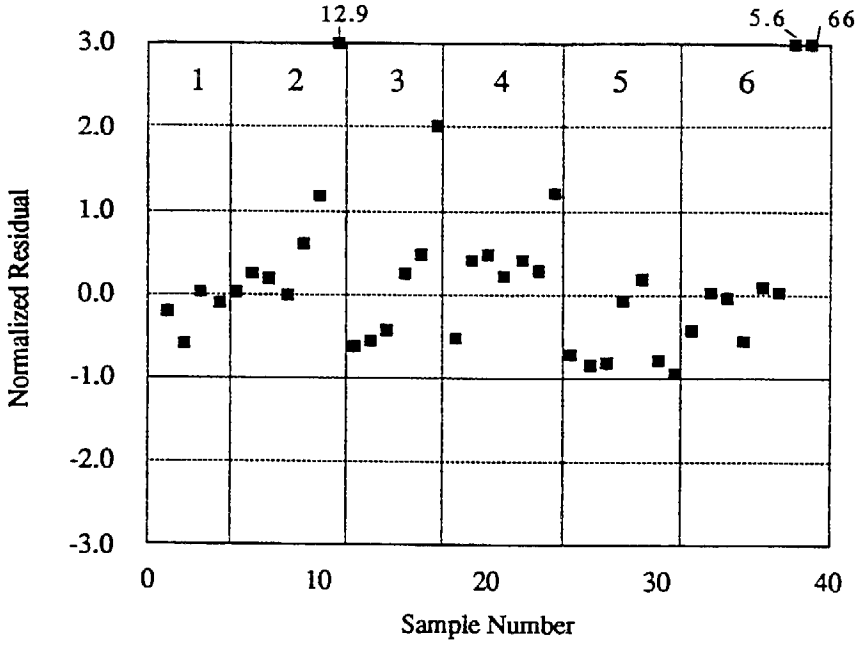

(a)

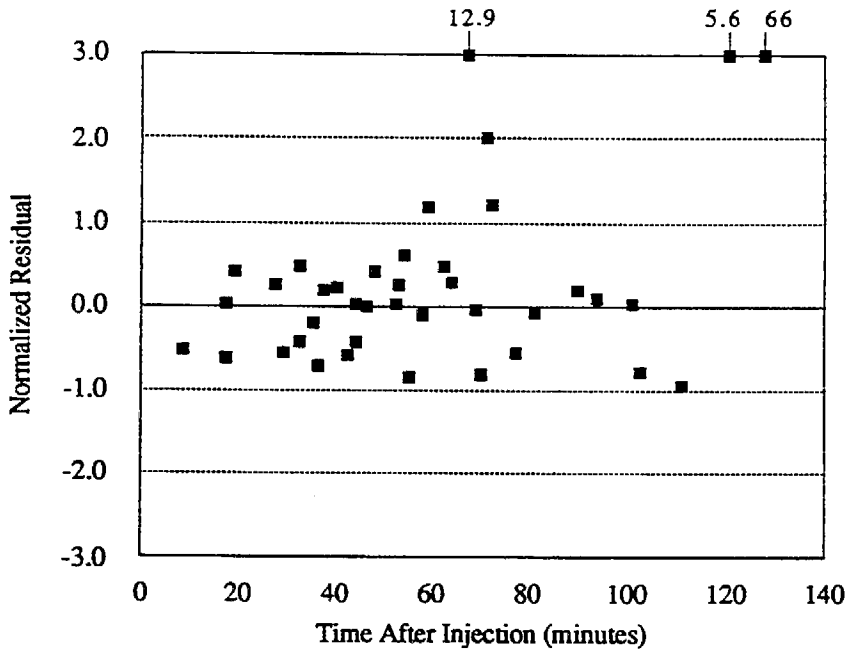

(b)

Figure 6-12. Normalized Residuals Indicating the Difference Between Measured and Predicted Concentrations of TCM-d in Sewer Atmosphere

Table 6-13. Summary of Steady-State Concentrations of TCM-d in Sewer Gas

Test	Average Concentration [$mg \cdot m^{-3}$]	Standard Deviation [$mg \cdot m^{-3}$]	cv	model / average
1	1.3	0.5	0.40	1.28
2	2.1	0.08	0.04	0.83
3	1.7	0.9	0.53	1.07
4	2.6	0.9	0.34	0.75
5	0.007	0.006	0.91	1.87[a]
6	0.019	0.006	0.30	1.06[a]

cv: Coefficient of variation (standard deviation / average).
model: Based on mixed (mass balance) initial liquid concentration.
a: Based on averaging model results for starting and ending flows during Tests 5 and 6.

and tracer concentrations. Individually, each measurement accounted for a ± 25% uncertainty in estimated transfer coefficients. Thus, overall uncertainties in mass transfer coefficients were estimated to be greater than 25% for Tests 1-4, and probably much greater than 25% for Tests 5 and 6.

Uncertainties in Sample Analyses

Greatest uncertainties in sample analyses were associated with preparation and analysis of TCM-d standards. A ± 20% uncertainty in standards led to a similar uncertainty in experimental gas concentrations and transfer coefficients. Thus, overall uncertainties in transfer coefficients caused by potential error in sample analyses were estimated to be greater than 20% for each experiment.

Uncertainties in Computational Analyses

Although uncertainties in Henry's law constant were estimated to be ± 30%, the impact of such variation was not linear under high ventilation conditions of Tests 5 and 6 (overall uncertainty to transfer coefficients based on Henry's law constant was approximately ± 10%). Thus, assumptions regarding extent of lateral and axial mixing, and appropriate values of Henry's law constant for TCM-d were the major contributors to uncertainties in computational analyses. Overall uncertainties in transfer coefficients caused by incorrect assumptions or applications of CORAL were greater than 20% for each experiment.

Overall Uncertainties

Overall uncertainty had to be greater than total uncertainty associated with experimental error. Thus, estimated lower bounds for overall uncertainties in transfer coefficients were ± 25% for all experiments. Actual uncertainties were greater based on combined, but not necessarily additive, effects of individual contributions listed in Table 6-14. Uncertainties for each

Table 6-14. Contributions to Uncertainties in Mass Transfer Coefficients

Experimental	
depth	± 10%
flow	± 15%
temperature	± 20% (Test 1); ± 5% (Tests 2-4) < ± 5% (Tests 5-6)
ventilation rate	± 10% (Tests 1-4); ± 25% (Tests 5-6)
tracer concentration	± 25%
injection rate	± 10% except > ± 10% (Test 3)
gas sample timing	± 10% except > ± 10% (first and last steady-state measurments for Test 1)
gas sampling rate	± 10%
gas and liquid sample loss	-10%
Sample Analysis	
standards	± 20%
TCM interference	negligible
trap or column contamination	< 5%
Computational	
gas mixing assumption	± 20% except > ± 20% (Test 5)
liquid mixing assumption	± 5%
Henry's law constant	± 20% (Tests 1-4); ± 10% (Tests 5-6)
Ψ_i	± 10%
initial conditions	negligible

experiment can also be assessed with regard to both gas and liquid concentration variations as described previously.

6.6 SUMMARY OF FIELD EXPERIMENTS

Volatile tracer experiments were conducted in two operating sewers, with the objective of developing a data base for evaluation of transfer coefficient models. Based on comparison of predicted and back-calculated (experimental) transfer coefficients, the Parkhurst-Pomeroy model, adjusted for differences in diffusivity between oxygen and VOCs, was selected for use in this study. Experimental and model results were also used to study axial and lateral mixing in wastewater and overlying sewer gases. It was concluded that wastewater and sewer gases are generally well-mixed laterally. Tracer experiments indicated that axial flow is best represented by a series of CFSTRs with characteristics between a single well-mixed reactor and a plug-flow reactor in the wastewater. However, axial flow appeared to approach a plug-flow reactor in the gas phase. Model applications indicated that the choice of reach divisions, i.e. number of CFSTRs, does not significantly change predicted VOC concentrations in the gas phase, or the comparison of predicted and experimental transfer coefficients.